Luís Ricardo Dias da Costa

NUMERICAL MODELLING APPLIED TO THE UNDERSTANDING OF GROUNDWATER FLOW AND MASS-TRANSPORT IN SOUTH PORTUGAL - A PERSPECTIVE OF REGIONAL HYDROGEOLOGICAL PROBLEMS AFFECTING GROUNDWATER STATUS

UNIVERSIDADE DO ALGARVE

Faculdade de Ciências e Tecnologia

2022

Luís Ricardo Dias da Costa

NUMERICAL MODELLING APPLIED TO THE UNDERSTANDING OF GROUNDWATER FLOW AND MASS-TRANSPORT IN SOUTH PORTUGAL - A PERSPECTIVE OF REGIONAL HYDROGEOLOGICAL PROBLEMS AFFECTING GROUNDWATER STATUS

Dissertação para obtenção do grau de Doutor em

Ciências do Mar, da Terra e do Ambiente

ramo Geociências

Trabalho efectuado sob a orientação de:

Prof. Doutor José Paulo Patrício Geraldes Monteiro

Prof. Doutor Luís Miguel Amorim Nunes

2022

NUMERICAL MODELLING APPLIED TO THE UNDERSTANDING OF GROUNDWATER FLOW AND MASS-TRANSPORT IN SOUTH PORTUGAL - A PERSPECTIVE OF REGIONAL HYDROGEOLOGICAL PROBLEMS AFFECTING GROUNDWATER STATUS

Declaração de autoria de trabalho

Declaro ser o autor deste trabalho, que é original e inédito. Autores e trabalhos consultados estão devidamente citados no texto e constam da listagem de referências incluída.

Luís Ricardo Dias da Costa

_____

(assinatura)

Aknowledgements

The current work would not have been possible without the support of a vast number of people and entities, to whom I am pleased to express gratitude for their contributions.

It is impossible to acknowledge all the professors, colleagues, friends, and family members who had a positive impact in the work developed, but I would particularly like to refer to:

My supervisors, for accepting the guidance of my dissertation theme, the encouragement, support and above all, the friendship bond developed. Professor José Paulo Monteiro your enthusiasm for hydrogeology, numerical modelling and water management was the main driver for me to persuade this field of studies. Professor Luís Nunes for the effort of reviewing the dissertation, your knowledge, professionalism, and capacity to synthetize complex subjects is an ongoing motivation for me to know and achieve more.

To several professionals who in some way contribute with knowledge or data sharing. From the Universidade do Algarve, to Professor Conceição Neves for introducing me to the big data analysis and climate comprehension and for the support with the analysis of the climatic effects on the groundwater levels in the region and to Professor Amélia Carvalho Dill for being willing to share the immense knowledge on hydrogeology. Edite Reis at *Agência Portuguesa do Ambiente*, for providing substantial data and information about water resources management and discussions about the groundwater-related problems in the Algarve region. To Ph.D. Judite Fernandes, at *Laboratório Nacional de Energia e Geologia*, for sharing the passion for the importance of field work. To my friend and colleague Bruno Rodrigues, Ph.D in Geology, for the long discussions about the geology of the Algarve which helped me to better understand the specific groundwater processes in the regions.

To my office colleagues Kathleen Standen, Thyago Lima and Katherine Malmgren, the everyday discussions and feedback, the spirit of camaraderie and support to share and overcome problems in an always respectful manner is a priceless office environment. A special remark should be made to Rui Hugman, a friend and a colleague who has always been available to share his knowledge and experience on numerical modelling, acting as an informal supervisor and providing a much-needed inspiration, at times. Thanks!!

To Andreia Martins, for understanding the late nights, the days away in the office, or field work, or congresses and putting up with my geekiness and above all, to inspire me to be a better person every day.

To my parents, without whom I would have never reach the stage of life I am today.

Finally, I wish to acknowledge the *Fundação para a Ciência e Tecnologia* for the PhD grant SFRH/BD/131568/2017, as well as DHI for supplying a student license of the FEFLOW software.

The research leading to these results has also received support from following projects:

- Project LIFE Charcos, financed by the LIFE program under contract Reference: LIFE12 NAT/PT/000997;

- MARSOL project financed by the European Union Seventh Framework Programme (FP7/2007 – 2013) under grant agreement GA-2013-619120;
- eGROUNDWATER project, financed by the Horizon 2020 under PRIMA partnership section Research and Innovation Programme, grant greement GA n.1921;
- ACORDO ESPECÍFICO DE COLABORAÇÃO ENTRE A AdA E A UALG - Execução dos Planos de Monitorização, em conformidade com o preconizado na DCAPE, no RECAPE e EIA da ETAR de Faro-Olhão (Projecto Financiado pela empresa Águas de Portugal em regime de prestação de serviços).

Resumo

A presente dissertação agrega diferentes trabalhos referentes à hidrogeologia do Algarve com foco para a análise de alguns problemas relacionados com as águas subterrâneas identificados na região. Foram empregues várias ferramentas numéricas de forma a caracterizar algumas das questões mais sonantes das águas subterrâneas no Algarve do ponto de vista institucional. Seleccionaram-se dois casos de estudo, o aquífero Querença-Silves e o conjunto de aquíferos em contacto com a Ria Formosa.

No primeiro caso de estudo apresentado, Querença-Silves, procedeu-se a uma análise de balanço com apoio de um modelo numérico de fluxo, com vista à evolução dos níveis de água subterrânea perante diferentes cenários de exploração e de Gestão da recarga de aquíferos. Adicionalmente, com recurso à relação de Ghyben-Herzberg, foi realizado um tratamento de pós processamento para identificar potenciais efeitos da evolução da interface água doce-água salgada, que resulta do contacto a Oeste deste aquífero com o estuário do Rio Arade. Apesar de nas condições actuais não se verificar ocorrência de intrusão salina, dados recolhidos e os resultados de modelação identificam que poderá haver um risco de ocorrência deste processo em cenários de seca prolongada aliados a extracções elevadas. Desta forma, procedeu-se à análise de cenários de Gestão da recarga de aquífero com injecção de água no sistema, de forma compreender como esta medida de mitigação poderá contribuir para a recuperação do sistema e recuo da interface água doce-água salgada.

No que respeita ao caso de estudo dos aquíferos em contacto com a Ria Formosa, foi feita uma primeira análise relativamente à evolução da pluma de contaminação por nitratos na Zona Vulnerável de Nitratos de Faro, com vista ao cumprimento das exigências legais impostas pela Directiva Quadro da Água e da Directiva Nitratos. Desta forma, com o apoio de um modelo numérico de escoamento e transporte de massa, procedeu-se à análise de diferentes cenários de ocupação de solo no que respeita à área agrícola e, consequentemente, carga de nitratos no sistema. Os resultados obtidos pelo modelo sugerem que mesmo num cenário em que se interrompa por completo a entrada de nitratos no sistema, não se conseguem atingir os objectivos ambientais no sistema até 2040, que, neste caso, corresponde a concentrações de

nitrato inferior a 50 mg/L. Este facto reforça a necessidade de adoptar medidas de mitigação alternativas às actuais para se conseguir reduzir o tempo necessário para cumprir com as exigências legais impostas pela Directiva Quadro da Água. Foi neste sentido que se apresentou uma análise de um cenário de Gestão de Recarga de Aquíferos com base na intercepção de água da chuva nas estufas, para posterior injecção no aquífero. Os resultados do modelo sugerem que este cenário não é suficiente para atingir a conformidade, mas que pode reduzir de forma algo significativa o tempo necessário para atingir a meta estabelecida.

Ainda no que respeita aos aquíferos em conexão com a Ria Formosa, com os exercícios de modelação efectuados tornou-se evidente que há conexões hidráulicas entre os diferentes sistemas aquíferos na área de estudo, com trocas de fluxo e massa entre si e que por isso, a sua gestão não poderá ser feita de forma individualizada para cada massa de água subterrânea. Adicionalmente, foi feita uma análise histórica de forma a tentar replicar o processo de contaminação do aquífero por nitratos desde o seu estado mais pristino, com a inclusão de processos de retorno de rega e reciclagem de nitratos, com base nos dados conhecidos. Na maioria dos sistemas, a inclusão destes processos explica os valores de nitratos na água subterrânea actualmente observados, com a excepção do sector centro-sul do aquífero da Campina de Faro, em que se observam valores mais elevados que os simulados, o que possivelmente se deverá a valores históricos de carga de nitratos mais elevados que os que são conhecidos ou à existência de barreiras hidráulicas locais que impossibilitam a descarga de nitratos para a Ria Formosa. Este facto reflecte também que os valores actualmente observados são um reflexo das práticas agrícolas realizadas no passado, e desta forma, o problema não pode ser resolvido simplesmente com a adopção de práticas agrícolas mais sustentáveis. Para tal será necessário implementar medidas de mitigação alternativas. Nesse âmbito, foram simulados vários cenários de mitigação, que envolvem a interrupção de cargas azotadas no sistema, a transição da origem de água para rega para água superficial e dois cenários de Gestão de recarga de aquíferos, um com base na recarga artificial ao longo do leito de ribeiras, outro com base na intercepção de água da chuva em estufas como anteriormente referido. A integração de cenários climáticos no modelo de transporte de massa revela que apesar da implementação de medidas de mitigação, poderá haver um retardamento no decréscimo dos

níveis de nitrato no aquífero superficial da Campina de Faro, resultado de processos de evapoconcentração associado à redução de recarga, aumento da extracção e processos de mistura incompletos no aquífero. Os resultados destes cenários reforçam o facto que a remediação de águas subterrâneas é uma tarefa ambiental complicada, especialmente no que se refere a processos de poluição difusa em áreas muito extensas e que para se atingirem as metas ambientais e o bom estado da água subterrânea, é necessário um conjunto de soluções convencionais e alternativas, de aplicação a escala local ou escala mais regional.

Através de ferramentas de estatísticas procedeu-se ainda a uma análise das relações entre padrões climáticos com a oscilação dos níveis de água subterrânea nos casos de estudo. Os resultados desta análise tarefa permitiram compreender melhor como os níveis das águas subterrâneas se podem comportar em diferentes cenários climáticos, e o que se pode esperar dos efeitos de curto e médio prazo de recarga na região do Algarve.

A implementação de modelos numéricos de fluxo e transporte de massa aliado à análise estatística das relações dos padrões climáticos com a oscilação dos níveis resultou numa ferramenta importante de caracterização dos sistemas aquíferos em estudo, com a redução da incerteza sobre os sistemas e a previsão de cenários de mitigação e cenários climáticos.

Termos chave: aquíferos costeiros, modelação numérica, fluxo subterrâneo, transporte de massa, gestão de recursos hídricos subterrâneos

Abstract

Numerical tools were developed to investigate some of the main groundwater management issues identified in the Algarve region (south Portugal). Two study areas are considered as case-studies, one consisting of the Querença-Silves aquifer which focuses on water balance issues, the other consisting of a set of aquifers in contact with the Ria Formosa coastal lagoon, with focus on the Nitrate Vulnerable Zone of Faro and the evolution of nitrate contamination in groundwater. Groundwater flow and mass-transport numerical models were developed to assess groundwater management issues identified in the study areas. Different types of scenarios have been simulated and analyzed, which take into account changes in land-use leading to different contamination input, changes in groundwater abstraction, mitigation scenarios, with particular focus for simulation of Managed Aquifer Recharge schemes and climate change effects. The use of numerical models was shown to be a powerful tool not only characterize hydrogeological problems, but also to predict the evolution of the current observed conditions under different scenarios. One of the main outcomes of the modelling showed that the nitrate contamination in the nitrate vulnerable zone of Faro is a persistent issue, which is a result of agricultural practices in the past. The current applied solutions rely on the adoption of good agricultural practices, but this was shown not be enough to achieve compliance within the Water Framework Directive. Groundwater remediation is one of the most difficult tasks in environmental clean-up, especially when it comes to large areas. Therefore, an ensemble of solutions, some local, some more regional, including land management measures, should be considered in order to attain a significant reduction of time in achieving good quality status of groundwater bodies. Together with the time-series analysis, the implemented models allowed to have a better understanding of the aquifer dynamics in terms of flow and mass-transport.

Keywords: coastal aquifers, numerical modelling, groundwater flow, mass-transport, groundwater resources management

Index

Index of figures

Index of Tables

Acronyms

AdA Águas do Algarve

APA Agência Portuguesa do Ambiente

CB Cerro do Bardo

COS2010 Portuguese land-use map 2010

EA East Atlantic Pattern

ENSO El Niño South Oscillation

EU European Union

M9 Almansil - Medronhal aquifer system

M10 São João da Venda – Quelfes aquifer system

M11 Chão de Cevada – Quinta João de Ourém aquifer system

M12 Campina de Faro aquifer system

M15 Luz-Tavira aquifer system

MAR Managed aquifer recharge

NAO North Atlantic Oscillation

ND Nitrate Directive

NVZ Nitrate Vulnerable Zone

QS Querença-Silves aquifer

WFD Water Framework Directive

WTP Water treatment plant

Chapter 1: Introduction

1.1 General introduction

The current thesis focus on the contribution to the current state of knowledge regarding the hydrogeology of Algarve aquifers, with the use of a wide variety of tools, including, numerical tools. The main scope of the thesis consists in providing a better insight on the main problems affecting groundwater bodies in the Algarve. To do so, two main study areas have been selected, namely, Querença-Silves karst aquifer system (QS) and the set of aquifers in connection with the coastal lagoon of Ria Formosa, of which, Campina de Faro (M12) is of particular interest.

The motivation leading to the selection of the QS study area, relies on the fact that this is the most important aquifer system in the Algarve, used not only for irrigation, but also for public supply. The main discharge of this aquifer system is to the estuary of the Rio Arade in the so called Fontes de Estômbar (a set of diffuse springs located in the westernmost point of the aquifer). Although there have not been any occurrences of seawater intrusion occurring through set of springs, the high abstractions in the system joint with the decrease of recharge may lead to an increased risk of seawater intrusion, which could put at risk the boreholes used for public supply located circa 1.5 km from the contact with the estuary. Therefore, it is important to characterize not only the risk of this system towards seawater intrusion, as well as address eventual mitigation measures.

Another important subject which is also approached in the current thesis consists in understanding the hydraulic connection between the different hydrostratigraphic units constituting the support of the central Algarve aquifers in connection with the Ria Formosa coastal lagoon.

There are aquifer systems whose geometric limits are clearly known since the earliest available geological cartographies dating from the end of the 20th century, such as the particular case of the Querença-Silves aquifer. Nonetheless, there cases in which the hydrostratigraphic units that constitute the support of some aquifer systems in the mesocenozoic basin of the Algarve still

do have hydraulic connections influencing the groundwater flow and transport, which are still far from being definitely characterised and understood. These same systems are subject to quantity and quality pressures that affect the groundwater status under the scope of the Water Framework Directive. Nitrate contamination at Campina de faro aquifer (Stigter et al. 2006b) is a particular subject highly depicted in this thesis. Aquifer contamination by fertilizers has been of concern for aquifers in South Portugal since the 1980s (Almeida 1985; Silva 1988). This is more evident for the case for the M12 aquifer, which is mostly due to extensive agriculture practices in the past. Arguably one of the main sources of nitrogen in groundwater, nitrogen fertilizers used in agriculture represent the largest diffuse pollution threat to groundwater quality not only for the M12 (Stigter et al. 2013) but also at a global scale (Rivett et al. 2008; Wick et al. 2012; Zhou et al. 2015).Therefore, the current work programme focus on the impacts from human activities and the effects of mitigation measures, such as the use of potential Managed aquifer recharge (MAR) scenarios. The application of MAR is a subject which is commonly referred to during this dissertation, and consists of manmade intentional enhancement of aquifer recharge with support of engineered systems (or nature based solutions) through which various techniques can be used to provide water infiltration into aquifers (Gale et al. 2002; Bouwer 2002; Gale 2005; Dillon 2005; Dillon et al. 2009). MAR has been proven to achieve success in many application worldwide in tackling water management problems (Stefan and Ansems 2018; Dillon et al. 2019), and should be considered as one of many water management tools to achieve sustainable water resources management (Gale et al. 2002).

Besides these quantitative and qualitative management issues, the current work programme also aims at improving the understanding of the conceptual flow model of the central Algarve aquifers since the connectivity between these systems is not well understood. This way, the developed models and analysis can contribute to a more precise assessment of the groundwater budget and flow directions in order to better represent the hydrologic processes in this area, as well as the mass transport mechanisms, which characterize the contaminant plume distribution originated from quality pressures identified in these systems.

The methodology applied in the current work program is based in the observation, characterization and modelling of groundwater flow and mass transport of the central Algarve, at Querença-Silves aquifer and to the set of aquifers in connection to the Ria Formosa. A thorough characterization of the flow - for both cases - and Nitrate contamination in groundwater, in the case of the Ria Formosa aquifers, was assessed and different management and climate scenarios were studied in order to try and predict their effect in the nitrate trend. The thesis also focuses on the uncertainty inherent to the understanding of these hydrologic processes, as well as the analysis of the impacts from human activities in these systems.

In order to support the knowledge on the groundwater oscillations of the case-studies, it is also important to consider their relations with climatic patterns. Therefore, an analysis on the time-series of groundwater and on how these relate with such climate patterns and indices, such as North Atlantic Oscillation (NAO) and East Atlantic pattern (EA) is included in the thesis document. This is a necessary step, in order to better understand the evolution of groundwater levels in the past, as well as to provide a tool to understand what changes can be expected in the future under different climate scenarios.

1.2 Objectives

During the last decade several numerical flow models of coastal aquifers in the region have been developed at University of Algarve and subsequently applied for management purposes (Monteiro et al. 2002, 2006b, 2007b, a; Vieira and Monteiro 2003; Monteiro and Costa 2004; Hugman 2017). In the current thesis, it is intended to continue the research being performed in terms of hydrogeology characterization with the support of numerical models.

By the practical point of view, it is expected that research will contribute to the improvement of water resources management in the Algarve region. The current state of development allowed the simulation of a number of scenarios related with the attenuation of the identified qualitative and quantitative problems according to different mitigation measures.

For the specific case of the Querença-Silves aquifer, this consists of a resilient karst system widely used for abstraction in irrigation and public water supply in the region. Nonetheless, the contact with the estuary of Rio Arade, together with the decrease of recharge and consisten demand for water in agriculture and touristic sectors may increase the risk of sweater intrusion in this system. Hence, under MARSOL project, a set of experiments has been performed, in order to provide possible MAR solutions to increase the resilience of this system. The numerical approach to simulate such solutions is described in this thesis, as a way of giving insight on the risk inherent in this system, as well as on the capabilities of such solutions in preserving the integrity of this aquifer system.

In the case of the Campina de Faro and the remaining aquifers in contact with Ria Formosa, a thorough analysis on the nitrate contamination in this system is assessed. Additionally, several mitigation and land-use scenarios are analyzed, and the outcomes are evaluated regarding regards to how such mitigation measures could benefit the chemical status of the aquifer under the Water Framework Directive demands. In fact, some of the land-use scenarios studied in this case were proposed by the water authority – Agência Portuguesa do Ambiente (APA) results of which were used to support the analysis of the groundwater body status in this area for the 3rd cycle of the River Basin Management Plan (2021-2027).

1.3 Thesis structure

The thesis is organized into seven chapters, including the current chapter – Introduction - which provides the outline and scope of the current work, with the general motivations and goals leading to the tasks performed.

The introduction is followed by **Chapter 2**, which presents the set of equations that describe groundwater flow and mass transport in porous media with the use of the finite element method.

Chapter 3 focus on the Querença-Silves aquifer system (QS) case-study and addresses the development and validation of a three-dimensional model in order to analyse the potential to use Managed Aquifer Recharge (MAR), in order to provide a safe and sound solution to for

groundwater level increase and, consequently, decrease the risk of seawater intrusion that may occur from the contact of this aquifer with the Rio Arade estuary. Additionally, an analysis of the numerical model mesh size in order to simulate local scale features (e.g. injection tests), is performed.

The following **Chapters 4 and 5** aim at the analysis of nitrate contamination in the set of aquifers in contact with the Ria Formosa coastal lagoon, with the support of a numerical flow and mass transport model. In **Chapter 4**, the focus lies on the Nitrate Vulnerable Zone of Faro and an analysis of the different types of land use and on how these affect the nitrate input into the system is performed. Additionally, a MAR scheme based on rainwater harvesting is proposed as a solution to contribute to the decrease of nitrate contamination in the NVZ. As for **Chapter 5**, the analysis focuses more on the intrinsic properties of the model, with an analysis regarding the contributions occurring between the aquifers located in the study area, as well as the impact of the recirculation of nitrates due to irrigation. Additionally, the developed model is used for the simulation of different mitigation scenarios and climate change scenarios.

Chapter 6 focuses on the analysis of long-term time series, and on the relationship between groundwater levels and climatic patterns in both study areas previously mentioned, QS and the aquifers in contact with the Ria Formosa coastal lagoon. Although this chapter does not include numerical modelling tasks, it provides a much-needed insight in order to understand how groundwater levels in the study-areas are controlled by climate.

Finally, **chapter 7** provides general conclusions and some additional considerations about perspectives for future development of work in terms of characterization and analysis at aquifers in the Algarve.

Chapter 2: Governing equations of groundwater flow and mass transport

The physical principles responsible for the groundwater flow and mass-transport simulation at regional scale are described in this chapter. Some developments of these basic principles related with the definition of boundary conditions and definition of initial mass-transport conditions are discussed in Chapter 5

2.1 Groundwater flow – Darcy's law

The more explicit form of the partial-differential equation describing three-dimensional transient flow of groundwater of constant density through saturated porous media is based on Darcy's law, expressing the momentum conservation coupled with an equation of continuity that describes the conservation of fluid mass (Freeze and Cherry 1979):

$$\frac{\partial}{\partial x}\left(K_{xx}\frac{\partial h}{\partial x}\right)+\frac{\partial}{\partial y}\left(K_{yy}\frac{\partial h}{\partial y}\right)+\frac{\partial}{\partial z}\left(K_{zz}\frac{\partial h}{\partial z}\right)+Q=S_s\frac{\partial h}{\partial t} \qquad (2.1)$$

where K_{xx}, K_{yy} and $K_{zz}$are values of hydraulic conductivity [LT^{-1}] along the *x*, *y* and *z* Cartesian axes; h is hydraulic head [L]. Q is a volumetric flux per unit volume [$L^3T^{-1}L^{-3}$] which represents sources and/or sinks in the porous media and; S_s is the specific storage [L^{-1}] and t is time. In the case of steady-state saturated flow conditions, variables are independent from time , hence, time is discarded and the right side of the equation 2.1 is equal to zero.

Hydraulic conductivity (*K*) is expressed by:

$$K=\frac{\rho g k}{\mu} \qquad (2.2)$$

where ρ is the density of the fluid [ML^{-3}], g is acceleration due to gravity [LT^{-2}], k is intrinsic permeability which is a function of the medium alone [L^2], and μ represents dynamic viscosity [$ML^{-1}T^{-1}$].

The hydraulic head [L] corresponds to the fluid potential, neglecting the kinetic energy of the fluid, and is expressed as the sum of the elevation of the point of measurement or elevation head z [L] and the pressure head p [$ML^{-1}T^{-2}$] and is defined as:

$$h = \left(\frac{p}{\rho g}\right) + z \tag{2.3}$$

Specific storage [L^{-1}] is defined as:

$$S_s = \rho g(\alpha + n\beta) \tag{2.4}$$

where α is the compressibility of the geologic media [LT^2M^{-1}], n is the effective porosity (dimensionless) and β is the water compressibility [LT^2M^{-1}].

Equation 2.1 is often expressed in a more compact form using the gradient and divergence operators:

$$S_s \frac{\partial h}{\partial t} + div\left(-[K]\,\overrightarrow{grad}\,h\right) = Q \tag{2.5}$$

Similarly to equation 2.1, for steady state conditions time is discarded and $S_s \frac{\partial h}{\partial t}$ is equal to zero.

2.2 Groundwater mass transport

Solving density-coupled flow and transport problems requires the solution of a complex system of coupled non-linear partial differential equations (Smith and Turner 2001). A complete solution for the solute transport problem includes four processes, which are advection, dispersion, decay and retardation (Freeze and Cherry 1979; Anderson and Woessner 1992; Appelo and Postma 2005).

The physical processes controlling the flux into and out of the elemental volume are advection and hydrodynamic dispersion (Freeze and Cherry 1979).

Advection is the component of solute movement that results from the transport by the flowing groundwater and its three-dimensional x, y, z cartesian distribution relates with concentration as follows (Cunha and Nunes 2011):

$$\frac{\partial C}{\partial t} = -\left(\frac{\partial}{\partial x}(v_x C) + \frac{\partial}{\partial y}(v_y C) + \frac{\partial}{\partial z}(v_z C)\right) \quad (2.6)$$

where C is the concentration of a contaminant in the fluid [ML^{-3}], t is time [T], v_i is the velocity of groundwater flow at a specific time [LT^{-1}].

Hydrodynamic dispersion refers to the spreading of a given contaminant caused by the fact that not all the plume particles move at the same average linear velocity is given by:

$$\frac{\partial C}{\partial t} = \frac{\partial}{\partial x}\left(D_x \frac{\partial C}{\partial x}\right) + \frac{\partial}{\partial y}\left(D_y \frac{\partial C}{\partial y}\right) + \frac{\partial}{\partial z}\left(D_z \frac{\partial C}{\partial z}\right) \quad (2.7)$$

where D is the dispersion coefficient [L^2T^{-1}].

If the hydrodynamic dispersion coefficients are considered constant, equation 2.7

simplifies to:

$$\frac{\partial C}{\partial t} = D_x \frac{\partial^2 C}{\partial x^2} + D_y \frac{\partial^2 C}{\partial y^2} + D_z \frac{\partial^2 C}{\partial z^2} \quad (2.8)$$

The chemical reaction term of the mass transport equation is controlled by the reactive components retardation and decay(Anderson and Woessner 1992).

Retardation is the result of adsorption of a contaminant by the rock or soil in the media, responsible for slowing down the rate of movement of a contaminant. Retardation factor (R_d)

can be explained as the ratio of average water particle velocity to average contaminant particle velocity (no units), which is given by:

$$R_d = \frac{v}{v_c} = 1 + K_d\left(\frac{\rho_b}{\theta}\right) \tag{2.9}$$

where R_d [-] is the retardation factor, v is the linear groundwater velocity [LT^{-1}], v_c is the velocity of the contaminant [LT^{-1}], K_d is the distribution coefficient [L^3M^{-1}], ρ_b is the bulk density of the porous media [ML^{-3}] and θ is the porosity [-]

Decay (λ) refers to the chemical and biochemical reactions affecting the half-life of a substance and is controlled by the half-life time of a substance:

$$\lambda = \frac{\ln(2)}{t_{1/2}} \tag{2.10}$$

Since nitrate transport in groundwater can be treated as a non-reactive constituent (Bear 1979; Freeze and Cherry 1979; Anderson and Woessner 1992), the numerical models implemented in the current thesis consider the advection-dispersion (equations 2.6 and 2.8) form of the mass transport equation, hence ignoring the decay and retardation processes. The general form of the mass-transport governing equation used in this thesis is then given by:

$$\frac{\partial C}{\partial t} = D_x\frac{\partial^2 C}{\partial x^2} + D_y\frac{\partial^2 C}{\partial y^2} + D_z\frac{\partial^2 C}{\partial z^2} - \left(\frac{\partial}{\partial x}(v_x C) + \frac{\partial}{\partial y}(v_y C) + \frac{\partial}{\partial z}(v_z C)\right) + \frac{q_s}{\theta}(C_s) \tag{2.11}$$

where the first term of the right side of the equation consists of the hydrodynamic dispersion as described in equation 2.8, the second term corresponds to the advection process described in equation 2.6 and the third term consists of the sources and/or sinks of contaminant into or out of the elementary volume, in which q_s is the volumetric flux of the contaminant [L^3T^{-1}] and C_s is the concentration of the respective source or sink.

2.3 The fresh-saltwater interface in coastal aquifers – Ghyben-Herzberg relation

Groundwater pumping from wells in coastal aquifers which are in hydraulic connection with the sea may result in an inversion of the hydraulic gradient, thus inducing a flow of saltwater towards the aquifer. This process is known as seawater intrusion (Bear 1979; Freeze and Cherry 1979). Inversely, the injection of freshwater in wells near the coast or the increase of recharge, may result in the recoil of the saltwater. This dynamic process is known as the saltwater-freshwater interface, and was first approached by Ghyben (1888) and Herzberg (1901), who showed that, assuming simple hydrostatic conditions in a homogeneous, unconfined coastal aquifer, the depth of this interface at a given point can be calculated as a function of the density of seawater and freshwater, and the hydraulic head in the same position(Verruijt 1968). This consists of a simple and useful method for estimating the depth of the fresh-saltwater interface, known as the Ghyben-Herzberg relation. It is based on the assumptions that (1) the interface is sharp, with no mixing, (2) there is no resistance to vertical flow and (3) at the shoreline freshwater head equals sea elevation. Thus, a point at depth z_s below sea level, pressure in saltwater is given by:

$$p_s = \rho_s g z_s \tag{2.12}$$

where ρ_s is saltwater density [ML^{-3}] and g is acceleration due to gravity [LT^{-2}]. The pressure in fresh water at the same point, is given by:

$$p_f = \rho_f g(z_s + h) \tag{2.13}$$

in which ρ_f is freshwater density [ML^{-3}] and h is hydraulic head [L] in the fresh water measured from the datum. As hydrostatic conditions are assumed, $p_s = p_f$, and therefore resolving for z_s yields the Ghyben-Herzberg relation:

$$z_s = \frac{\rho_f}{\rho_s - \rho_f} \tag{2.14}$$

For ρ_s=1025 g.cm^{-3} (typical ocean densities) and ρ_f=1000 g.cm^{-3} the above equation reduces to the simple relation:

$$z_s = 40h \tag{2.15}$$

Chapter 3: Modelling contributions at Querença-Silves aquifer system

In the current chapter, a characterisation of the karst Querença-Silves aquifer system (QS) Portugal is performed jointly with an analysis regarding the water flow and storage of the system. Additionally, a theoretical analysis is performed, in order to assess the outcome of Managed Aquifer Recharge (MAR) scenarios, in what concerns the increase of groundwater storage in the aquifer system. A three-dimensional numerical groundwater flow model has been applied in order to provide the analysis outcome.

The work presented on this chapter is based on the outcomes of the MARSOL project (FP7 MARSOL-619120 Project) and the congress presentations Costa et al. (2015a) and Costa et al. (2015c).

- FP7 MARSOL-619120 Project (Demonstrating Managed Aquifer Recharge as a Solution to Water Scarcity and Drought);
- Costa L, Monteiro J, Oliveira M, et al (2015a) Modelling Contributions of the Local and Regional Groundwater Flow of Managed Aquifer Recharge Activities at Querença-Silves Aquifer System. In: EGU General Assembly 2015. Vol. 17, EGU2015-146, poster presentation. Copernicus GmbH, Wien, Austria.
- Costa L, Monteiro JP, Oliveira MM, et al (2015c) Interpretation of an Injection Test in a Large Diameter Well in South Portugal and Contribution to the Understanding of the Local Hydrogeology. In: 10o Seminário de Águas Subterrâneas - Associação Portuguesa de Recursos Hídricos (APRH). Universidade de Évora, 9 e 10 de Abril de 2015, Évora. pp 61–64

3.1 Introduction

The Querença-Silves aquifer system (Figure 3.1) is the largest aquifer in Algarve, located in the center of the Algarve region, in south Portugal, a region characterized by a Mediterranean climate with dry and warm summers and cool wet winters. It is considered a karst aquifer formed by Jurassic (Lias-Dogger) carbonate sedimentary rocks covering an irregular area of 324

km^2 from the Arade River (at the west) to the village of Querença (at the East) (Monteiro et al. 2006b, 2007a, b). The system is delimited south by the Algibre thrust, which is the main onshore thrust in the Algarve Basin, separating the Lower/Early and the Upper/Late Jurassic and to the north by the Triassic-Hettangian rocks (Terrinha 1998). The Estômbar springs on the west limit of QS aquifer constitute the main discharge area of the system towards the Arade River, supporting several important groundwater dependent ecosystems.

Manuppella et al. (1993) presents a cross-section of the central Algarve region (Figure 3.2). This cross-section allows a synthetized visualization of the geometric relations of the Early/Lower Jurassic lithology which support the Querença-Silves aquifer system Identified in blue, in Figure 3.2.

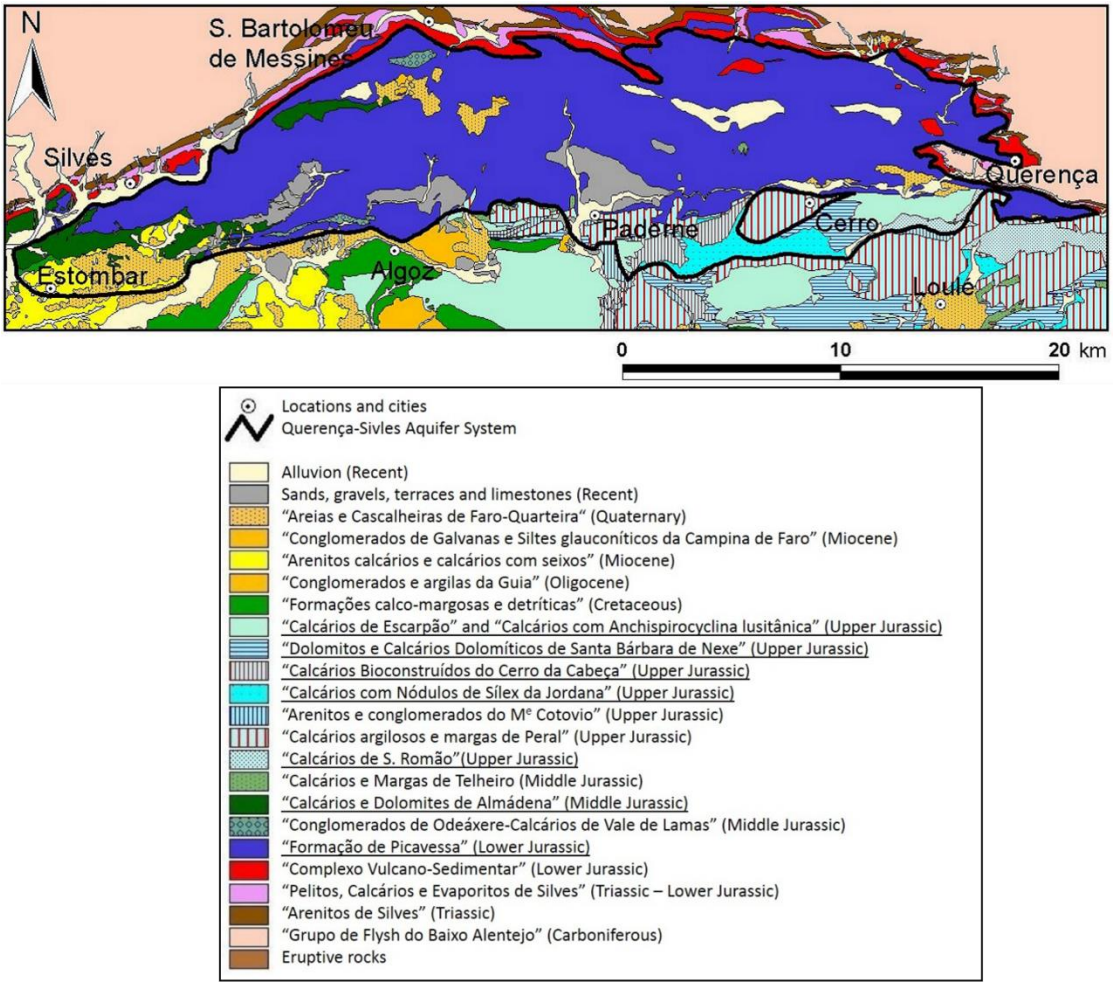

Figure 3.1 - Querença-Silves aquifer system's geology. Underlined features are the ones identified within the aquifer limits. (source: Almeida et al. (2000))

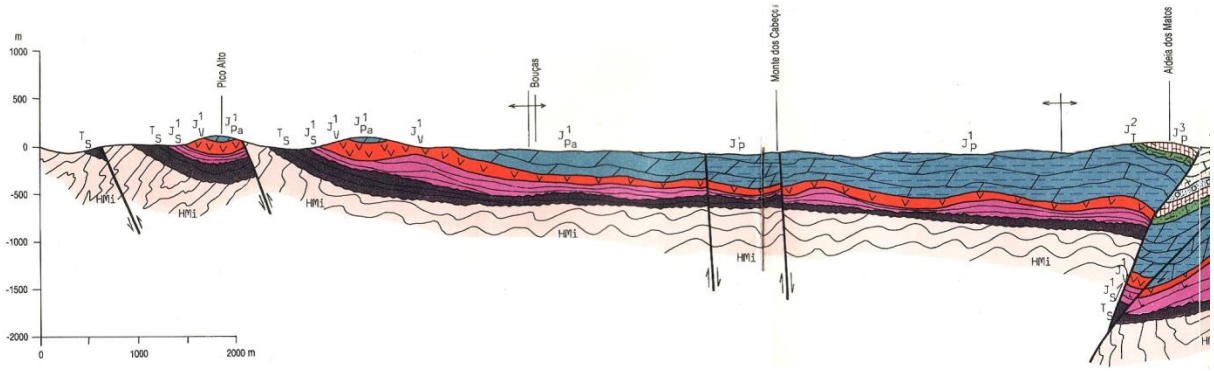

Figure 3.2 - Geometry of the carbonated rocks of early Jurassic which constitute the most important support of the aquifer system Querença-Silves (dark blue colour, to the left of the Algibre thrust). (Source: Manuppella et al. (1993))

According to previous studies, the hydrogeological setting of the QS aquifer, has a complex compartmented structure, with two distinct domains separated by a fault: a western domain and an eastern domain. Its western domain has a well-developed karst, westward flow direction, with the main discharge areas along the Arade river, with particular relevance to Estômbar springs (westernmost point of the aquifer, where main discharge occurs). Its eastern domain has more random flow directions, less regular piezometric surfaces (Figure 3.3) and a lower karst development. The tectonic activity of this region results in its widespread fracturing, defining a significant number of semi-independent aquifer blocks, with more or less constrained and restricted hydraulic links between them. Such hydraulic restrictions are more expressive in the eastern domain, because in the western domain the pervasive karstic network largely obliterates such tectonic setting (Mendonça and Almeida 2003; Monteiro et al. 2006b).

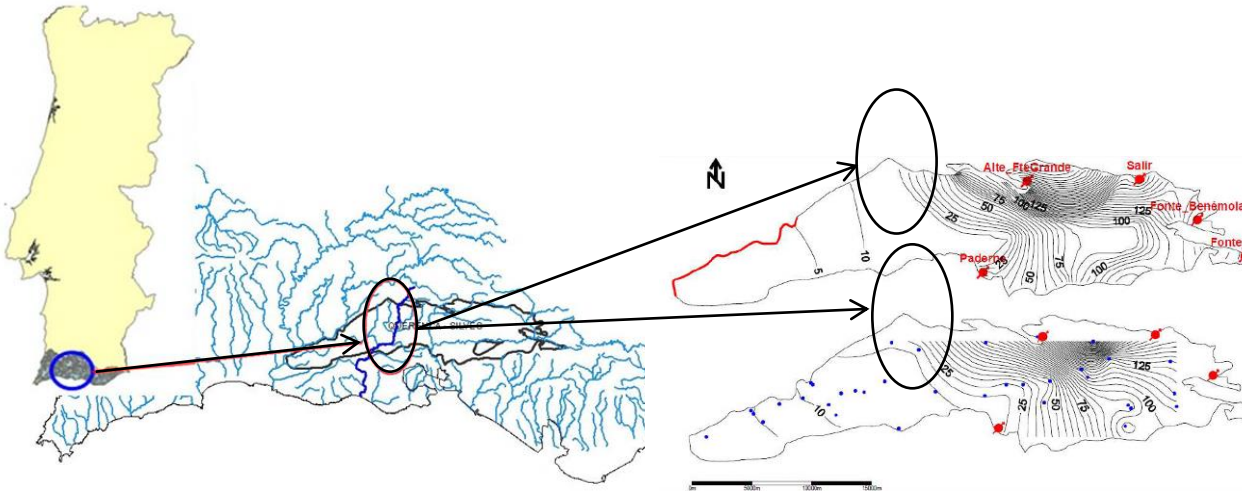

Monteiro *et al*., 2006

Figure 3.3 - Site location along Ribeiro Meirinho stream and central-western area of Querença-Silves aquifer and its piezometry (upper right: modelled; lower right: measured) (Source: Leitão et al. (2014))

The Ribeiro Meirinho stream is located in the central-western area of Querença-Silves aquifer and its upper reaches are located outside the aquifer, in Algarve hills. The latter are Palaeozoic terrains, composed mainly of schist and graywackes, essentially impervious lithologies, being

therefore, the main source of water for this stream until it reaches the Jurassic limestones, dolomites, dolomitic limestones and other, less important, calcareous formations composing the karst aquifer.

3.2 Data and Methods

3.2.1 Modelling context

A 3D finite element flow and transport, calibrated and validated, model is being used to study and predict the regional effect of injecting wet year's surface water surplus in the large diameter Cerro do Bardo well and surrounding area.

This analysis was performed under steady-state conditions and considered two water supply abstractions scenarios. Scenario 1 which is equivalent to the current extraction conditions and scenario 2 which is equivalent to the maximum abstraction period ever registered at QS aquifer, which corresponds to the drought of 2004/2005.

QS supported an important part of the Algarve urban water supply system during the severe drought that affected Portugal during 2004 and 2005. During this period the extractions in the QS were the most intense in all the historic period of water use in the Algarve region. The extraction volumes for urban supply in municipalities settled in the area of the QS in this period were: 4.6×10^6 m^3/year (Silves); 1.9×10^6 m^3/year (Lagoa); 3.5×10^6 m^3/year (Albufeira) and 0.4×10^6 m^3/year (Loulé) (Monteiro *et al.,* 2007a). Additionally to these abstractions, Águas do Algarve SA extracted in this same period 11.0×10^6 m^3/year in the Vale da Vila well field (also for urban supply in other areas of the Algarve). Finally, as the average of extractions for irrigation in the area of the QS is in the order of 30.91×10^6 m^3/year (Nunes *et al.,* 2006), it is estimated that the total extractions in the QS, in its period of more intense water exploitation, was in the order of 52.31×10^6 m^3/year. Such extraction scenarios may induce a decrease in the hydraulic head at a regional level in the aquifer and contribute to the intrusion of saltwater coming from the Arade river, at the westernmost border of the aquifer. The location of the main well fields, used for urban supply in QS, is represented in Figure 3.4.

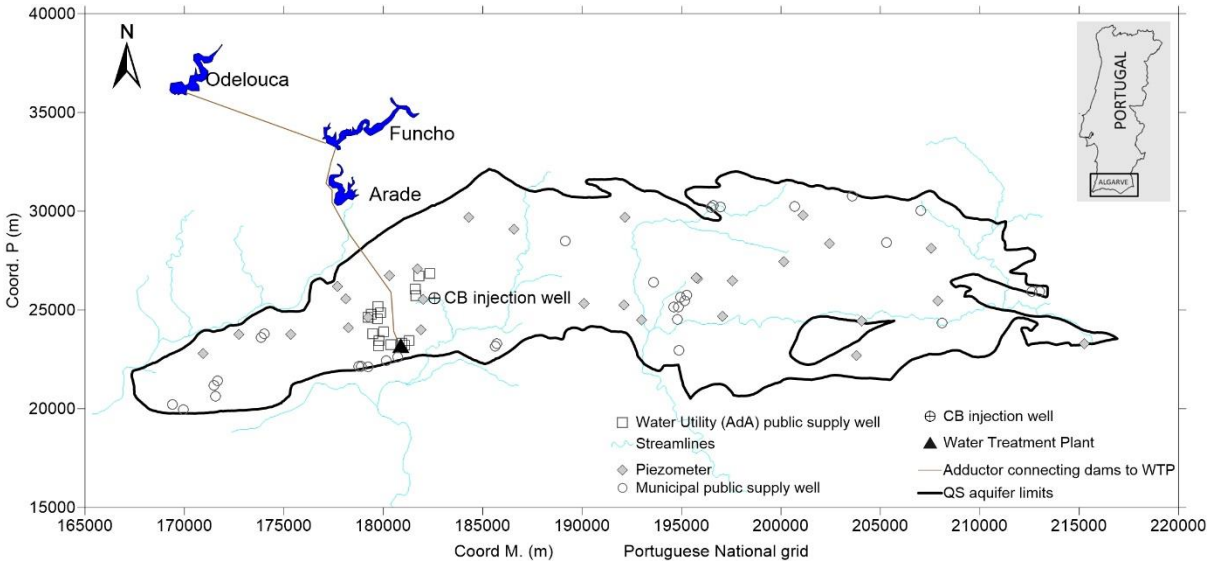

Figure 3.4 - Location and main supply wells in Querença-Silves aquifer system

3.2.2 Water balance

Oliveira *et al.* (2008) estimated an aquifer balance of 104 hm^3/y with a sequential Daily water balance model, later updated by Oliveira *et al.* (2011) to 94 hm^3/y. This model, BALSEQ_MOD, estimates a spatial distribution of infiltration by incorporating methodologies to estimate the processes of soil infiltration, real evapotranspiration, and deep infiltration. The last estimates from 2011 and its spatial distribution were incorporated into the numerical model, as presented in Figure 3.5.

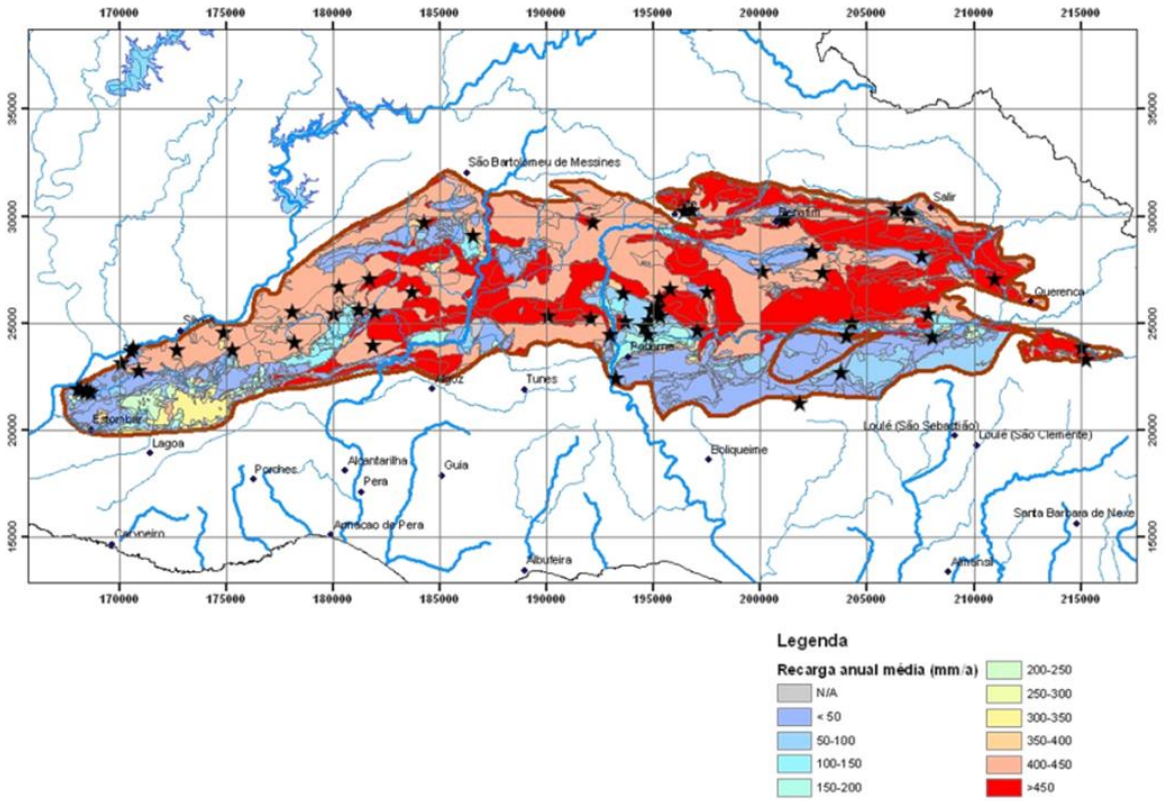

Figure 3.5 – Average Querença-Silves aquifer recharge (period 1941-1991) (source: Oliveira et al. (2008))

3.2.3 Infrastructures for MAR

The main infiltration infrastructure at the demo site consists of the CB handmade large dug well, originally built in the late 1970's, with a diameter of 2 meter and 32 meters deep, located close to Aivados stream at Cerro do Bardo (Figure 3.4). During MARSOL project, injection tests with and without tracers were performed on the CB well (Deliverable 4.3), the results of which indicated high infiltration capacity (around 400 m/d), with a groundwater flow pattern mostly towards East, contrary to the regional aquifer main flow direction. A weir is located 200 m downstream CB, which acts as a small dam, retaining some water losses from the well to the stream, when the injected water volume exceeds the injection capacity at the well. These infrastructures provide good conditions for implementing a MAR system, in which the infiltration process is enhanced by natural existing sinkholes in the riverbed. These same sinkholes allow the infiltrated water to reach the regional aquifer.

3.2.4 Water origin for MAR (water budget)

For the Cerro do Bardo site, the theoretical water availability for MAR would be originated from the surplus of surface water dams (Funcho, Odelouca and Bravura), which is typically discharged downstream during wet years. This discharge occurs mostly for security measures when the dams are in risk of reaching full capacity of the reservoir (in order to avoid dam overtopping which would result in serious infrastructure damage), therefore, there is no direct relation between yearly rainfall and the discharged surplus. According to the water supply company *Águas do Algarve, Lda.* responsible for managing the dams, Odelouca dam alone has an average annual inflow in wet years of 122 hm^3, of which an annual supply to the Alcantarilha Water Treatment Plant (WTP) is estimated at 50 – 55 hm^3/year. This would result in an average remainder storage of ~70 hm^3 every year in the Odelouca dam alone.

A fraction of this surface storage could be used for MAR at the CB well and weir system, which are located upstream the groundwater pumping wells of Alcantarilha WTP. A pipeline connecting the three dams to the WTP Alcantarilha is already active (Figure 3.4), which passes around 2 km from the Cerro do Bardo well at its closest point. Currently, there is no pipeline connection to the CB injection site.

3.2.5 Numerical groundwater flow model for Querença-Silves aquifer

The numerical model developed within this work consist of the commercial modelling software FEFLOW(Diersch 2014). Detailed descriptions of the governing equations and theoretical development and benchmarking of the FEFLOW code can be found in Kolditz et al. (1998), Diersch and Kolditz (1998), Diersch (2014).

With the support of numerical models, it is intended to show how the QS aquifer may be influenced by seasonal pumping effects and how this impacts the regional water level and the evolution of the saltwater-freshwater interface, as well as how MAR can contribute to decrease the level of such impacts and contribute to augment the groundwater piezometric levels. This was done by simulating two extraction scenarios, one scenario with the highest registered

abstraction, during the 2004/05 drought and another with the actual abstraction rates. Then, for both scenarios, several MAR scenarios were tested, injecting from 1 to 25 hm^3/year at the existing infiltration infrastructures. The results from the large infiltration and tracer test performed during the MARSOL project in April 2016 have shown an infiltration capacity of the injection site of 4060 m^3/d, i.e. 1.48 hm^3/y (MARSOL Deliverable 4.3, Leitão et al. (2016)).

3.2.5.1 Background models developed for QS aquifer

The model used in this project is the result of ongoing research in relation with monitoring and modelling of aquifers at the University of Algarve.

The first variants of this model implemented for the QS aquifer system were presented in Monteiro et al. (2003) and Vieira and Monteiro (2003) and were related with understanding the types of boundary conditions controlling the regional flow pattern and evaluation water balance of the aquifer in terms of recharge and discharge. Monteiro et al. (2006b) performed an initial inverse calibration of transmissivity (T) for the model allowing a considerable improvement in the reliability of the simulation of the observed regional flow pattern. Subsequently, Monteiro et al. (2007b) and later, Salvador et al. (2012) used the model to investigate stream-aquifer interactions and quantify recharge occurring from streams, as these are relevant to the ecological conditions of riparian groundwater dependent ecosystem. Stigter et al (2009) undertook simulations of hypothetical extraction scenarios as part of an effort to determine sustainable sources of groundwater for integration into a regional water supply system, in which the spatial distribution of abstraction for irrigation was refined and applied to the location of known irrigation wells. Later, the model has been adapted by Hugman et al. (2012) to perform an analysis of sustainable yield of the aquifer system based on several properties (aquifer properties, temporal distribution of recharge, temporal distribution of groundwater pumping and spatial distribution of wells), whereas Hugman et al. (2013) focused on the optimization of time-scale abstractions in order to maximize groundwater use with minimum impacts. In more recent years, Hugman et al. (2017a) developed a vertical cross-section model with density-coupled flow and transport for the western sector of the QS, to

assess seawater intrusion risk against several scenarios, namely, an ensemble of climate, water-use and adaptation scenarios from 2010 to 2099 taking into account intra- and inter-annual variability in recharge and groundwater use.

The work presented in this chapter consists of an adaptation of the model developed by Hugman et al. (2012) and Hugman et al. (2013), which focus mainly in converting the previously defined 2d model to a three dimensional mesh.

3.2.5.2 Model geometry

Monteiro et al. (2007a) calculated a thickness of the QS model based on the geological cross section presented by Manuppella et al. (1993) and the maximum observed hydraulic head map at the QS aquifer. For a better representation of the experiments developed under MARSOL project, the QS model has been converted to a 3D version based on the thickness map calculated by Monteiro et al. (2007a) with 6 layers and 7 vertical slices, accounting for a total of 134454 elements and 81641 nodes (Figure 3.6).

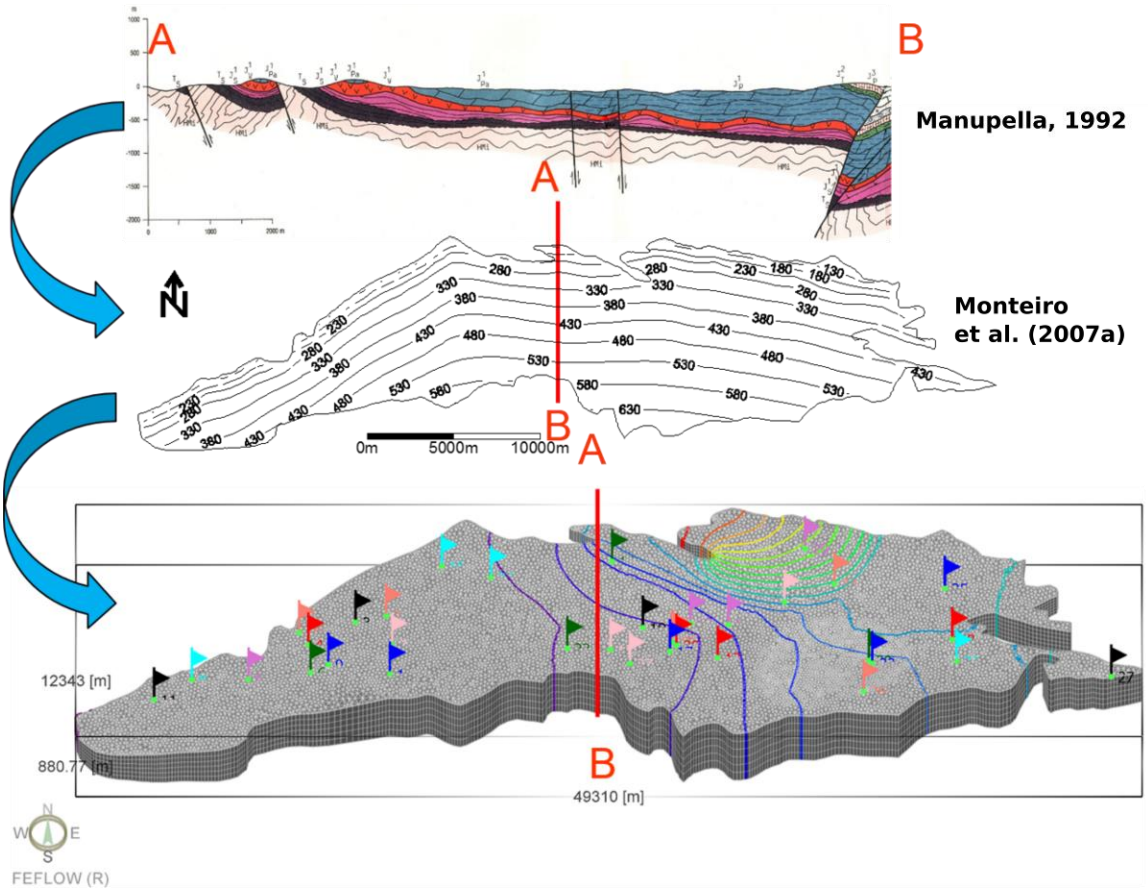

Figure 3.6 – Development steps of the 3D geometrical mesh of the Querença-Silves aquifer model

3.2.5.3 Numerical model parameters, calibration and boundary conditions

Although QS is a karst aquifer, the developed model flow domain, is represented as a single continuum equivalent porous media. The representation of the flow domain of karst systems as single continuum equivalent porous media, using concepts of hydraulic conductivity (K), is valid when modelling hydraulic heads and flow on a regional scale, as is discussed by Scanlon et al. (2003). Notwithstanding, it is important to bear in mind that this methodology may result in significant uncertainty when simulating smaller scale effects such as drawdown of wells at a local scale or travel times.

Areal recharge rates according to what was presented at chapter 3.2.2 were imposed in the model and estimated average recharge was set to 45% of rainfall, according to calculations by Oliveira et al. (2011). The spatial distribution of the recharge was applied as in Figure 3.7.

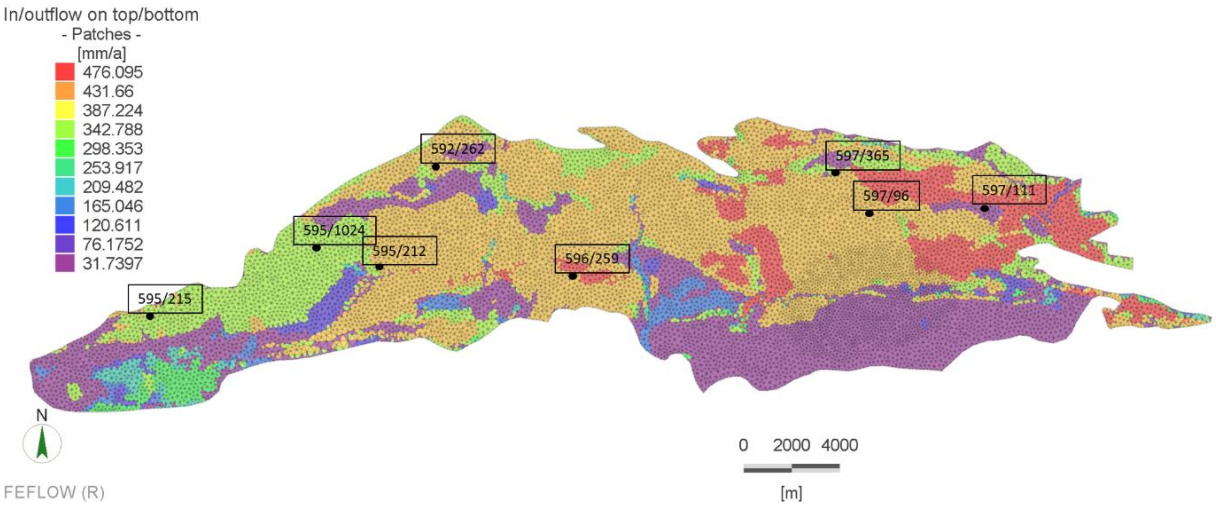

Figure 3.7 - Average recharge (period 1941-1991) imposed in the model, according to calculations by Oliveira et al. (2011)

Hydraulic conductivity at each element was estimated by dividing the calibrated transmissivity calculated in the 2D model developed by Hugman et al. (2012) by the element thickness calculated according to Monteiro et al. (2007a). The resulting hydraulic conductivity distributions is shown in Figure 3.8.

Dirichelet boundary conditions were set along the border of the aquifer with the Arade River, with fixed hydraulic head of zero meters, thus simulating aquifer discharge at the Estômbar Springs. Fixed abstraction boundary conditions to represent the groundwater abstractions were defined and imposed on known abstractions located as previously shown on Figure 3.4, according to extraction scenarios 1 and 2. Private irrigation well abstractions were applied to 150 nodes based on known well locations. The estimated annual abstraction for irrigation according to Nunes et al. (2006) was distributed equally among these nodes and under transient conditions being active for the period of the last week of May to the end of September, such as previously defined by Hugman et al. (2012). Withdrawals for public supply

were applied to the nodes corresponding to the Water supply company, Águas do Algarve (AdA) wells (Figure 3.4 and Figure 3.8), which provided monthly values of abstraction.

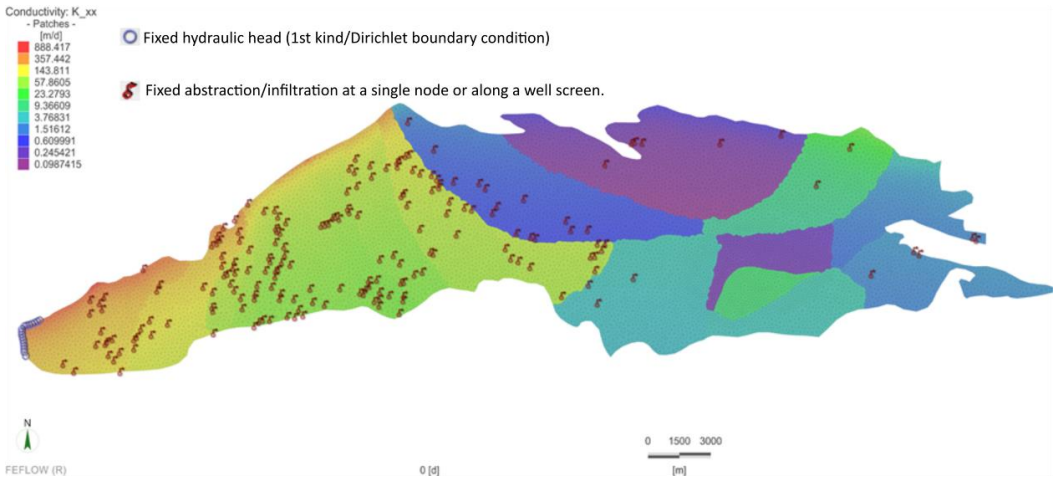

Figure 3.8 – Calculated hydraulic conductivity distribution for the three-dimensional model and location of Dirichlet boundary conditions and fixed abstraction boundary conditions

Since the 2D model has previously been calibrated (Monteiro et al. 2006b, 2007a; Hugman et al. 2012, 2013), a simple validation of the observed vs calculated time series of hydraulic head was performed, which is shown in Figure 3.9, results of which appear to have a satisfactory fit the observed trends in general.

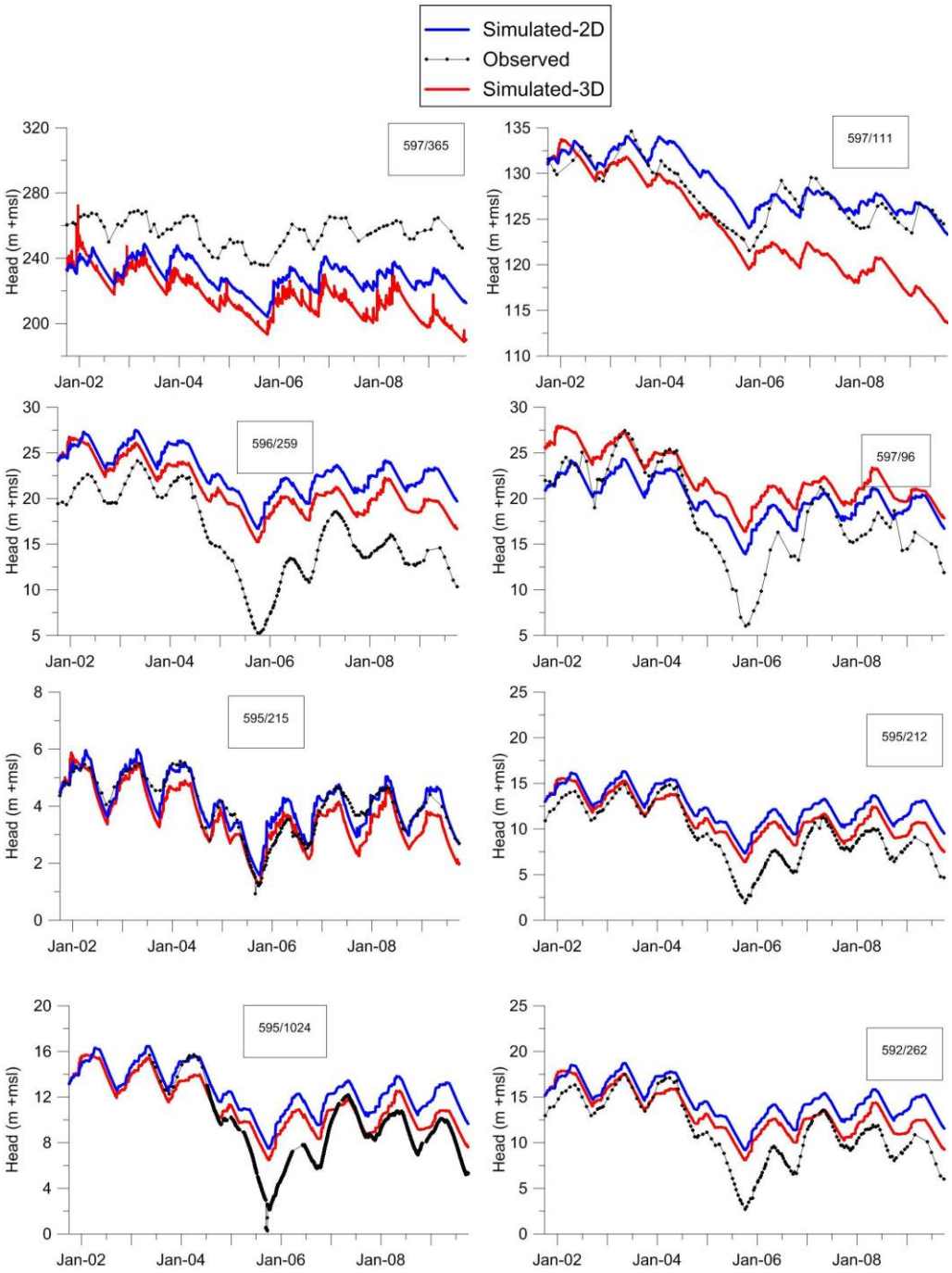

Figure 3.9 – Observed and simulated hydraulic head at several observation wells used to calibrate and validate the QS numerical flow model for the 2D and 3D geometry

3.2.5.4 Modelling scenarios

Two abstraction scenarios were considered for the numerical model (Table 3.1). Scenario 1 considers water currently exploited by the Water supply company (Águas do Algarve, Lda.) used for urban supply, which is 11.00 hm^3/year (Stigter et al., 2009) and for irrigation withdrawals which is estimated as 30.91 hm^3/year, mostly concentrated in the western sector of the aquifer (Nunes et al., 2006), summing a total abstracted value of 42 hm^3/year.

Scenario 2 represents the period during which extractions in QS were the most intense in all the historic period of water use in the Algarve region according to existing records, corresponding to the drought of 2004-2005. During this period, extraction volumes for municipal urban supply were 4.6 hm^3/year (Silves); 1.9 hm^3/year (Lagoa); 3.5 hm^3/year (Albufeira) and 0.4 hm^3/year (Loulé), which makes a total of 10.40 hm^3/year (Monteiro et al., 2007a; Monteiro et al., 2007b). These values together with the abstractions from scenario 1 sum up to a total water abstraction value of 52.31 hm^3/year and are summed up on Table 3.2.

Table 3.1 - Abstraction volumes per category for scenario 1 and 2

	Private irrigation (hm^3/year)	**Water Utility (AdA) public supply (hm^3/year)**	**Municipal wells for urban supply (hm^3/year)**	**Total abstraction (hm^3/year)**
Scenario 1	30.91	11.00	0	41.91
Scenario 2	30.91	11.00	10.40	52.31

For both scenarios, new simulations were performed under steady state conditions, considering the injection of different surface water surplus volumes, ranging from 1 hm^3/year to 25 hm^3/year at Cerro do Bardo injection site and surrounding Water Utility AdA inactive water wells. The aim of this analysis is to determine the resilience of the aquifer towards higher abstractions as were observed during the 2004/05 drought, as well as using surface water surplus from dams in order to mitigate the excess of groundwater explored.

3.2.6 Results

Results allow estimating the influence of 10 hm^3/y of MAR with an increase of the hydraulic head upstream the injection area, and the drawback of the saltwater-freshwater interface

downstream the injection area (Figure 3.10). In addition, a saltwater-freshwater sharp interface analysis according to the Ghyben-Herzberg relation (Ghyben 1888; Herzberg 1901; Verruijt 1968) was performed, to address the evolution of the interface at different MAR and abstraction scenarios (Figure 3.11). In this case, the location of the interface was calculated using the Ghyben-Herzberg relation at each node.

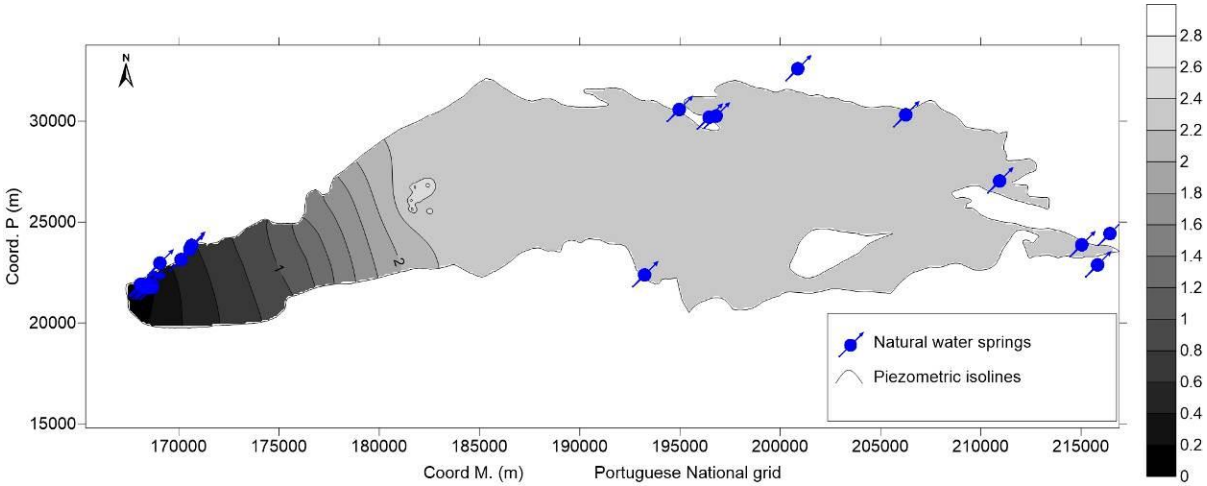

Figure 3.10 – Residual between hydraulic head without and with injection of 10 hm^3/year

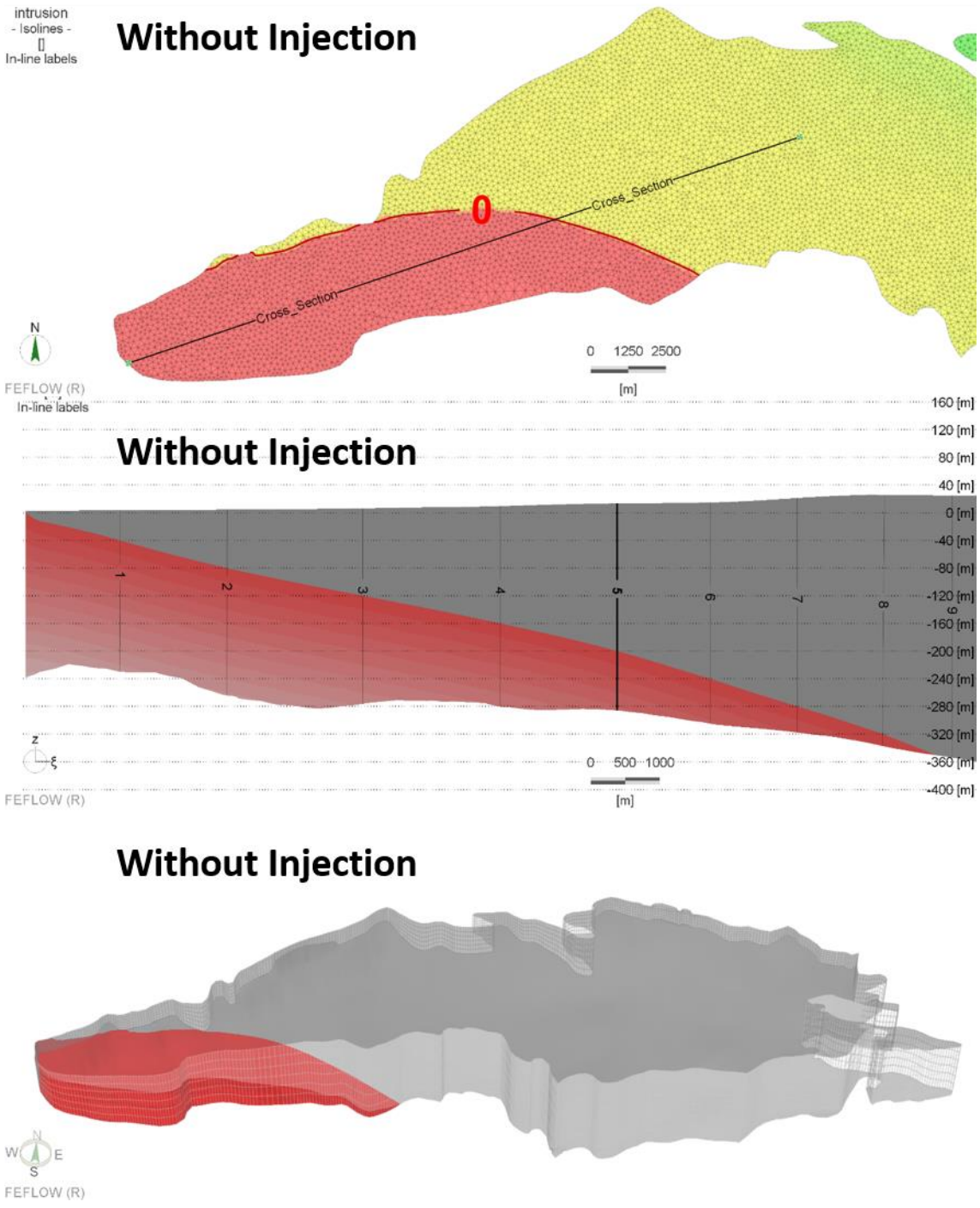

Figure 3.11 – Sharp interface analysis of saltwater-freshwater interface at Querença-Silves. The red contours indicate the seawater fraction of the seawater-freshwater interface, calculated according to the Ghyben-Herzberg relation.

Important to note that from Figure 3.11, the top image shows the extension of the interface at the bottom slice of the model, representing the bottom of the aquifer. The middle image is a vertical profile representation of seawater-freshwater interface. The bottom image shows the seawater intrusion plume on a 3D perspective. This example is a simulation of a scenario with the maximum groundwater abstraction recorded at Querença-Silves (period of 2004/2005) without MAR.

Considering the know-how developed during MARSOL project, one of the MAR scenarios simulated was the injection of 3 hm^3/year under scenario 1 conditions, i.e. current groundwater abstraction. This consists of a theoretical surplus of water from the WTP Alcantarilha that could be available for use in MAR, although scenarios of different injection volumes have also been simulated. The model simulation results for this scenario are presented in Figure 3.12, which shows the residual hydraulic head between business as usual and injecting 3 hm^3/year at Cerro do Bardo, or in other words, the resulting increase in groundwater level upon injecting 3 hm^3/year.

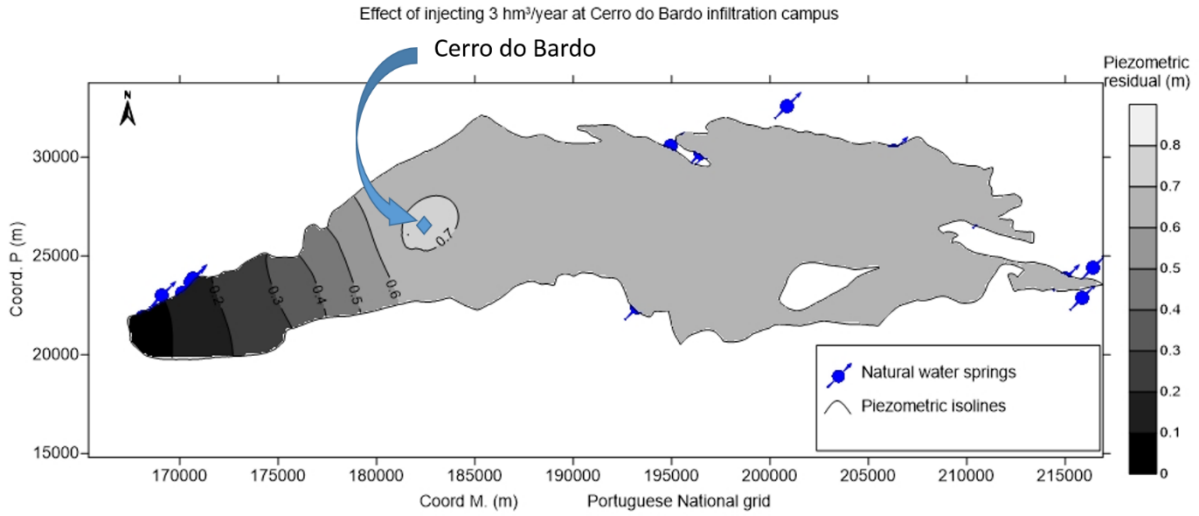

Figure 3.12 – Residual between hydraulic head without and with injection of 3 hm^3/year

Modelling shows that a very impressive effect can be observed upstream of the MAR facilities, due to its barrier effect with the general flow, resulting in an increase in groundwater level of about 0.6 to 0.7 m in most of the aquifer. Also, MAR activities might mitigate and avoid further

saltwater intrusion in the Arade river estuary. By applying a sharp interface approach based on Ghyben-Herzberg relation it is possible to obtain rough estimates on the total affected area by the seawater intrusion. Considering business as usual, a total volume of 22.43 km^3 at the aquifer model are being affected by seawater intrusion. On the other hand, when injecting 3 hm^3/year the volume of the aquifer model affected by seawater intrusion decreases to 20.24 km^3. Hence, a total volume of 2.13 km^3 of aquifer in the waterfront can be relieved from seawater intrusion by injecting 3 hm^3/year.

3.2.6.1 Local scale analysis at Querença-Silves

Parallel to the previous efforts, the same model was also used to simulate the influence of the local scale injection at Cerro do Bardo (CB) large diameter well on April 1st, 2014. The interpretation of this injection test is depicted in MARSOL deliverables 4.3 and 4.2. It consisted of an injection test at CB well (with a depth of 32 meters and a diameter of 2 meters). In order to obtain early estimates for the well infiltration rate capacity, an infiltration test with a flow of 125.20 m^3/h and 40 m^3 of water was performed on the well (during approximately 19 minutes). The injection of water has produced a maximum water rise of 6.38 m though stabilization of the water level has not been achieved. Table 3.2 summarizes the estimated infiltration rate for the recovery period of the injection test.

Table 3.2 – Results of the recovery period from the injection test. Water displacement and infiltration rate

Time (hours)	**1**	**2**	**3**	**4**	**5**	**6**	**7**
Δh (m)	3.28	0.88	0.51	0.36	0.26	0.18	0.14
Infiltration rate (m/d)	78.82	21.17	12.22	8.52	6.26	4.3	3.26

As can be seen from Figure 3.13, results indicate an expected relation between the infiltration rate and the hydraulic load in the well (i.e. water level in the well).

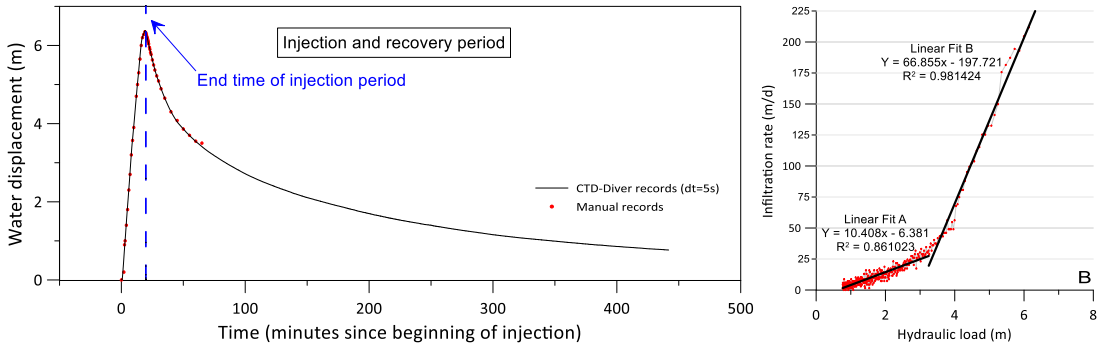

Figure 3.13 – LEFT: Records for water displacement in the well as a function of time. RIGHT: Scatter plot between hydraulic load and infiltration rate and its linear fits

Two different phases can be evidenced from Figure 3.13-Right in the relation between the infiltration rate and the hydraulic load. The first one is set by lower hydraulic load (up to around 3.25 m), in which infiltration rate can reach up to 25 m/d. The second phase, for higher hydraulic loads (above 3.25 m) originates infiltration rates higher than 25 m/d, reaching, in this test, a maximum of 211 m/d, at 6.35 m. The two linear fits identified could possibly be associated with the existence of a double porosity system, to the wellbore storage, or to existing infiltrating conditions inside the well above 3.25 m displacement elevation.

The numerical modelling efforts results show that the simulated hydraulic response of the aquifer with the regional model underestimate the observed behavior monitored at the scale of the well. This happens mainly due to the characteristics of well among other factors, like the element size of the mesh around the well.

As can be seen on Figure 3.14, by refining the mesh node density, and thus, decreasing the element size, the calculated hydraulic head error decreases. Yet, a rather dense mesh than the ones presented here would be necessary to effectively reach a calculated hydraulic head similar to the observed during the injection test.

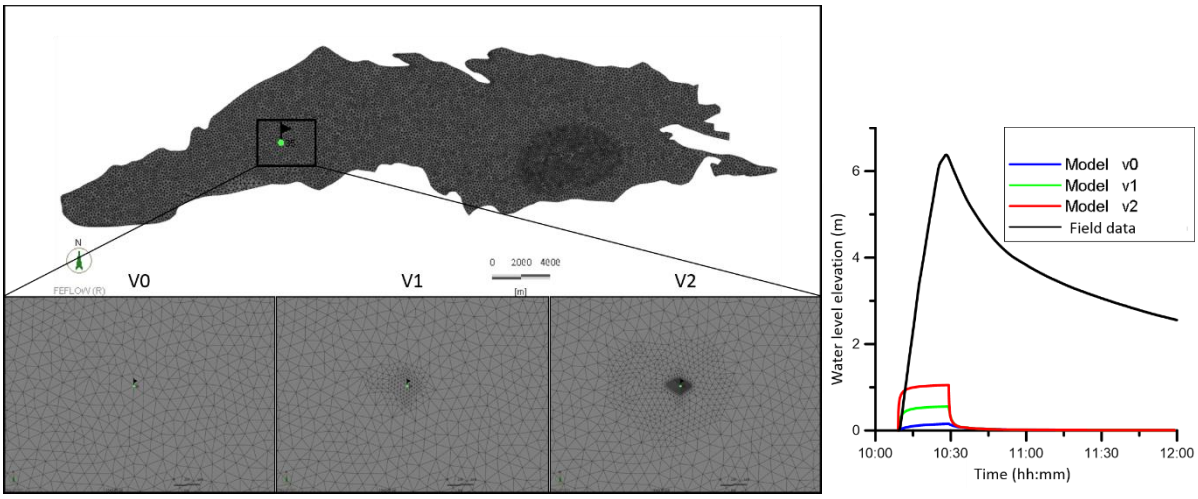

Figure 3.14 – Effect of mesh density on simulated hydraulic head during injection test

In this case, the use of analytical solutions of well hydraulics consists of a more suitable approach in order to determine the hydraulic properties controlling the flow in the well, as well as for representing the observed hydraulic heads in the well. Costa et al. (2015) presents an analysis on an injection test performed at Cerro do Bardo under MARSOL project, in which an analytical model was used in order to represent the hydraulic head behavior in the well, as well as to determine the hydraulic properties at the well local scale.

Detailed insight and methodologies on analytical solution methods for different configuration pumping tests can be found in bibliography. Injection tests are considered conceptually identical to pumping tests, except that flow is into the well rather than out of it (Horne 1990; Kruseman and de Ridder 1990). Notwithstanding, there is generally a tendency to increase hydraulic conductivity when extracting and to decrease hydraulic conductivity during injection. Extraction removes fines whereas injection may create clogging.

In order to better understand the factors controlling the infiltration of water in the well into the aquifer and estimate aquifer parameters (transmissivity and storage) and well parameters (storage and skin factor), an aquifer parameter analysis was performed with the support of the aquifer test analysis software MLU version 2.25.63 (Hemker and Post 2014), which consists of an analytical groundwater modelling tool to compute drawdowns, analyze well flow and aquifer test data based on a single analytical solution technique for well flow. Due to the high level of

uncertainty regarding both the aquifer and the well configuration, a sensitivity analysis was performed, considering several possible aquifer and well configurations.

From the sensitivity analysis, transmissivity values were found ranging from 14.99 to 36.64 m^2/day and storage coefficient from $7.09x10^{-02}$ to $6.38x10^{-1}$. The configuration that better appears to represent the reality is the one which considers the well is installed on an upper unconfined aquifer (thickness 10.75 m) separated by the regional aquifer by an implicit aquitard. For this configuration, transmissivity for the top layer is estimated as 14.99 m^2/d. Figure 3.15 shows the correlation between the observed and calculated drawdown data of the injection test for this configuration.

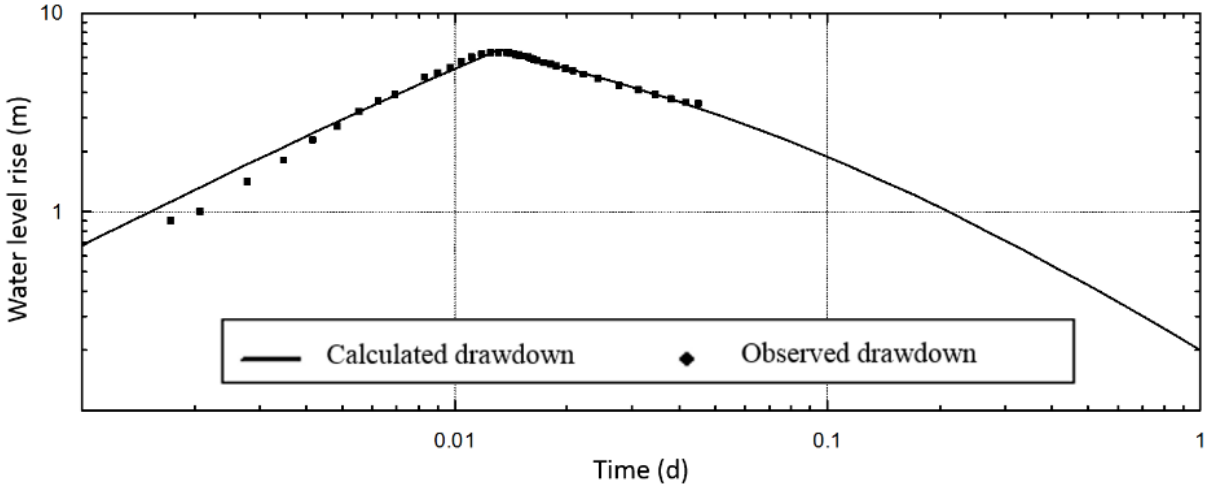

Figure 3.15 – Comparison of observed and calculated data based on optimized values of aquifer parameters

There lies a high degree of uncertainty regarding the Cerro do Bardo well characteristics, the local aquifer geometry, and the connection between the well and the aquifer. On one hand, the information supplied by the local inhabitants suggests that flow in the area is from West to East, opposing to the regional flow. Also, it appears there is a confining or lower permeability layer at around 30 to 40 meters depth, which coincides with the Cerro do Bardo wells depth. This probably means the well is not in direct contact with the regional aquifer or any of its karst conduits. On the other hand, parameter estimation during the injection test at the well returned transmissivity values much lower than the average transmissivity values determined by previous pumping tests in the surrounding (and much deeper) wells. This fact also indicates

that Cerro do Bardo well isn't directly linked with the regional aquifer, which would increase the residence time of any injected water at this site.

With the support of MLU software several possible aquifer and well configurations were simulated, achieving transmissivity values ranging from 14.99 to 36.64 m^2/d. The results obtained from the analytical models for interpreting pumping tests suggest Cerro do Bardo well is locally separated from the regional aquifer by an implicit local aquitard or a confining layer. Nonetheless, the non-uniqueness of the factors contributing for the observed hydraulic responses, as well as geophysics experimental results gathered by LNEC at the test site, raises doubts related to the non-connectivity in localized areas. In these areas the regional aquifer and the top aquifer would be in direct contact. If this is the case, then the MAR into the well would be directly incorporated in the regional aquifer, for later use down-gradient.

3.3 Conclusion

During the development of the current work, the Querença-Silves limestone karstic aquifer system was a subject of study in order to perform an initial analysis to the potential benefit of Managed Aquifer Recharge, in order to increase groundwater storage when there is water availability for later use. Additionally, there is a risk of seawater intrusion occurrence through connection of the aquifer with the Arade river, near the main discharge area of the system, in the Westernmost sector of the aquifer, which could possibly be averted, or diminished using MAR. In order to proceed to this analysis, a three-dimensional numerical groundwater flow model was used, with the simulation of different abstraction and MAR scenarios. This model is a result of several years of development, starting in early 2000's, with the work Monteiro et al. (2003) and Vieira and Monteiro (2003). In the current work, the model was converted to a three-dimension model and groundwater level time-series were validated.

Regarding the analysis of the simulated scenarios, results suggest that the conjugated effects of increased abstraction and reduction of natural recharge may increase the risk of seawater intrusion through the westernmost discharge area of the aquifer, where the Fontes de

Estômbar are located. This is a concerning situation, since not only is this area served by a large number of abstractions for intensive and extensive irrigation (mainly citrus trees, and a recent growth of avocado area) but also due to the location wells used by the in Águas do Algarve Lda. (the company responsible for the water supply in Algarve) used for urban water supply.

The inclusion of MAR hypothesis, shows that this could be a viable solution to consider in order to increase groundwater levels and to a point diminishing the risk of seawater intrusion in the Fontes de Estômbar area. Considering the BAU scenario of abstraction and irrigation, results show that the inclusion of at least 3 hm^3/year in the Cerro do Barro injection site could result in an increase of circa 0.6 – 0.7 m upstream of the injection point, which gradually decreases towards west, until the discharge area at Fontes de Estômbar.

The theoretical affected area by seawater intrusion was also compared with and without MAR, By applying the Ghyben-Herzberg relation. Model results that in current conditions, an area od 22.43 km^3 are potentially affected by seawater intrusion, mostly occurring in depth. The inclusion of a MAR scenario as presented in this work, would contribute to reduce the affected area to 20.24 km^3.

Chapter 4: Potential use of rainwater harvesting for managed aquifer recharge to improve chemical groundwater status in central Algarve and the impact of land-use scenarios.

The current chapter describes the analysis of different land-use scenarios and its effect on the chemical status of groundwater in in a set of aquifers draining to the Ria Formosa coastal lagoon, in South Portugal followed by an assessment of a Managed Aquifer Recharge (MAR) scheme based on rainwater harvesting in order to comply with the European Union (EU) Water Framework Directive (WFD).

To do so, a groundwater flow and mass-transport numerical model has been developed and the scenarios have been simulated. The main driver for the study consists of the analysis of the evolution of nitrate contamination at the Nitrate Vulnerable Zone (NVZ) of Faro and its compliance within EU WFD and the Nitrate Directive (ND). Previous studies have shown agriculture to be the main source of the nitrate in the NVZ Faro, and many efforts have been implemented by the regional agriculture authority over the years, in order to decrease the nitrate load into the aquifers. Nonetheless, the expected impact of the current land-use scenarios on the distribution of the nitrate contaminant plume, as well as mitigation measures have not been properly assessed until the developments presented in the current thesis.

The land-use analysis part of this task was performed in collaboration with the Portuguese environment agency, Agência Portuguesa do Ambiente (APA) and the Faculdade de Ciências – Universidade de Lisboa and is based on the project “Metodologia para avaliação da evolução da qualidade das massas de água subterrâneas nas zonas vulneráveis aos nitratos de origem agrícola no âmbito da diretiva nitratos e diretiva quadro da água” (Carvalho et al. 2017), of which the author of this thesis was a co-author, whereas the MAR scheme assessment is based on the peer-reviewed paper Costa et al. (2020).

- Carvalho MR, Zeferino J, Silva C, et al (2017) Metodologia para avaliação da evolução da qualidade das massas de água subterrâneas nas zonas vulneráveis aos nitratos de origem agrícola no âmbito da diretiva nitratos e diretiva quadro da água. Lisboa

- Costa LRD da, Monteiro JPPG, Hugman RT (2020) Assessing the use of harvested greenhouse runoff for managed aquifer recharge to improve groundwater status in South Portugal. Environ Earth Sci 79:1–15. https://doi.org/10.1007/s12665-020-09003-5

4.1 Introduction

The evolution of groundwater exploitation, agriculture, and soil use in south Portugal during the last 5 decades has led to several groundwater management problems, namely depression of groundwater levels, which can lead to seawater intrusion and groundwater contamination problems mainly related to the excessive use of fertilizers. Besides the identified groundwater management problems, the low infiltration rates in some of these aquifers lead to severe drainage problems during high-intensity rainfall events that affect land use in the flatter topography in the region.

Aquifer contamination by fertilizers has been of concern for aquifers in South Portugal since the 1980s (Almeida 1985; Silva 1988). This is particularly the case for the Campina de Faro aquifer system (M12), which is mostly associated to extensive agriculture practices in the past. Arguably one of the main sources of nitrogen in groundwater, nitrogen fertilizers used in agriculture represent the largest diffuse pollution threat to groundwater quality not only for the M12 (Stigter et al. 2013) but also at a global scale (Rivett et al. 2008; Wick et al. 2012; Zhou et al. 2015).

The NVZ Faro was established in 1997 to manage water quality in the M12 and in surrounding groundwater bodies, where current nitrate concentrations can reach values as high as 300 mg/l (Figure 4.1). According to the EU Nitrates Directive and the EU Water Framework Directive (WFD), measures should be implemented in order to improve groundwater chemical status of every groundwater body by 2027, which, in the case of nitrates in groundwater, corresponds to a 50 mg/L threshold.

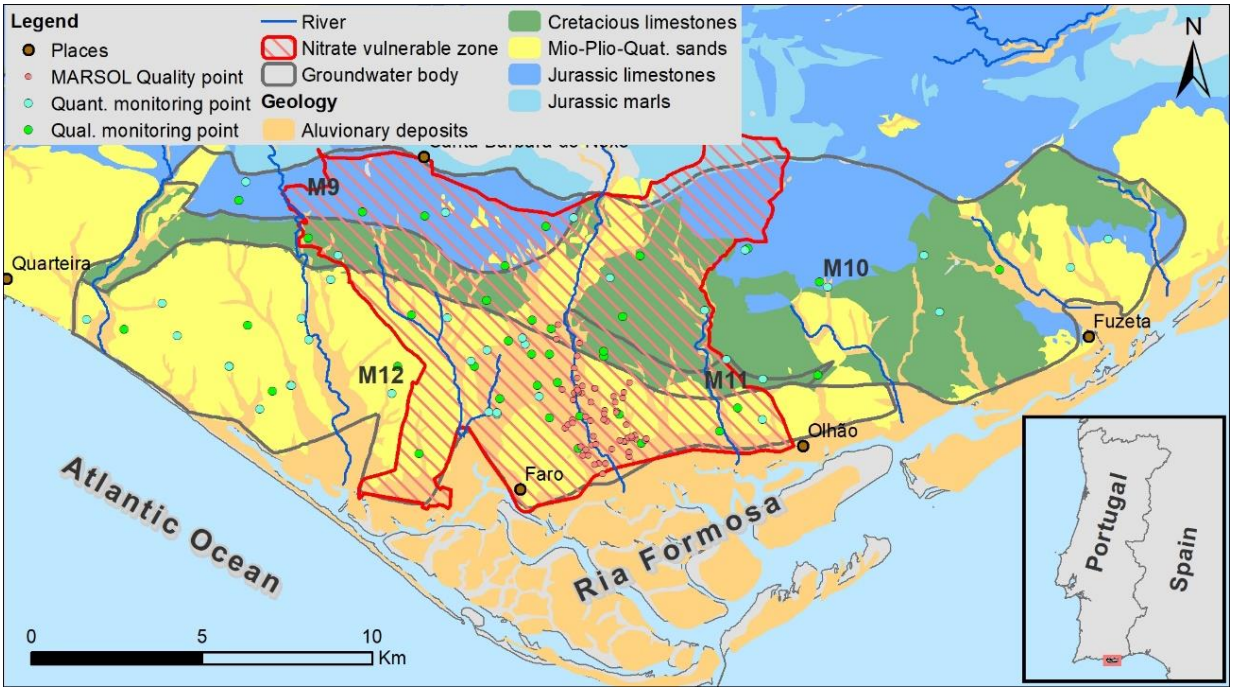

Figure 4.1 - Study area, main groundwater bodies, simplified geology, nitrate vulnerable zone, monitoring network (quality and quantity)

Managed aquifer recharge (MAR) techniques, which include artificial aquifer recharge solutions, could contribute to achieve the good status of groundwater by augmenting infiltration in the aquifer and thus contribute to either the dilution or the flushing of nitrates from the aquifer. MAR consists of manmade intentional enhancement of aquifer recharge with support of engineered systems (or nature based solutions) through which various techniques can be used to provide water infiltration into aquifers (Gale et al. 2002; Bouwer 2002; Gale 2005; Dillon 2005; Dillon et al. 2009). MAR has been proven to achieve success in many application worldwide in tackling water management problems (Stefan and Ansems 2018; Dillon et al. 2019), and should be considered as one of many water management tools to achieve sustainable water resources management (Gale et al. 2002).

Water for MAR can be derived from many sources, including rainwater, stormwater, river flow water, desalinated water, treated wastewater or even groundwater from another aquifer. With the appropriate treatment water from an MAR scheme can be used for irrigation, industrial use, as a source of drinking water, to prevent seawater intrusion and to sustain ecosystems (Bouwer

2002; Dillon et al. 2009). Amongst these water sources, rainwater harvesting for MAR has an important role for water management due to the low-cost of its implementation, and there are many examples of this being carried out all over the world (Abdulla and Al-Shareef 2009; Jones and Hunt 2010; Domènech and Saurí 2011; Beckers et al. 2013; Hashemi et al. 2014; Ashraful and Islam 2015).

Some additional advantages of collecting and storing rainwater in urban or rural areas are the increase of water supply availability, increase of groundwater levels and the reduction of storm-water floods (Gale et al. 2002; Kim and Lee 2013; Kim et al. 2013).

In the current chapter of the thesis, different land-use scenarios and their impact on the nitrate plume contaminant within the NVZ of Faro are analyzed, in order to quantify the necessary mitigation time to achieve compliance according the WFD. Additionally, the current chapter also describes an assessment of the potential application of a MAR scheme as a tool to improve groundwater quality, specifically regarding nitrate contamination in groundwater at NVZ Faro, south Portugal. The availability of source water for the MAR scheme at this location was estimated from the amount of rainfall that was intercepted by greenhouses with the support of satellite imagery and GIS tools. The recharge infrastructure for the scheme consists of old dug wells, whose infiltration capacity was estimated through injection tests on the field. A numerical model was used to assess the impact of such a scheme on groundwater nitrate concentration at NVZ Faro. The presented MAR scheme has the advantage of being a low-cost solution, since the infrastructure for collecting water, as well as the injection infrastructure are already available and thus, there is no need for significant construction works.

4.2 Study area

The study area is the NVZ Faro in Algarve, the southernmost province of Portugal as indicated in Figure 4.3. This area is underlain by a set of aquifer systems which are in hydraulic connection and discharge to the Ria Formosa coastal lagoon (Leote et al. 2008; Hugman 2017; Hugman et al. 2017b; Malta et al. 2017). The NVZ Faro covers an area of 97.73 km^2 and is underlain by the

Almansil - Medronhal (M9), São João da Venda – Quelfes (M10), Chão de Cevada – Quinta João de Ourém (M11) and Campina de Faro (M12) groundwater bodies.

South Portugal is characterized by a Mediterranean climate (Csb Köppen classification in the western Littoral region and Csa in the remaining area), with dry summers and wet winters. Monthly average temperatures range from 12 to 24 ºC with a mean annual temperature of 17.3 ºC (Silva 1988). The mean annual precipitation of the region is 531 mm, varying from about 500 to 1000 mm (Loureiro and Coutinho 1995).

4.2.1 Geological and hydrogeological setting

The study area is located in the Algarve basin, which contains sediments of Mesozoic to Cenozoic age and which overlies schists and greywackes of Carboniferous age (Almeida et al. 2000) that comprises the basement in the area. Sediments in this basin contain a number of aquifers which are highly heterogeneous in nature. The northernmost aquifer systems (M9, M10 and M11) are located in an area with a relatively rugged topography composed by Jurassic limestones which are overlain by Cretaceous limestones. The Cretaceous formations dip to the south (at about 20º to 30º) and subcrop at depths below 200 m near the city of Faro (Stigter 2005) where they are overlain by Miocene and Plio-Quaternary sandy limestones and detritic formations in an area with a more moderate topographic relief (Figure 4.1 and Figure 4.2). A brief description of the hydrogeology and geology of these aquifers is provided below based on more detailed descriptions presented by several authors (Almeida 1985; Silva 1988; Manuppella et al. 1993; Terrinha 1998; Almeida et al. 2000; Stigter 2005; Hugman 2017).

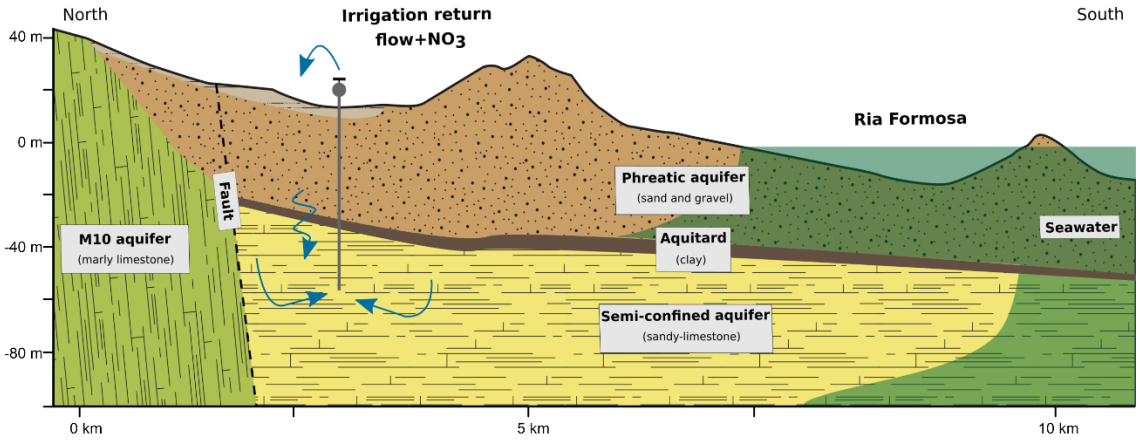

Figure 4.2 - North-South hydrogeological profile of Campina de Faro (adapted from Hugman (2017))

In general, the M9 aquifer is a semi-confined karstic system formed by Jurassic limestones and dolomites. Groundwater flows in a southerly direction in this aquifer, towards the M10 aquifer, which consists of a multi-layered system. The M10 aquifer consists of Jurassic limestones with a thickness of about 300 m in the northeastern part of the study area, and of Cretaceous limestones in most of its meridional region followed by a sequence of marls and limestones and detritic Miocene deposits with an average thickness of 75 m. The main groundwater flow direction in M11 is towards the south and southeast. Aquifer M11 is comprised of dolomites and limestones of Cretaceous age with an estimated thickness of 200 m that forms a highly productive semi-confined system. Groundwater level data is limited for the aquifer, but the surrounding systems and the topography profile suggest main flow-direction should be in a southerly direction.

Aquifer M12 is a complex coastal multi-layered system located on a flattened platform surface. The upper part of the system is a phreatic aquifer that mainly consists of sands of Plio-Quaternary that have a thickness varying from 8 m to 60 m (Stigter 2005). The lower semi-confined aquifer is formed by Miocene fossil-rich sandy-limestones deposited in an westwards-deepening graben-like structure, with few surface outcrops in the study area. This formation has a typical thickness of circa 50 m but may reach a thickness of up to 200 m near the coast (Silva 1988; Stigter 2005).

Since this formation is mostly confined, most of its recharge is derived from seepage from stream that are connected with fault systems, or from leakage from upstream Cretaceous and Jurassic limestones through a system of faults. The phreatic and semi-confined aquifers are separated by an extensive confining layer of sand, silt and clay, that has a variable thickness (Silva et al., 1986 in Diamantino, 2009). Nevertheless, one cannot exclude the possibility of hydraulic connection in sectors where the confining layer is absent or in situations it has been artificially established after the drilling of new boreholes within existing wells (Almeida et al. 2000). A generalized cross-section of the stratigraphy regarding aquifer M12 is presented in Figure 4.2.

The general direction of groundwater flow in the M12 aquifer is in a southerly direction, and this is increased by preferential flow paths formed by N-S trending faults (Stigter 2005). Groundwater discharge from this aquifer takes place in the Ria Formosa coastal lagoon and offshore.

4.2.2 Water and land use

Citrus orchards, greenhouse crops and open-air horticulture are the dominant agricultural activities in the area and have been responsible for high inputs of nitrates fertilizers from fertilizer use. It is likely that historically, nitrate inputs to groundwater were much higher than what currently takes place (Quelhas dos Santos 1991; Stigter et al. 2011, 2013). In addition, the recirculation of nitrates in groundwater caused by return flows from irrigation with contaminated groundwater along with the leakage from septic tanks are considered significant sources of nitrogen, especially for the M12 aquifer (Stigter et al. 2006c; CCDR-Alg 2007; Diamantino 2009; Stigter et al. 2013).

In general, agriculture in the study area relies on private irrigation wells, which in the case of M12, abstract groundwater from both the upper and lower aquifer. Although most of the public water supply is currently from surface water resources, until the 1990's, most of public supply was supplied from groundwater wells. In fact, most of these wells were drilled between the 1960's and 1990's, during which period groundwater was the main source of water in the

region. This lead to overexploitation of the M12 aquifer (Monteiro 2006). After the late 1990's public supply changed from groundwater to surface water reservoirs, although in the M12 area, irrigation for agriculture and golf courses is still mostly supplied by groundwater abstractions (Monteiro 2006; Monteiro et al. 2006a).

4.2.3 Nitrate contamination

Nitrate concentrations in M12 became a major concern in the 1980's, with the observation of values from 300-400 mg/l, leading to the establishment of the Nitrate Vulnerable Zone (NVZ) in 1997 which was subsequently expanded in 2003 to the current extent shown in Figure 4.3(Stigter et al. 2011, 2013). The Nitrate Directive and WFD resulted in the implementation of measures by the regulatory agency, such as encouraging good agriculture practices to achieve 'good' chemical status.

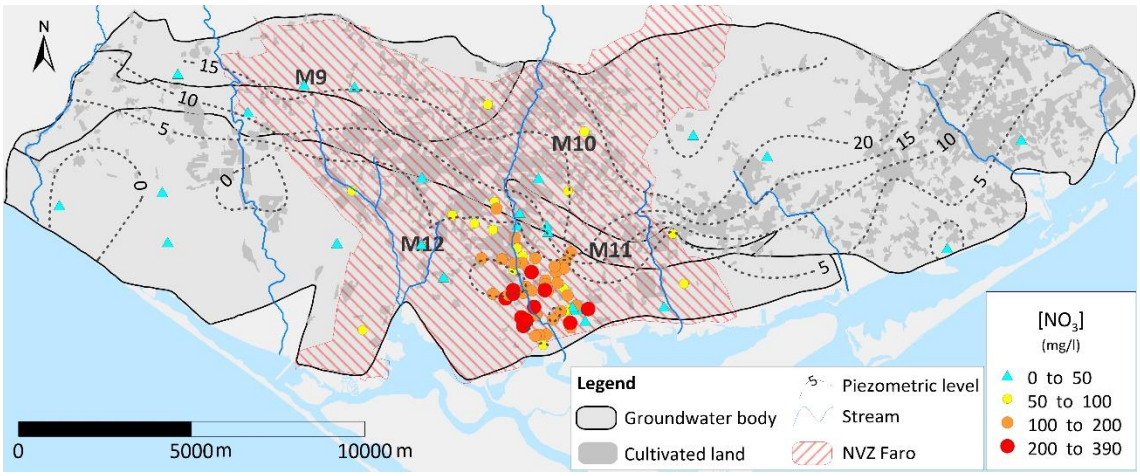

Figure 4.3 - Observed nitrate concentrations and piezometric levels from May 2016 according to observation points from the Environmental Protection Agency and the MARSOL Project sampling campaigns

Nonetheless, groundwater quality has not improved significantly since the implementation of these measures, most likely due to the low hydraulic gradient in the M12 aquifer and the recycling of nitrates through irrigation (Stigter 2005). In fact, monitoring of nitrates in the NVZ provide evidence that well-defined nitrate contaminant plumes are slowly heading towards the

Ria Formosa coastal lagoon, with evidence of decreasing concentrations of nitrates in the northernmost region and increasing concentrations in the southern part of the region (Stigter 2005; Diamantino 2009; Stigter et al. 2011, 2013; Leitão et al. 2015).

During the FP7 MARSOL project (FP7/2007-2013 GA619120) groundwater sampling campaigns around the city of Faro were performed in order to assess the evolution of the nitrate contamination between 2014 and 2016. The results of these campaigns, together with data from the official monitoring network of the regulatory water agency (Agência Portuguesa do Ambiente - APA), have shown that there has been no significant improvement of the nitrate contamination plume. The spatial distribution of nitrates for 2016 (from the MARSOL campaign and the APA sampling) in the study area is shown in Figure 4.3. Also shown are the piezometric levels, which were obtained from the kriging interpolation of data from the official monitoring sampling points indicated in Figure 4.1.

The observed nitrate concentrations for the year 2016 at the 91 groundwater quality monitoring points (from APA official network and MARSOL project) are presented in Figure 4.3. Of these monitoring points, 65 show exceedances according to the nitrate directive, (i.e., they have nitrate concentration higher than 50 mg/l). Of the 37 monitoring points of the official water quality network, there were 17 nitrate exceedances, mostly in the M12 aquifer.

4.3 Methodology

The highest nitrate concentrations in groundwater in the study area occur within the M12 aquifer, and therefore the study is focused on this aquifer system. Consequently, the assessment of the viability of an MAR scheme and the identification of injection points were carried out within the M12 aquifer limits.

The potential source water for this scheme is derived from rainwater that is intercepted by greenhouses in the study area, with injection points consisting of the existing traditional dug wells. In order to assess the effect of such a MAR scheme at the study area, the work has developed in three stages: (1) estimate the volume of the available source water for the MAR

scheme; (2) identify potential infiltration sites and infrastructure and their infiltration capacity; and (3) simulation of scenarios with support of a groundwater flow and mass transport numerical model.

4.3.1 Estimating source water availability - rainwater harvesting potential

The first stage of the project was to estimate the total volume of rainwater that could be harvested from greenhouse rooftops in the study area and injected into the M12 aquifer. The applied methodology consisted of three main tasks:

1 - Estimate the average annual and monthly rainfall and its distribution over the M12 aquifer;

2 - Determine the location and the total greenhouse surface area over the M12 aquifer;

3 - Intersect the rainwater distribution calculated in 1) with the area calculated in 2) in order to estimate the potential water availability.

Estimated of the temporal and spatial rainfall distribution in the study area were obtained from a 31 year average (1959/60- 1990/91) rainfall distribution model for Portugal developed by Nicolau (2002), which provided average annual and average monthly multiannual rainfall. This model was developed using an orthogonal grid with a resolution of 1 km×1 km matrix and was calculated using kriging with elevation as external drift.

Estimates of greenhouse surface area and their locations were obtained from a land use survey based on aerial photographs from 2007 and 2008 developed by the Portuguese Environment Agency - *Agência Portuguesa do Ambiente* - (APA-ARH Algarve I.P., unpublished).

Finally, with the support of GIS tools, rainfall distribution values were intercepted with the distribution of greenhouses and their surface area, thus calculating the potential rainwater that could be harvested at each greenhouse location. These calculations were made assuming a runoff coefficient of 1. Therefore, it was assumed that all rainfall intercepted by the greenhouses is collected and diverted to the infiltration infrastructure.

4.3.2 Infiltration infrastructure

The second stage of the project consisted of assessing the infiltration capacity of the system. It was assumed that infiltration would take place through large traditional dug wells in the study area. These large dug wells are very common in the rural area around Faro and are still widely used for irrigation. Usually not deeper than 20 – 30 meters, these structures intersect the phreatic aquifer. To assess the infiltration capacity of the system, an injection test was performed in a traditional well that was 19 m deep and had a diameter of 4.5 m. The test consisted of a three-step injection test, during which the inflow rate was increased at each step from 6.5 m^3/h to 16m^3/h and finally to 35 m^3/h over a total period of 14.5 hours. The Injected water was pumped from a well located 15 m east of the injection well, which intersects the Miocene confined aquifer. Previous tests performed during the MARSOL project revealed there is no hydraulic connection between the two aquifers locally (Costa et al. 2015b; Leitão et al. 2015). During the injection test, water level, electrical conductivity and temperature variations in the test well were recorded with an automatic CTD diver at 1-minute intervals. These measurements were also undertaken manually during the test.

Finally, a set of large traditional wells were identified not only from field work, but also from the APA inventory of wells. With the support of GIS tools, wells located within a 150 m buffer from the greenhouses were selected as infiltration infrastructure for each of the greenhouses. This buffer was selected to limit the potential capital costs associated with the connection pipework.

4.3.3 Numerical model – reference model

The numerical model used to simulate the nitrate mass transport was adapted from previous studies (Hugman 2017; Hugman et al. 2017b) using the finite element code FEFLOW (Diersch 2014). For the current work, a calibrated three-dimensional version of the prior model was adapted (Hugman et al. 2017b), which was built according to the main geostratigraphic units in the study area. The boundary conditions (BC) and point sources of nitrate in the model were

adapted in order to assess the evolution of nitrate contamination with and without the injection of harvested rainwater.

The model consists of three layers, with 715,107 triangular prism elements and 483,688 nodes equally distributed across the four slices, with particular refinement of the mesh within the limits of the NVZ (Figure 4.4A). The surface layer of the model consists of surface elevation data which was obtained from digital elevation model of the study area. The remaining slices were distributed equally to obtain a model thickness of 100 m. The exception to this was the M12 aquifer, which was simulated as a multi-layered system with a phreatic and a confined aquifer separated by an aquitard.

The stratigraphy of these features, model recharge, the BC, the point sources imposed in the model and the latter calibration of hydraulic parameters that used information from prior studies (Hugman 2017) are fully described in (Hugman et al. 2017b).

Recharge was defined according to the distribution of rainfall defined by Nicolau (2002) and the outcropping recharge rates from infiltration defined by Almeida et al. (2000) (Figure 4.4B). A constant head BC with an elevation of 0 meters above sea level was imposed along the coast to simulate groundwater discharge to the Ria Formosa coastal lagoon. Temporary streams were assigned a constant head BC equal to surface elevation, but these were constrained to only allow flow out of the model and not in. BC for wells were assigned to nodes corresponding to golf courses irrigated with groundwater and within cultivated irrigated areas, with abstraction rates calculated according to the water demand and irrigation efficiency for each specific plot of agricultural land. Both the additional recharge and nitrate input from Irrigation return flow were not included in the current simulations.

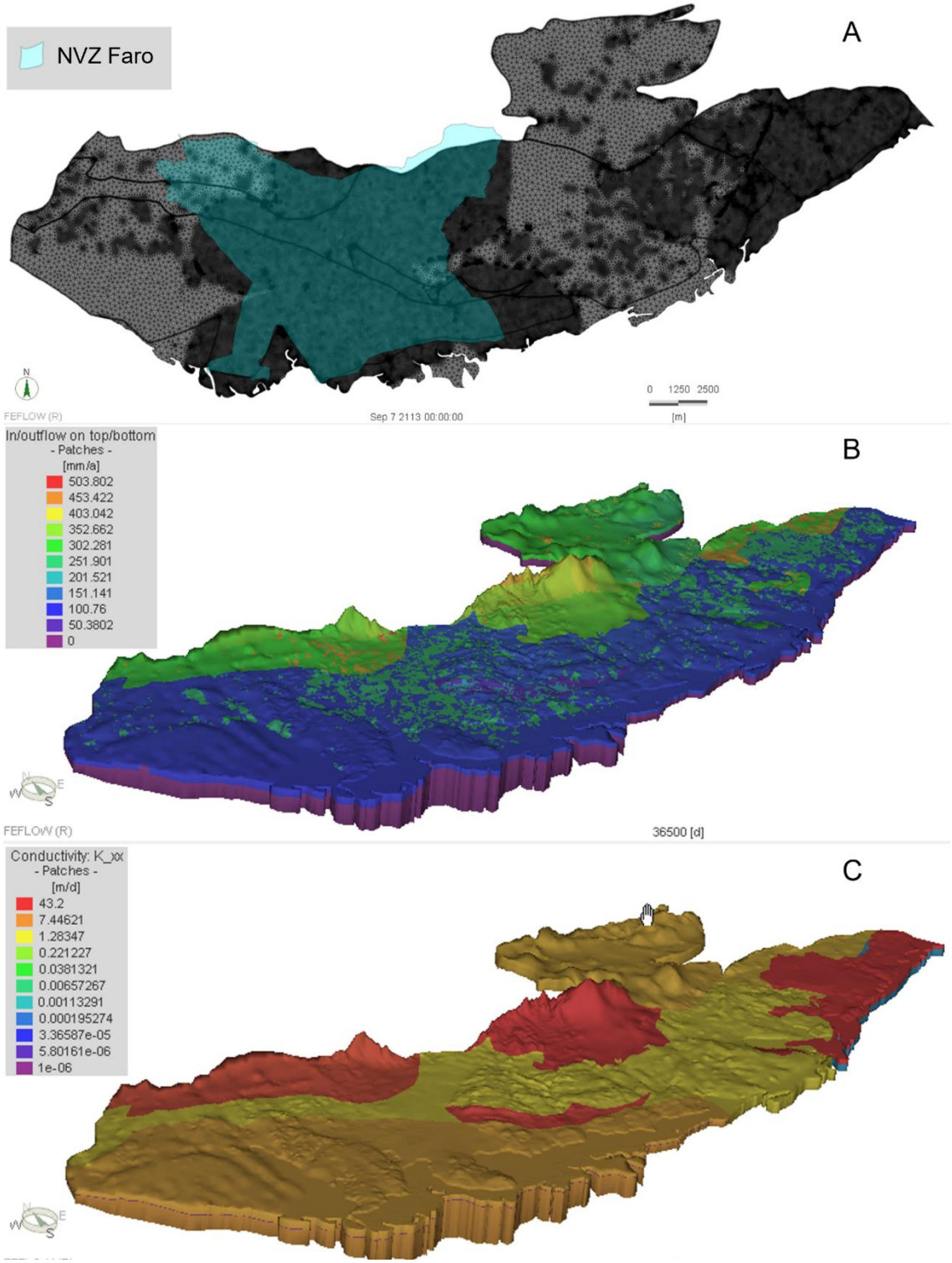

Figure 4.4 - A: Finite element mesh generated for the numerical flow and mass transport (Nitrate) model for the NVZ Faro; B: 3D view of the generated geometry of the mesh(vertical exaggeration of 5x) and the recharge input in the model; C: Hydraulic conductivity distributed in the model

Nitrate inputs to the model were defined according to estimates by (Carvalho et al. 2017), and were distributed according to the distribution of cultivated land-use identified in the Portuguese 2010 Land-use survey (Carta de Ocupação de Solos 2010). This value was estimated based on nitrate reference values defined by the River Basin Management Plan (APA 2016) and imposed within the NVZ limits at the top slice of the model as a point-source mass-transport BC. About 81.24 km^2 (83%) of the study area issued for agriculture or is occupied by forests that may result in nitrogen inputs into the system. An important part of the cultivated land (36%) comprises almond and citrus orchards, which are the main contributor to the nitrogen inputs to groundwater. Diffuse nitrate input within the NVZ Faro for the different groundwater bodies and sectors are shown in Table 4.1.

Table 4.1 – Diffuse nitrogen input according to sector and groundwater body within the NVZ Faro. Others category includes the urban, industrial, tourism and golf activities (adapted from Rosário Carvalho, et al. (2017))

Groundwater body	**Sector**	**N Total Kg/year**
Almansil-Medronhal (M9)	Agriculture	5483
	Livestock	508
	Others	48
São joão da Venda – Quelfes (M10)	Agriculture	26700
	Livestock	1859
	Others	508
Chão de cevada – Quinta João de Ourém (M11)	Agriculture	1291
	Livestock	93
	Others	0
Campina de Faro (M12)	Agriculture	9725
	Livestock	1096
	Others	1130

The definition of hydraulic and transport parameters, zonation and calibration of the model is described in Hugman et al. (2017). Uniform hydraulic property zones were considered for all

systems, except for the M10, M12 and Luz-Tavira (M15) aquifers. The latter aquifer is located outside of the boundaries of the NVZ. The M10 and M15 aquifers were divided in zones according to subcropping geology (Jurassic, Cretaceous and Miocene).

Aquifer M12 was divided into three vertical layers with different hydraulic properties representing the aquitard and the phreatic and semi-confined aquifer systems. The spatial distribution of hydraulic conductivity (K) values was estimated by inverse modelling for the period of 1999 using the Gauss-Marquardt-Levenberg method with the nonlinear parameter estimation software PEST (Doherty 2002). The determined K values for the model (Figure 4.4C) are:

- M9 Jurassic formation: 25.82 m/day
- M10 Jurassic formation: 42.16 m/day
- M10 Cretaceous formation: 1.77 m/day
- M11 Cretaceous formation: 35 m/day
- M12 Plio-Quaternary formation: 4.46 m/day
- M12 Miocene formation: 6.0 m/day

Zones of uniform effective porosity were assumed according to those of K and values were calibrated by trial and error and validated with simulations between 1995/96 and 2012/13. The correlation coefficient (R^2) and root mean square error (RMSE) between calculated and observed values of nitrate for this period are 0.84 and 417.5 respectively. In general, the coupled groundwater mass transport-flow model can represent changes in nitrate concentration between 19195/96 and 2012/13 with a relatively uniform distribution of error, except for the observed values at the monitoring point 611/260, which are much higher than the calculated values.

In this study, two scenarios were defined: the business as Usual (BAU) scenario, and the scenario with the injection of harvested rainwater into wells (INJ). Both scenarios were simulated for the period 2016 until 2040 and results were compared. During the period of simulation, recharge was considered to be constant and Nitrate inputs were assumed according

to the previously defined values. The simulations used automatic time-steps, where an appropriate length of the time step was determined based on the change in the primary variables (head and mass concentration) between the time steps.

4.3.4 Impact of Land-use scenarios on nitrate contamination

The analysis of Land-use scenarios consists of a task performed in cooperation with the Agência Portuguesa do Ambiente and the Faculdade de Ciências - Univesidade de Lisboa within the project "Metodologia para avaliação da evolução da qualidade das massas de água subterrâneas nas zonas vulneráveis aos nitratos de origem agrícola no âmbito da diretiva nitratos e diretiva quadro da água" (Carvalho et al. 2017). The aim of the project was to analyze the necessary time to achieve compliance with EU WFD regarding Nitrate contaminants, and how different land-use scenarios may affect such evolution of contamination. In order to do so, apart from the Business as Usual, 4 scenarios of nitrate input from agriculture and livestock pressures have been simulated, using the model configuration described in the previous chapter for the time period 2017-2040, namely:

- Scenario A: No input
- Scenario B: "Agriculture"
- Scenario C: "Agriculture+Livestock"
- Scenario D: "Agriculture 10 kg N/ha"
- Scenario D: "Agriculture 20 kg N/ha"

The simulated scenarios were compared with the reference situation, which consists of the contaminated area for the year 2016/2017 according to official data by the Agência Portuguesa do Ambiente. For this period, the interpolated nitrate data shows that 43.3% of the NVZ is above the quality standard, 50 mg/L.

The description of these simulated scenarios is depicted below.

Business as Usual

This consists of the current reference scenario in terms of nitrate pressure in the aquifer system, according to observed values from 2016-2017, which is described in chapter 4.3.3, and resumed in Table 4.1.

Scenario A: No input

This consists of a no qualitative pressure scenario, assuming there is no more nitrate input into the system. It is an unrealistic scenario intended to analyze how the contamination in the system would evolve in a "natural environment" and serves as a reference outcome to compare with the following scenario simulations, in order to assess the impact of livestock and agriculture activities in the system. In this scenario, results depend solely on the initial conditions (nitrate concentration and hydraulic heads) and the hydraulic/mass transport parameters of the model.

Scenario B: "Agriculture"

Scenarios B considers only the nitrate input originated from agriculture pressures assumed in the 2nd cycle of the River Basin Management Plan (RBMP) (APA 2016), which are set in Table 4.2.

Table 4.2 – Land use typology classes and corresponding nitrogen input and nitrate conversion, corresponding area for each land use typology and calculated nitrate load for the NVZ Faro.

COS2010 Land Use typology	COS2010 Land Use code	Nitrogen input kg N/ha/year	Nitrate input kg NO_3^-/ha/year	Area ha	Nitrate load kg NO_3/year
Agriculture area with temporary cultures	2.1	3.50	15.50	1211.98	18786
Agriculture area with permanent cultures	2.2	1.89	8.37	3567.04	29856
Permanent pastures	2.3	1.05	4.65	337.27	1568
Heterogeneous agricultore area	2.4	2.70	11.94	1478.69	17648
Forests	3.1, 3.2	1.40	6.20	1272.98	7892
				Total nitrate Load at NVZ Faro:	75751

Total nitrate load for this scenario is 75751 kg/year, of which, 39% corresponds to permanent agriculture cultures, 25% to temporary agriculture cultures, 23% to permanent to permanent pastures.

The nitrate input values from agriculture identified in the 2nd RBMP were distributed in the model according to the mapped agriculture area in the Portuguese land use map – Carta de Ocupação de Solos 2010 (COS 2010).

Scenario C "Agriculture and Livestock"

Scenario C consists of the agriculture input defined in scenario B plus the livestock pressures according the 2nd RBMP estimates (APA 2016).

Estimates for livestock pressures are defined according to city council limits (Faro, Olhão and Loulé), which do not coincide with the NVZ area. Therefore, the contribution from each city council was set as the proportion of the city council area which intercepts the NVZ, hence resulting in the NVZ livestock pressures shown on Table 4.3.

Table 4.3 – Nitrate loads from livestock in the NVZ Faro according to city council

City council	Area (ha)	NO_3 (kg/year)	Total livestock load (kg NO_3 / year)	Total livestock + agriculture load (kg NO_3 / year)
Faro	7164.90	1552	1938	77689
Loulé	1166.28	254		
Olhão	1041.81	132		

The current scenario results in a total nitrate input of 77689 kg/year, of which, 1938 kg/year correspond to the livestock pressure, i.e., about 2.5% of total nitrate input in the system. It is noted that the livestock activity is of low importance in the study-area, hence the low percentage of the total nitrate input.

Scenario D: "Agriculture 10 kg N/ha"

Scenario D is characterized by a uniform nitrate input of 10 kg Nitrogen/ha (44,29 kg NO_3/ha) in all areas identified as agriculture use in the study-area, according to the Portuguese land-use map, which is identified with the COS2010 code 2, and includes the following land use types:

- Agriculture area with temporary cultures
- Agriculture area with permanent cultures
- Permanent pastures
- Heterogeneous agriculture area

According to this criteria, the total agriculture area in NVZ Faro area is 6595 ha (65% of the total area). Assuming an input of 10 kg Nitrogen/ha (44,29 kg NO3/ha), the resulting nitrate load to the system is 292064 kg/year (Table 4.4).

Table 4.4 –Calculated nitrate load for scenario D, which considers an input of 10 kg Nitrogen/ha/year (44.29 kg NO_3/ha/year) in agriculture areas.

Land use type	NO_3 input (kg/ha/ano)	Input area (ha)	NO_3 load (kg/ano)
Agriculture	44.29	6595	292064

Scenario E: "Agriculture 20 kg N/ha"

Scenario D is similar to the previous scenario, although, the Nitrogen input is doubled to match 20 kg/ha/year. This corresponds to 88.57 kg NO_3/ha/year, which, considering the agriculture area, results in a total nitrate load of 584127 kg/year (Table X)

Table 4.5 –Calculated nitrate load for scenario E, which considers an input of 20 kg Nitrogen/ha/year (88.57 kg NO_3/ha/year) in agriculture areas.

Land use type	NO_3 input (kg/ha/ano)	Input area (ha)	NO_3 load (kg/ano)
Agriculture	88.57	6595	584127

4.4 Results

4.4.1 Estimating Source Water availability

Data compiled for the study area overlying the M12 aquifer indicates that it has an annual average of 570 mm with the spatial distribution shown in Figure 4.5. The location of the greenhouses and their surface area was obtained from the land use survey provided from APA-ARH Algarve I.P. Only the greenhouses that are totally within or intercept the M12 limits were considered in this study and their total surface area account for 2.74 km^2 with the spatial distribution as seen in Figure 4.5.

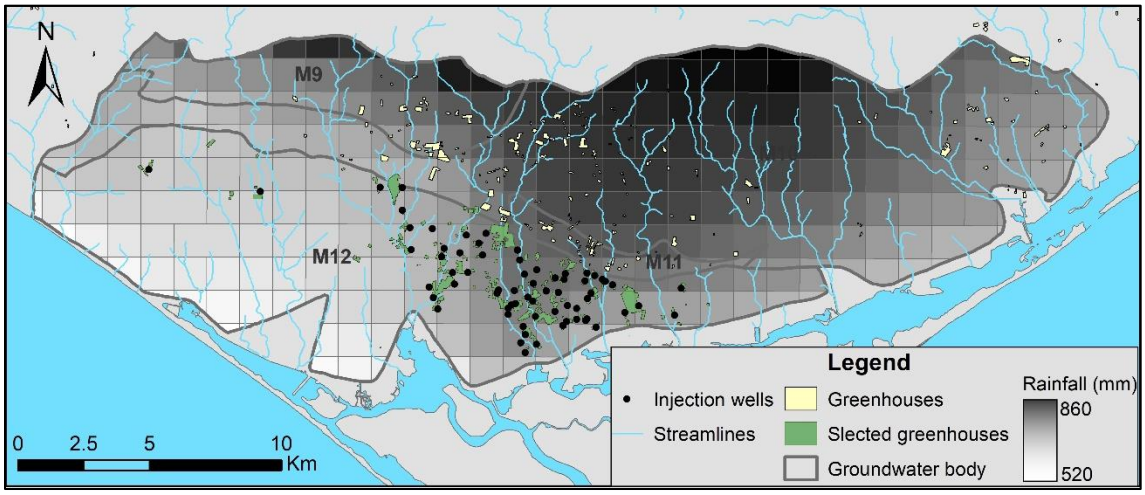

Figure 4.5 - Average annual rainfall spatial distribution on the study area (based on Nicolau (2002)) and greenhouse location (based on APA-ARH Algarve, unpublished) and selected injection wells

According to the rainfall model developed by Nicolau (2002), the rainfall distribution over the M12 aquifer in the stud area varies from 520 to 629 mm (and up to 860 mm on aquifer systems to the north), with lower values at the western coast and the highest average at the Center-Eastern inland sector of the aquifer. According to the multiannual monthly averages, the highest rainfall months in the M12 aquifer area are in January (87 mm), February (81 mm),

October (68 mm), November (91 mm) and December (101 mm) which, together account for 75% of the annual precipitation.

The amount of average annual rainfall that was intercepted by greenhouses overlying the M12 aquifer was calculated with the support of GIS tools and is estimated as to be 1.63 hm^3/yr, with the monthly distribution as presented in Figure 4.6.

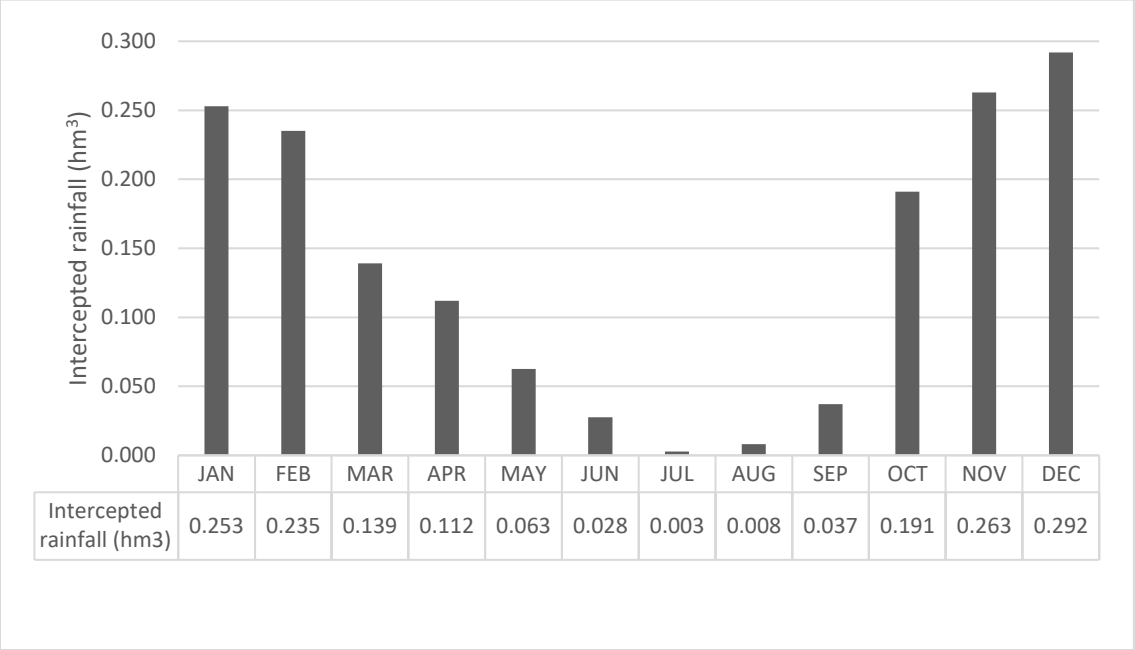

	JAN	FEB	MAR	APR	MAY	JUN	JUL	AUG	SEP	OCT	NOV	DEC
Intercepted rainfall (hm3)	0.253	0.235	0.139	0.112	0.063	0.028	0.003	0.008	0.037	0.191	0.263	0.292

Figure 4.6 - Estimated monthly volume of rainfall intercepted on greenhouses at M12 based on monthly pluri-annual average rainfall distribution periods

Most of the intercepted volume at greenhouses (75%) occurs between October and February, with a maximum of 0.292 hm^3 in December, corresponding to about 18% of the annual intercepted rainfall

4.4.2 Estimating the infiltration capacity of existing wells

4.4.2.1 Injection test

The infiltration capacity of large diameter dug wells was assessed with an injection test that was carried out in one well during this study. The depth to water level (i.e. static water level) at

the beginning of the test was 10.28 m and at the end of the test, the maximum water level registered was at 7.97 m. That is, for a flow of 35 m^3/h, there was a water rise of 2.31 m in the well. The water levels during the injection test in the large diameter well are presented in Figure 4.7.

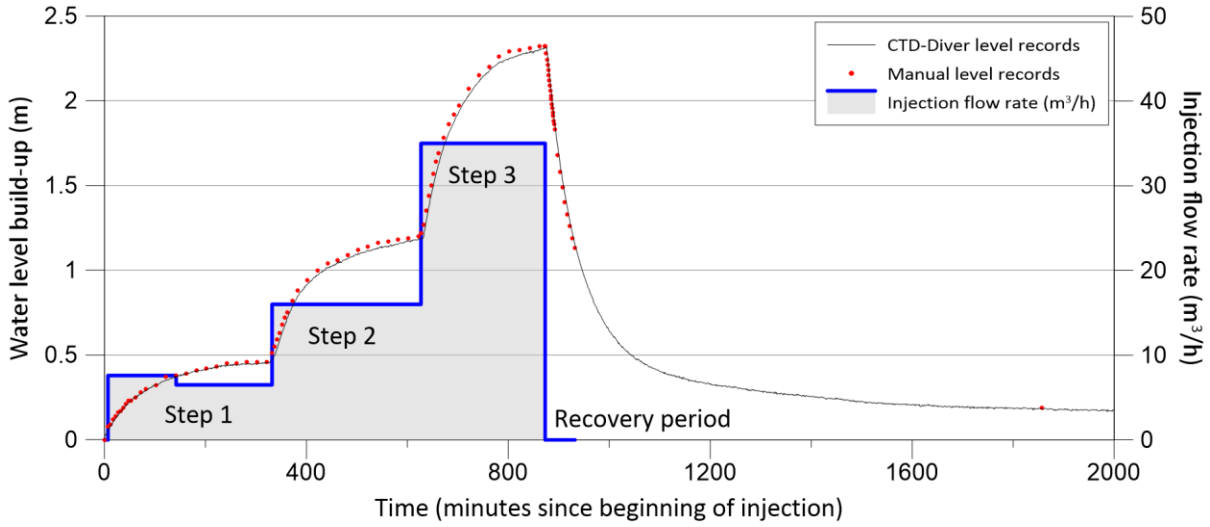

Figure 4.7 - Injection flow rate (right axis), Manual and CTD records (left axis) for water displacement in the well as a function of time, for all the injection stages and recovery period

The stepwise injection test was performed as a steady-state test, i.e. each injection step was carried out until a stable water level was achieved. During the period for which water level was stable, it can be assumed that the infiltration rate is the same as the injection rate. The injection test results are synthetized in Table 4.6 where Step Δh (m) stands for the observed water level rise with reference to the beginning of each step water level, and Total Δh (m) stands for the observed water level rise with reference to static water level before injection started. The injected volume was calculated at each step by multiplying the injection rate by the step duration.

Table 4.6 Injection test results

	Duration (min)	**Injected volume (m^3)**	**Injection rate (m^3/h)**	**Total Δh (m)**	**Step Δh (m)**	**Specific recharge capacity ($m^3/h/m$)**
Step 1	322	37.5	7.6 & 6.5	0.456	0.46	15.32
Step 2	299	79.7	16	1.183	0.73	13.52
Step 3	249	145.3	35	2.314	1.13	15.13

The injection flow rate for step 1 was originally 7.6 m^3/h, but at minute 142 of the injection step 1 there was a decrease in the flow rate to 6.5 m^3/h due to a pump fail. Hence, total injected volume for step 1 is equal to [(7.6 m^3/h × (141 min / 60 min/h)) + (6.5 m^3/h × (181 min / 60 min/h))] = 37.47 m^3.

Observed water level rise was 0.46 m, 0.73 m and 1.13 m for steps 1, 2 and 3 respectively, which corresponds to specific recharge capacities (i.e., the unit of water injection flow rate per unit of rise of water in the well) of 15.32, 13.52 and 15.13 $m^3/h/m$ respectively. Considering that specific recharge capacity does not show an apparent decrease during the test and depth to water level at the end of the test was at 8 m from the top of the well, the well's capacity for recharge is possibly much higher than the values tested. This hypothesis is supported by the data shown in the plot of the infiltration rate as a function of the hydraulic head in the well (i.e. the height of water column in the well) and the water level rise level shown in Figure 4.8. The plot on the left side of Figure 4.8 shows that the rate of change for the water level rise remained constant during the entire injection test. The plot on the right presents the same but for the recovery period.

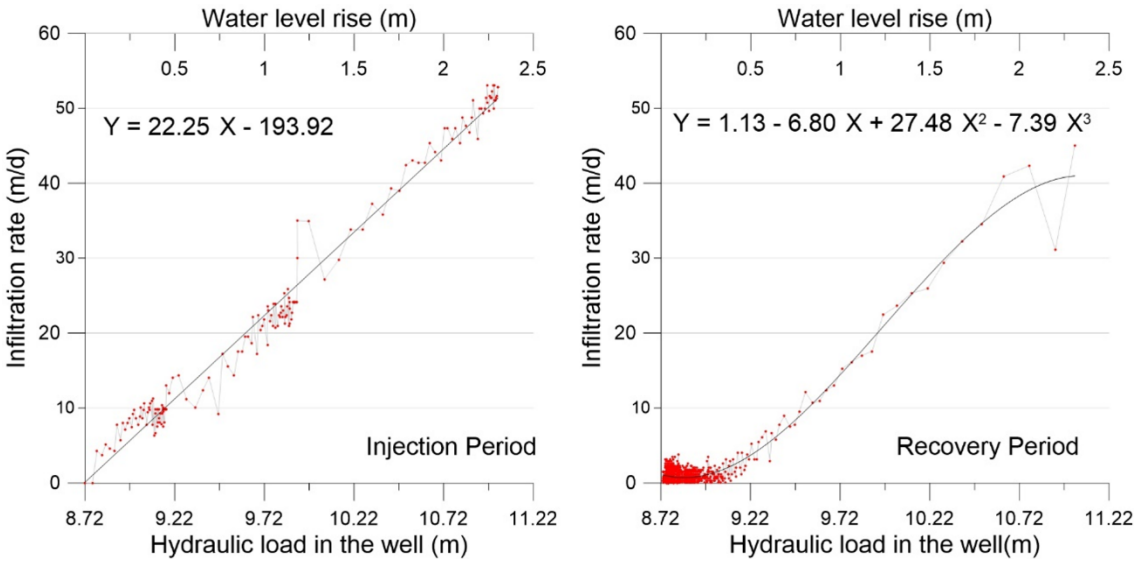

Figure 4.8 - Calculated infiltration rate versus hydraulic load in the well (bottom X-axis) and water level rise (top X-axis) for the injection period (left) and the recovery period (right) and the respective linear and polynomial fit

Nonetheless it is important to take into account a possible decrease in the recharge capacity of wells over time, due to several factors like well clogging by means of air binding in the aquifer pores, incrustations of screen opening, bacterial obstruction and chemical reactions between source water, formation water and formation material (Bouwer 2002; Martin 2014; Dwivedi et al. 2015). Moreover, the heterogeneity of the system should be taken in account, as wells in different locations, depths and diameters may have different infiltration capacities due to differences in geologic/lithological characteristics and shape factors.

4.4.2.2 Infiltration capacity

In order to infiltrate rainwater harvested from greenhouse rooftops, there is the need to divert this volume of water to recharge infrastructure near each greenhouse. The database of potential large diameter wells for injection was compiled from the wells registered at the regulatory agency database (APA-ARH Algarve) together with field surveys in order to identify further large wells. With the support of GIS tools, 67 large diameter wells were selected according to their distance to greenhouses, considering a maximum distance of 150 m.

However, it was not possible to associate wells to all the greenhouses identified in the aquifer, therefore, the greenhouses without wells in their vicinity were excluded from potential sources of rainwater collectors for MAR. After this filtering, it was assessed that a total of 1.51 hm^3/year of rainwater could be harvested from a total greenhouse surface of 2.21 km^2 and diverted into wells located nearby (selected greenhouses and infiltration wells presented in Figure 4.5). This value corresponds to about 15% of the aquifer average balance based on estimates by Almeida et al. (2000a).

According to injection test results (section 4.4.2.1) it is assumed each of the chosen injection wells has an infiltration capacity of 16 m^3/hour (the half step of the injection test) which would be equivalent to 0.14 hm^3/year. Based on this assumption and the greenhouse–well distribution presented in Figure 4.5, the water volume diverted from each greenhouse to the respective infiltration well corresponds to a lower injection volume than the mid-step injection volume for 66 of the 67 selected wells. One of the selected wells was assigned flow rates higher than 16 m^3/hour, yet the maximum value would be 0.18 hm^3/year (21.4 m^3/h), which is still much lower than step 3 of the injection test. These results suggest that the infiltration capacity of the selected wells is adequate to support the total water volume generated in an average one-year period. Nevertheless, the intra-annual seasonality of rainfall shows that there will be large variations in runoff produced between rainy and dry seasons, with December being the month with the highest contribution of generated water volume for injection (0.292 hm^3).

Daily rainfall data ranging from January 1st, 2000 until December 31st, 2019 from the rainfall gauging station of Patacão, in Faro, from *Direcção Regional de Agricultura e Pescas do Algarve* (DRAP-Alg) was statistically analyzed to assess the daily maximum rainfall extreme events and compared to the scheme's infiltration capacity. From the obtained data for the 20 years daily rainfall series, it was found that about 69% of the days had no rainfall, which correspond to 5006 dry days and 2299 days with recorded rainfall. Considering days with rainfall events, the maximum recorded daily rainfall for this period was 117.2 mm/day, with Q25%, median and Q75% of 0.2, 0.8 and 5.4 mm/day.

Converting the mid-step and 3rd step of the injection tests, (16m^3/h and 35m^3/h) to the total system (67 injection points) daily infiltration capacity, results in total values of 2.57x10^{-3} hm^3/day and 5.63x10^{-3} hm^3/day, which correspond to 11.64 mm/day and 25.47 mm/day, respectively. Considering only the rainfall events, 87% of which (i.e. 1995 of the 2299 rainfall events) have precipitation equal or lower than 11.64 mm/day, the infiltration capacity corresponding to mid-step injection flow, so it is assumed that the system's infiltration capacity is capable of absorbing the volume of water intercepted by greenhouses during these events. As for the 3rd step injection flow, the corresponding infiltration capacity can accept up to 95.00% (i.e. 2184 of the 2299 rainfall events) of the rainfall events recorded.

For the whole rainfall series there is a 4.2% chance of a rainfall event surpassing 11.64 mm/day and 1.6% of surpassing the 25.47 mm/day mark, which correspond to approximately 15 rainfall events per year for the first and 6 events per year, for the latter. According to the application of Weibull's formula, the probability of occurrence for rainfall events higher than 11.64 mm/day and 25.47 mm/day is 4.15% and 1.57% respectively and these represent return periods of 24 days for the first and 63 days for the latter. It is important to say that this is a theoretical return period, which does not take into account the rainfall seasonal distribution and in fact, these circa 15 events with rainfall distribution higher than 11.64 mm/day do occur in general between October and March.

It is assumed that for the highest 95% rainfall events, the system's infiltration capacity is enough to fully sustain the generated volume at the greenhouses by direct infiltration. The events with rainfall higher than 25.47 mm/day need to be taken cautiously into consideration, since the injection test performed has not been tested to such values, although the results obtained suggest that the system is capable of inflows higher than these values, as suggested by Figure 4.8. In cases where rainfall events exceed the wells infiltration capacity the generated flow should be discarded, since the capital costs of designing a solution to include these volumes would likely be prohibitive.

4.4.3 Numerical model – Managed aquifer recharge scenario

Simulated results of nitrate concentration were compared for both the BAU and INJ scenarios, based on monitoring points available (Figure 4.5). Both scenarios were simulated from 2016 to 2040. In general, model results for 2027 (i.e., the end of the 3rd river basin management cycle plan according to the WFD) show that for BAU, there will be 33 observation points with a nitrate concentration higher than 50 mg/l (Figure 4.9) of which, 10 belong to exceedances of the official monitoring network. As for INJ scenario, the number of exceedances by 2027 is 30, of which 9 belong to the official network. Considering the final step of the simulation, i.e. 2040, model results show 9 exceedances for the INJ scenario and 14 exceedances for the BAU scenario, of which, 2 and 3 respectively belong to the official network for each scenario.

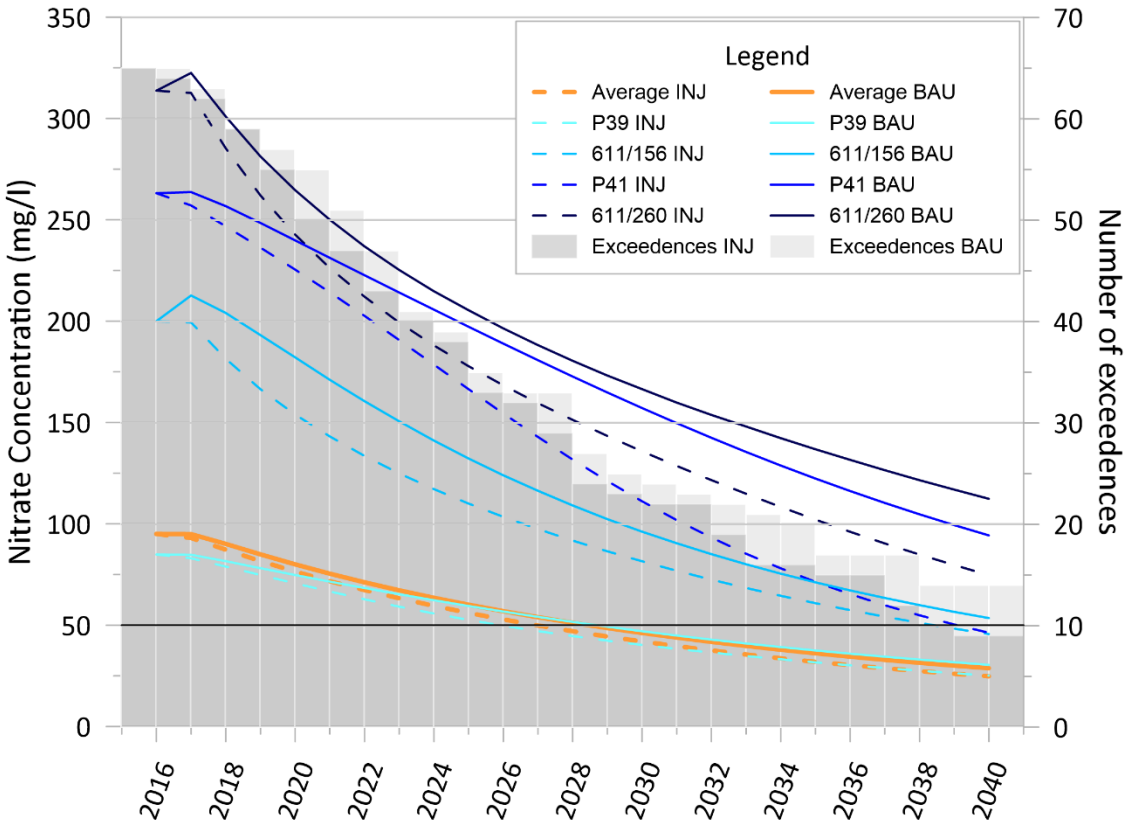

Figure 4.9 - Left Axis: simulated evolution of groundwater nitrate concentration for both scenarios at four monitoring points (P39, P41, 611/156 and 611/260) and annual average of all 91 quality monitoring points. Right Axis: simulated evolution of the number of exceedances of groundwater nitrate concentration

Analyzing individual observation results by 2027 show that INJ scenario contributed to the decrease of nitrates concentration below 50 mg/l in three additional points, when compared with BAU (P17, P36 and P39, the latter shown in Figure 4.9). For the INJ scenario, the majority of the observation points tend to achieve the nitrate concentration limit approximately 2-3 years before the INJ scenario (as shown with the example of observation point 611/156 in Figure 4.9). In 5 observation points, results by the end of the simulation (2040) show the threshold value is only achieved for the INJ scenario, as shown by the plots 611/156 and P41 in Figure 4.9. For 9 observation points the 50 mg/l threshold would not be achieved either in the INJ or BAU scenarios (see example 611/260 in Figure 4.9). In these cases, the maximum difference between both scenarios is nearly 40 mg/l, registered for both 611/260, P42 and P56. It is important to note that by the end of the simulation, some observation points show higher nitrate concentration for the INJ scenario than BAU, in particular for 10 observations points. In such cases, the calculated nitrate concentrations for the INJ scenario are 1 to 5 mg/l higher than those observed in BAU. In fact, the INJ scenario resulted in a decrease of groundwater quality in most of the modeled area, although for some areas BAU presented better results (Figure 4.10). This is probably either because of the mounding effect caused by the injected water, which resulted in a local barrier to groundwater flow and mass transport and local gradients opposite to the regional groundwater flow, or due to the transport mechanisms in groundwater simulated by the model, as response to the type of BC implemented to simulate the nitrate input and the injection of the harvested water, which may induce numerical instability in the model.

Regarding average calculated concentration of all monitoring points for each year, it can be seen from Figure 4.9 that for BAU, a value of 51 mg/l is calculated by the end of 2027, while for INJ scenario this value is 47 mg/l. Also, for INJ scenario, the 50 mg/l barrier is reached by the end of 2026, whereas for BAU this threshold is achieved early 2029. By the final timestep (2040) average concentration is 25 mg/l in INJ scenario and 29 mg/l for BAU.

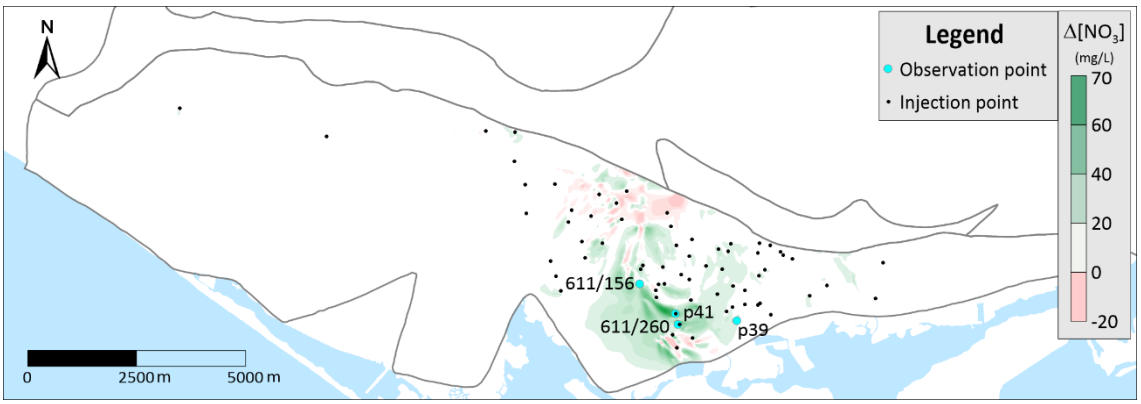

Figure 4.10 - Difference between simulated nitrate concentrations in groundwater for the BAU and INJ scenarios. Positive values (green) indicate lower concentration for the INJ scenario and negative values (red) indicate lower concentration for BAU

In general, results obtained with the model show there is a slight improvement regarding the decrease of the number of observation points with exceedances of nitrate quality for the INJ scenario, which, from the water resources management point of view is not a significant improvement. Nonetheless, a decrease of nitrate concentration specifically in observation points with a high nitrate concentration (such as P41 and 611/260) is observed, as well as the general geographic distribution of nitrate decrease for the INJ scenario. These two facts show that this scheme could reduce nitrate concentrations in groundwater in the study area. Moreover, the presented scheme is expected to be a low-cost and low impact solution, since most of the infrastructure is already available, except for the connection between the greenhouses and the injection wells and eventually a filtration-based pre-treatment.

These results must be taken cautiously, since the implemented numerical model does not account significant processes such as the recirculation of nitrate and additional recharge resulting from irrigation return flows, a process which is known to be important in causing the salinization of groundwater in the study area (Stigter 2005; Stigter et al. 2006a).

The presented MAR scheme is one of many mitigation measures that could be implemented in the study area to mitigate the high concentrations of nitrate in groundwater. The main advantage of the proposed scheme in this study is the use of existing infrastructure for collecting water and traditional dug wells as a mean to inject the harvested water in the

aquifer. These wells are widely distributed in the most contaminated area, thus reducing the costs of implementing such MAR scheme.

Other potential source of water for recharge identified in the study area include treated wastewater or surface water from rivers. Currently, treated wastewater is used in MAR frequently in many countries with a low cost of implementation (Missimer et al. 2014). Comparing the current MAR scheme with the reuse of treated wastewater it is expected that the MAR scheme outlined in this study would be cheaper to implement, since it would be necessary to pipe treated discharged from sewage water treatment plants to the aquifer injection points, or design and construct infiltration basins or other recharge structures. Additionally, there are potential water quality issues that could result from the use of treated wastewater as a source of aquifer recharge (Casanova et al. 2016). Regarding river streamflow, during FP7 MARSOL project, an overview of different types of water availability for MAR and recharge options were investigated , including the construction of infiltration basins in the beds of intermittent rivers to enhance recharge (Leitão et al. 2015). Although the implementation of such infiltration basins may have a reduced cost, the results shown during MARSOL project suggest that the water availability for recharge in such scheme's is relatively low, when compared with the MAR scheme presented in this work, since the streams in the study area are intermittent with flow generated only during strong rainfall or storm events and only a part of this flow infiltrates in the aquifer.

The results presented in the current task show the use of runoff from greenhouses for MAR could help lower nitrate concentrations in groundwater, particularly in the M12 aquifer. Such a scheme would also raise awareness of the need to improve the management of urban water resources and would help to develop a water sensitive city.

Nonetheless, this is an approach based on a theoretical analysis and does not take into consideration several factors that may influence the success of this approach, that would require further investigation. These issues are mostly related to the availability and suitability of infrastructure for water collection (the greenhouses), the infiltration infrastructure (the large traditional dug wells) and water quality issues, among others. These issues are discussed below.

Greenhouse conditions

Some of the greenhouses in the study area are very rudimentary and either do not have or have very inefficient water drainage systems. These factors can limit the amount of water that could be intercepted by the greenhouse and diverted for MAR. That is, for many greenhouses, the runoff coefficient could be significantly lower than 1.

Ownership issues

This is a scientific study based on existing greenhouses and wells in the study area that belong to private users. Therefore, authorization and cooperation from the owners would be required to implement a MAR scheme using these structures. Additionally, in many cases the wells and the greenhouses may have different owners, potentially increasing the complexity of implementing the MAR scheme outlined in this work.

Well clogging

As mentioned before, the potential for recharge wells to become clogged must be considered in every MAR project. Clogging is one of the main challenges for MAR and can lead to loss of performance of the recharge scheme, a decrease of the local hydraulic conductivity (and therefore, infiltration capacity) of aquifer sediments and can result in costly redevelopment of bores and infiltration basins (Martin 2014). The most common causes of clogging at wells are the presence of suspended solids in the injected water, biological clogging (Martin 2014) and air entrapment/binding (Pyne 1995). The implementation of retention devices with capacity for sedimentation and other types of pre-treatment should be taken into account to decrease clogging effect.

Water quality

It is important that the source-water for a MAR scheme is of a suitable quality to prevent clogging by suspended solids. Generally, for rainwater harvesting, the first precipitation episodes of the year are usually discarded due to the high level of accumulated dirt in the collection area. A bypass system to the water networks should be taken in consideration. In the

case of injection through wells, water should be filtered in order to reduce the input of suspended solids, one of the main causes for clogging.

Injection method

The injection method tested in the injection test that was carried out in this study consisted of a gravitational direct injection method. This meant that water was discharged into the upper part of the well and was allowed to flow naturally by gravity into the well. This method may induce air entrapment in the well, and thus, contribute to clogging.

Additionally, some of the large-diameter wells that were inspected in this study were unsuitable for use as recharge structures due to their poor level of maintenance or because of their use for "garbage disposal". In those cases, further work would be necessary to restore the proper conditions for the use of these as infiltration wells and assess the individual wells infiltration capacity.

Increase of groundwater levels / well overflow

Although increasing groundwater levels and aquifer storage is in general a beneficial result of a MAR scheme, excessive infiltration of water in an aquifer with variable permeability can lead to groundwater mounding and potentially to the discharge of groundwater to the land surface. Ultimately this could result in the water overflow in a given well and could cause damage in nearby infrastructure and crops.

Rainfall distribution

This study assessed the recharge potential of runoff using average monthly and daily precipitation and therefore monthly water availability but did not consider what would happen in extreme rainfall events when a large amount of rain falls in a few hours. Variations of rainfall intensity would need to be considered when designing the MAR scheme outlined in this study, and this could require the construction of additional infrastructure to accommodate high-rainfall events.

4.4.4 Numerical model – Land-use scenarios

As previously mentioned, for the land-use assessment, simulation was performed for the period 2017-2040, being 2016 the reference year. A time-lapse of the simulated results indicating the nitrate concentration higher than 50 mg/L for the different scenarios are shown in Figure 4.11 (scenario A), Figure 4.12 (scenario B), Figure 4.13 (scenario C) Figure 4.14, (scenario D) and Figure 4.15 (scenario E).

In general, the area with nitrate concentration higher than 50 mg/L is rather similar for scenarios A, B, C and D, noting a decrease in the contaminated area when compared with the reference scenario or scenario E, which considers an increase of the nitrate input. Nonetheless, compliance was not achieved for the simulated period, i.e. until the year 2040.

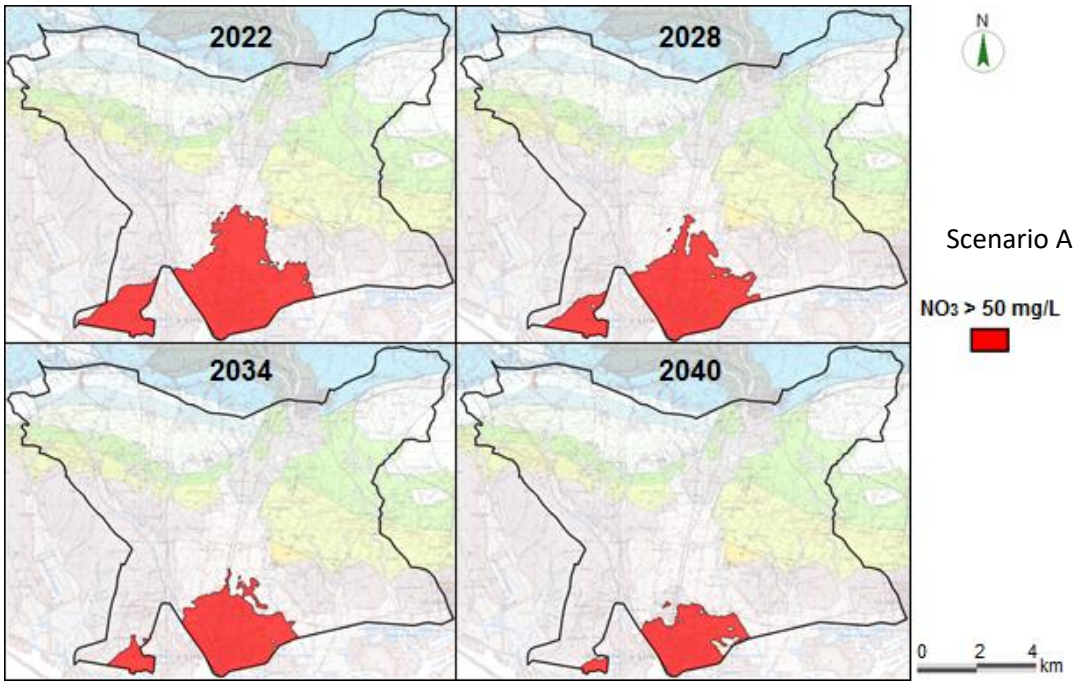

Figure 4.11 – Time-lapse of simulated nitrate concentration showing areas higher than 50 mg/L at NVZ Faro for Scenario A: Input 0 (source: (Carvalho et al. 2017))

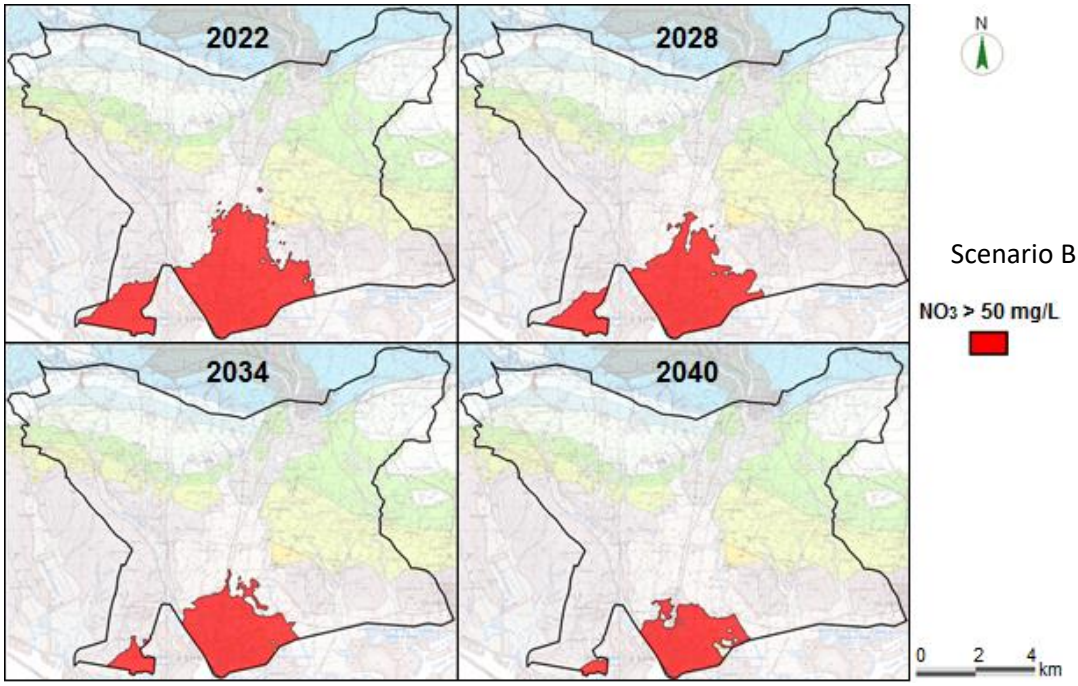

Figure 4.12 - Time-lapse of simulated nitrate concentration showing areas higher than 50 mg/L at NVZ Faro for Scenario B: “Agriculture” (source: (Carvalho et al. 2017))

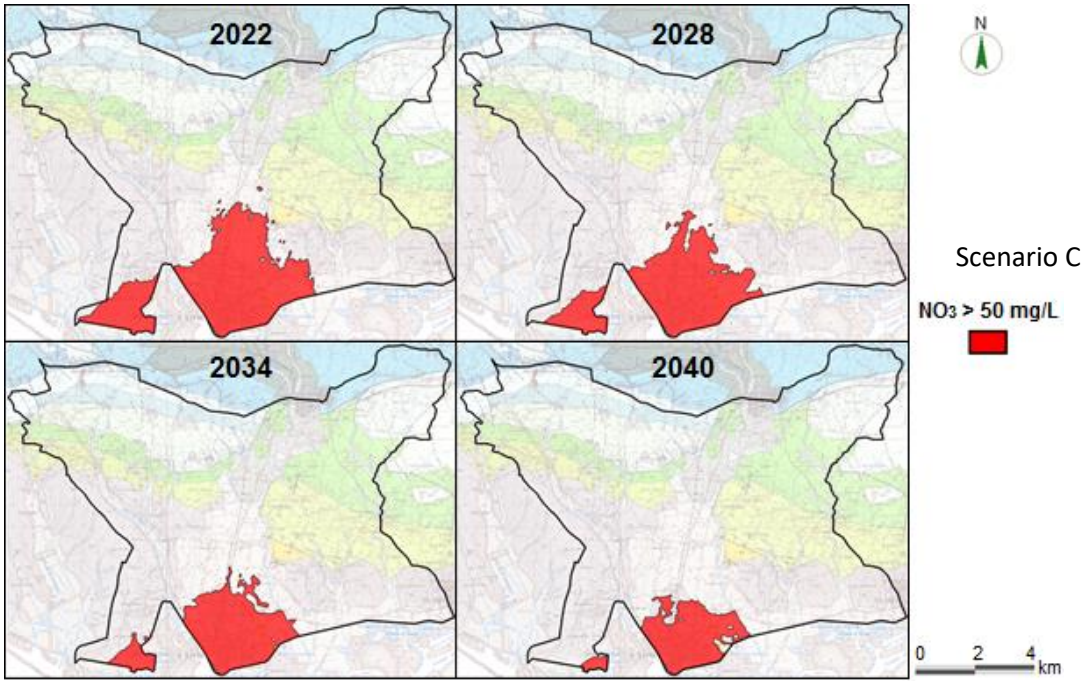

Figure 4.13 - Time-lapse of simulated nitrate concentration showing areas higher than 50 mg/L at NVZ Faro for Scenario C: “Agriculture+Livestock” (source: (Carvalho et al. 2017))

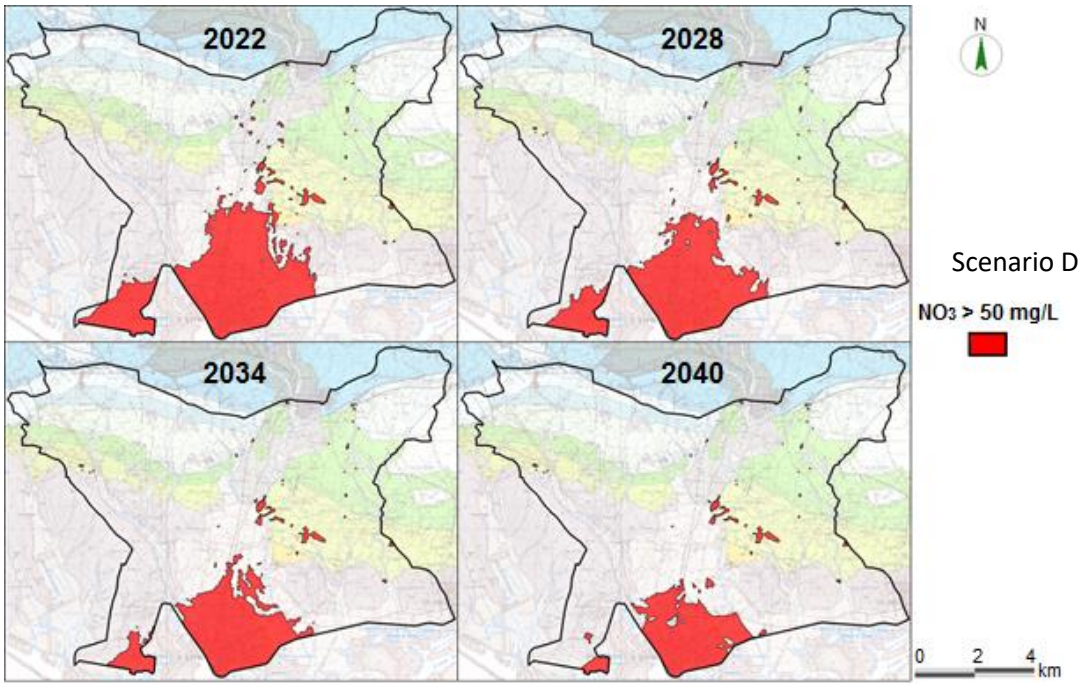

Figure 4.14 - Time-lapse of simulated nitrate concentration showing areas higher than 50 mg/L at NVZ Faro for Scenario D: “Agriculture 10 kg N/ha” (source: (Carvalho et al. 2017))

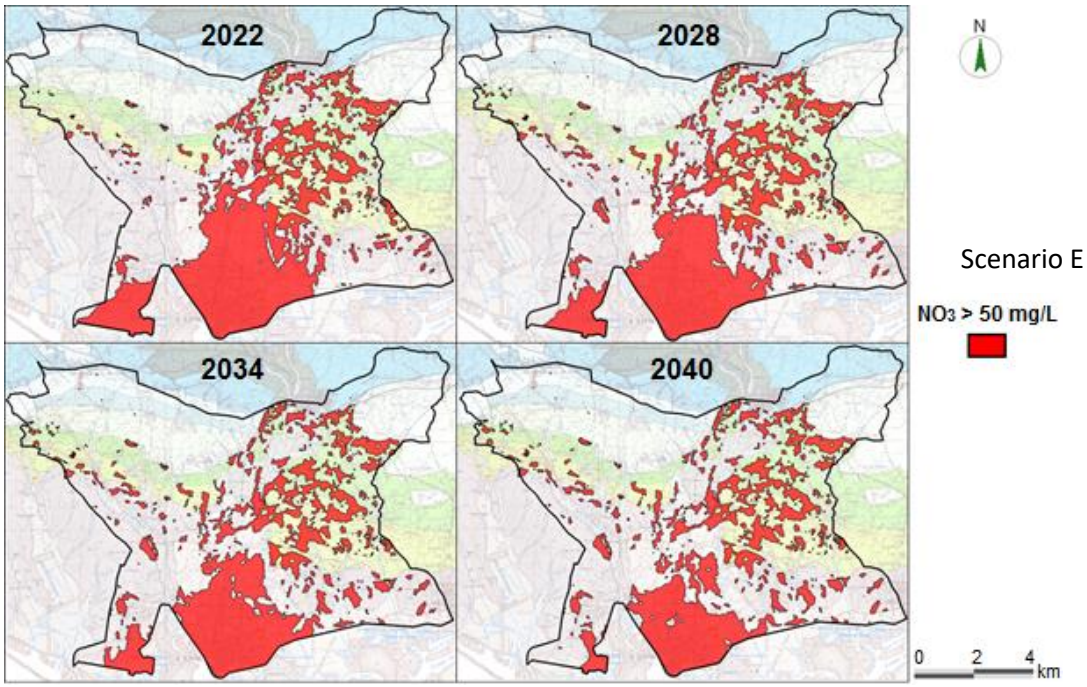

Figure 4.15 - Time-lapse of simulated nitrate concentration showing areas higher than 50 mg/L at NVZ Faro for Scenario E: “Agriculture 20 kg N/ha” (source: (Carvalho et al. 2017))

Results for the modelled scenarios are summarized in the Table 4.7.

Table 4.7 – Simulated results for the mass transport analysis for each land use scenario at NVZ Faro

Scenario	**NO_3 input kg/year**	**% area under pressure**	**% area exceedance $[NO_3]$> 50 mg /L**	
			2016	**2040**
A: No Input	0	0	42.3	5.3
B: “Agriculture”	75751	82.9		5.7
C: “Agriculture + livestock”	77689			5.7
D: “Agriculture 10 kg N/ha”	292063	69.5		7.4
D: “Agriculture 10 kg N/ha”	584127			20.6

Simulated results for scenario A, which considers no input whatsoever, still registers a maximum nitrate value of 105 mg/L by the end of the simulation, with one of official the monitoring points (611/260) resulting in 95 mg/L, which is still higher than the quality standard for nitrate, 50 mg/L. By the end of the simulated period, the contaminated area is limited to the M12 aquifer, since the remaining aquifers covered by the NVZ do show values below 50 mg/L Simulated results show that the contaminated area consist of 14% of the NVZ by 2022, 10% by 2028, 8% by 2034 and 5% by the 2040.

Regarding Scenario B: “Agriculture” and Scenario C: “Agriculture+Livestock”, which considers the agriculture (Scenarios B and C) and livestock (Scenario C) pressure indicated in the 2nd RBMP (APA 2016), results are quite similar, which is due to the fact that livestock in the study area has a very expression. Obtained results for both scenarios B and C show that the contaminated area (i.e. nitrate concentration > 50 mg/L) is about 14% of the NVZ by 2022, 10% by 2028, 8% by 2034 and 5% by 2040.

Results for scenarios D and E consider a fix annual rate of nitrogen input of 10 kg/ha and 20kg/ha respectively, in the agriculture areas identified in the Portuguese land-use map

(COS2010). Both scenarios do show an increase of the contaminated area comparing with the previous scenarios A, B and C.

Although the area under pressure for scenarios C and D is smaller than that for scenarios B and C (69.5% of the NVZ for scenarios C and D, 82.9% for scenarios B and C), the nitrogen input rate into the system is higher, resulting in a total nitrate load of 292.06 ton/year for scenario C and 584.12 ton/year, whereas scenarios B and C are 75.75 ton/year and 77.69 ton/year respectively, and similarly, highest nitrate concentration by the end of the simulation is higher for scenario C (circa 120 mg/L) and D (200 mg/L).

By the end of the simulation, two observation points exceed the quality standard for scenario C (611/156 with 51 mg/L and 611/260 with 102 mg/L), whereas for scenario D, 8 exceedances are observed, of which, 7 are in M12 (maximum value observed are 611/260 with 111 mg/L) and 1 in M10 (607/478 with 90 mg/L).

Unlike the previous scenarios, results show that by the end of the simulation, groundwater bodies North of M12 also have nitrate concentration higher than 50 mg/L for both scenarios D and E. Obtained results show that the contaminated area (i.e. nitrate concentration > 50 mg/L) for the years 2022, 2028, 2034 and 2040 is respectively 16%, 13%, 10% and 7% for scenario D and 27%, 25%, 23% and 21% for scenario E.

According to the obtained results, it is evident that the compliance regarding nitrate concentration will not be achieved until 2040 at the NVZ Faro. In the majority of the scenarios, results indicate there is a decrease in most of the North area of the NVZ, corresponding to the aquifers north of Campina de Faro aquifer (M12), which, in general, do achieve compliance within the simulated period. For M12, however, there appears to be a concentration effect near the Coastal lagoon of Ria Formosa, resulting from a retardation of the flushing of nutrients to the coastal lagoon. Even for the best-case scenario A, after extending the simulation 10 more years, until 2050 high concentration of nitrate are observed still near the south limits of M12, as shown in Figure 4.16

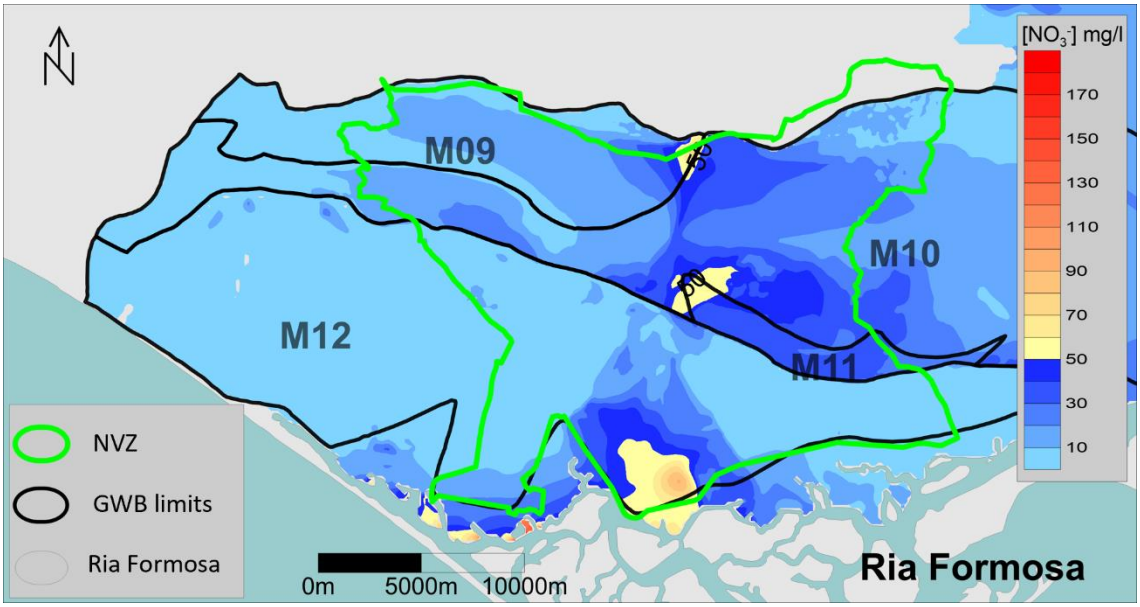

Figure 4.16 – Simulated nitrate concentration for land use scenario A by 2050

This could be due to a number of factors, namely: a) the contact with the coastal lagoon Ria Formosa, the main natural discharge point of the aquifer; b) the low permeability of the Plio-Quaternary aquifer of Campina de Faro; likely due to the low hydraulic gradient in the aquifer as well as the low natural recharge (which vary between 100-125 mm/year), hence reducing the system's resilience for water renewal; c) The initial conditions for the reference situation (2016/17), in the highest nitrate concentration were already higher in this area of the aquifer.

4.5 Conclusions

An assessment of a proposed MAR scheme using rainwater harvested greenhouse rooves indicates that this water could be discharged through existing large-diameter wells to increase recharge and reduce nitrate concentrations in an aquifer near the city of Faro in Portugal.

The volume of rainfall that could be intercepted by the greenhouses was estimated to be 1.67 hm^3/year from a total greenhouse surface area of 2.74 km^2, in an average rainfall year. Due to the limited number of large-diameter wells that are located within 150 m from greenhouses the surface area of greenhouses available to intercept rainfall is reduced to

2.21 km^2, which reduces water availability to 1.5 hm^3/year. Nevertheless, this is a significant volume in comparison to the natural aquifer recharge (15% of annual average rainfall).

An infiltration test was performed in this study to assess infiltration capacity of one of the large diameter wells, and results were extrapolated to the 67 identified wells that were located within 150 m range from existing greenhouses in the area. The results of the infiltration test show that the existing large-diameter wells would be capable of sustaining the total amount of water generated from the intercepted rainfall from the greenhouses in an average year. It was determined that the proposed MAR scheme would be capable of sustaining the direct infiltration of runoff produced by rainfall events of up to 25 mm/day. This would correspond to about 95% of the daily rainfall events in the region.

A numerical groundwater flow and transport model was adapted in order to assess whether nitrate concentrations in groundwater in the study area would be lowered with the proposed MAR scheme. Two scenarios were considered, a Business as Usual and a MAR scenario, which included the injection of the harvested rainwater into the selected wells for an average year of rainfall. The scenarios were simulated from 2016 until 2040 and indicated that the injection of the harvested rainwater results in a slight decrease of the number of nitrate exceedances (3 by 2027 and 5 by 2040). The greatest impact, though, was observed in areas with high nitrate concentration where a decrease up to 70 mg/l by 2027 was calculated by the model.

Though the results of the numerical model simulation of the MAR scenario are encouraging, some issues that may decrease the potential for this solution should be taken into consideration in future studies. These include the potential for clogging of infiltration wells, the integrity and conditions of both the greenhouse and the wells, the need for obtaining the permission of landowners to use this infrastructure, injection methods and water quality concerns. Notwithstanding, given the water availability this solution can provide, it results in an alternative and low-cost mitigation measure that could easily be implemented to contribute not only to improve the groundwater chemical status at NVZ Faro, in particular the Campina de Faro aquifer as well as augment groundwater levels.

Regarding the analysis of the land-use scenarios, simulations suggest that a compliance can not be achieved by 2040, even for the best case scenario, which consists of eliminating the nitrate pressures into the system. In most scenarios, by the end of the simulation, Campina de Faro aquifer (Plio-Quaternary layer) is the only contaminated area, which is mainly due to the interaction of this system to the coastal lagoon Ria Formosa (the main discharge area of the system) as well as the low permeability and recharge values, reducing the systems capacity to regenerate. The mostly affected area by the end of the simulation corresponds to the current highest nitrate observed values, i.e., in the central area of Campina de Faro aquifer, supporting the fact that there appears to be some kind of hydraulic barrier, entrapping the nitrate contamination in this area.

Chapter 5: Numerical modelling to assess intrinsic hydraulic properties and conceptual model regarding the chemical status of aquifers in central Algarve

The analysis preformed on Chapter 4: focused mainly on the Nitrate contamination problems occurring in central Algarve aquifers within the NVZ of Faro, focusing on the impact of different land-use scenarios and estimating the effect of a mitigation measured based on rainwater harvesting. In this chapter, research focus more on intrinsic hydraulic properties of the aquifers connected with the Ria Formosa, and how the numerical model approaches such features, with a specific analysis on the nitrate recirculation effect. After, a set of mitigation measures and its effect on the chemical status of groundwater is assessed, followed by the analysis of climate scenarios.

The work presented in this chapter results from the peer-reviewed publication Costa et al. (2021).

- Costa LRD, Hugman RT, Stigter TY, Monteiro JP (2021) Predicting the impact of management and climate scenarios on groundwater nitrate concentration trends in southern Portugal. Hydrogeol J 29:2501–2516. https://doi.org/10.1007/s10040-021-02374-4

5.1 Introduction

The combined pressure from overexploitation and inadequate agricultural practices in some areas of southern Portugal since the 1970s has led to a number of groundwater management problems, such as the lowering of groundwater levels in some areas near the coast, localized seawater intrusion and groundwater contamination by excessive use of fertilizers (Stigter et al. 2007, 2013; Hugman et al. 2016; Hugman 2017; Costa et al. 2020). Due to the health and environmental hazards associated with nitrate in groundwater (e.g. Zhou et al. 2015), the European Union (EU) has implemented legislation on restoration and conservation, through the Nitrates Directive and the Water Framework Directive (WFD). These directives aim to implement measures that assure the achievement of good water status in all water bodies by

2027. For the case of groundwater contamination by nitrate, the threshold value for good status corresponds to 50 mg/l. Complying with this legislation can be extremely challenging in several regions, further revealed by the still rising trend in nitrate concentrations observed in both surface waters and groundwater over the last few decades (Jackson et al. 2008; Musacchio et al. 2020).

The aquifers located in the southern Portuguese Meso-Cenozoic basin, in the Algarve, are an important water source in the region, sustaining circa 70% of the total water abstracted for agriculture and the majority of the golf courses. In total, groundwater contributes to about 60% of the annual total abstracted water volume (221 hm^3/year) in the region, according to the Portuguese Water Authority (APA 2016).

The overexploitation in some coastal aquifers in the Algarve during the final decades of the 20th century led to a gradual decrease in their water quality. The current regulatory agency (the Portuguese Environment Agency - APA) responded by prohibiting the drilling of new boreholes along the coast. However, since the switch to a surface-water-based public supply in the region, groundwater levels have stabilized, and water quality has improved in some of these aquifer systems. Parallel to this situation, aquifer contamination by nitrate fertilizers has been a matter of concern for the water authority since the 1980s. This led to the implementation of two nitrate vulnerable zones (NVZ) in compliance with the EU Nitrates Directive to further monitor and implement mitigation measures. The highest levels of contamination and salinization are observed in the Campina de Faro Aquifer System (M12) located in the western part of the drainage basin of the Ria Formosa lagoon, an ecologically sensitive and economically important wetland (Stigter et al. 2013).

There are a number of aspects in the M12 system that deserve more detailed study. First, estimated groundwater abstractions from M12 are higher than average annual recharge, which would give the aquifer a status of “overexploited” from an initial water balance perspective. Long-term decreasing trends in groundwater levels are however not observed, which seems to indicate that this aquifer is receiving inflow from other hydraulically connected groundwater bodies, a phenomenon that has not been properly assessed so far. If so, then this also

contributes to the difficulty of assessing the status of individual groundwater bodies in compliance with the WFD.

Second, although changes in water use and improved agricultural practices have led to improvements in some of the aquifers in the region, this is only partly the case for M12. Continuous monitoring provides clear evidence of the continued elevated levels of nitrate and movement of the contamination plume towards the Ria Formosa coastal lagoon (Stigter et al. 2007, 2013; Costa et al. 2020), which demands deeper investigation. This may have serious consequences for the Ria Formosa lagoon, recognized as an important wetland at both European and International level and designated as a Natura 2000 and a Ramsar site. Coastal lagoons are particularly vulnerable to eutrophication as they are regions of restricted exchange with the adjacent ocean and may accumulate nutrients supplied by the surrounding watershed (Newton et al. 2003). The role of groundwater discharge as a vector for nutrient transport to the lagoon has been well established from a water and nutrient balance perspective (Stigter et al. 2013; Malta et al. 2017), as well as in field studies of groundwater seepage under the lagoon (Leote et al. 2008; Ibánhez et al. 2011; Rocha et al. 2015). However, these aspects have not been simulated and confirmed through numerical modelling, making it impossible to simulate scenarios of (management and/or climate) changes, a third aspect that motivated the current study. Initial estimates of the contribution of groundwater borne nitrogen (N), based on a regional water balance and N loads suggests that total transport towards the lagoon is in the order of 300 ton/a, significantly larger than the annual contributions from surface run-off (6 ton) (Malta et al. 2017), though lower than the point-source contribution from waste water treatment plants (477 ton). However (and a fourth aspect justifying the current research), studies in the area have also shown that the N loading alone does not explain the high values of nitrate observed in the field (Stigter et al. 2011, 2015), and that salinization processes caused by irrigation return flow may be an additional driver.

From a climate change perspective, southern Portugal is located in an area expected to be heavily affected by more intense rainfall and longer droughts, and long-term drier conditions (e.g. Giorgi 2006; Raymond et al. 2019). As water availability becomes scarcer, groundwater demand for irrigation will actually increase, putting further pressure on the groundwater

resources. In flat lying areas with low hydraulic gradients, sea-level rise may pose an additional threat to groundwater quality near the coast (Werner and Simmons 2009; Ferguson and Gleeson 2012a; Taylor et al. 2013a).

In the current study a groundwater flow and nitrate transport model is developed and used to assess how nitrate transport in M12, and similar coastal aquifers worldwide, is controlled by intrinsic properties, human activities and restoration measures, and how the system is hydraulically connected to neighboring aquifers. In addition, the model is used to assesses the feasibility of achieving good water quality status in all groundwater bodies connected to the Ria Formosa coastal lagoon within the timeframes outlined in the WFD, under current conditions, proposing alternative management scenarios, and facing predicted climate changes in the long run.

5.2 Study area

The onshore Meso-Cenozoic Algarve basin is an east-west trending sedimentary basin, with a south-dipping monocline structure, lying on Carboniferous schists and greywackes (Manuppella et al. 1993). The main aquifer systems within the Ria Formosa catchment (M9-M15 in Figure 5.1) are characterized by limestone and highly karstified dolomites from the Jurassic and Cretaceous, overlain to the south by sandy-limestone and detritic (sands and silt) formations from the Miocene and Plio-Quaternary. Figure 5.1 (b) Western and Eastern presents representative cross-sections of the eastern and western sectors of the study area.

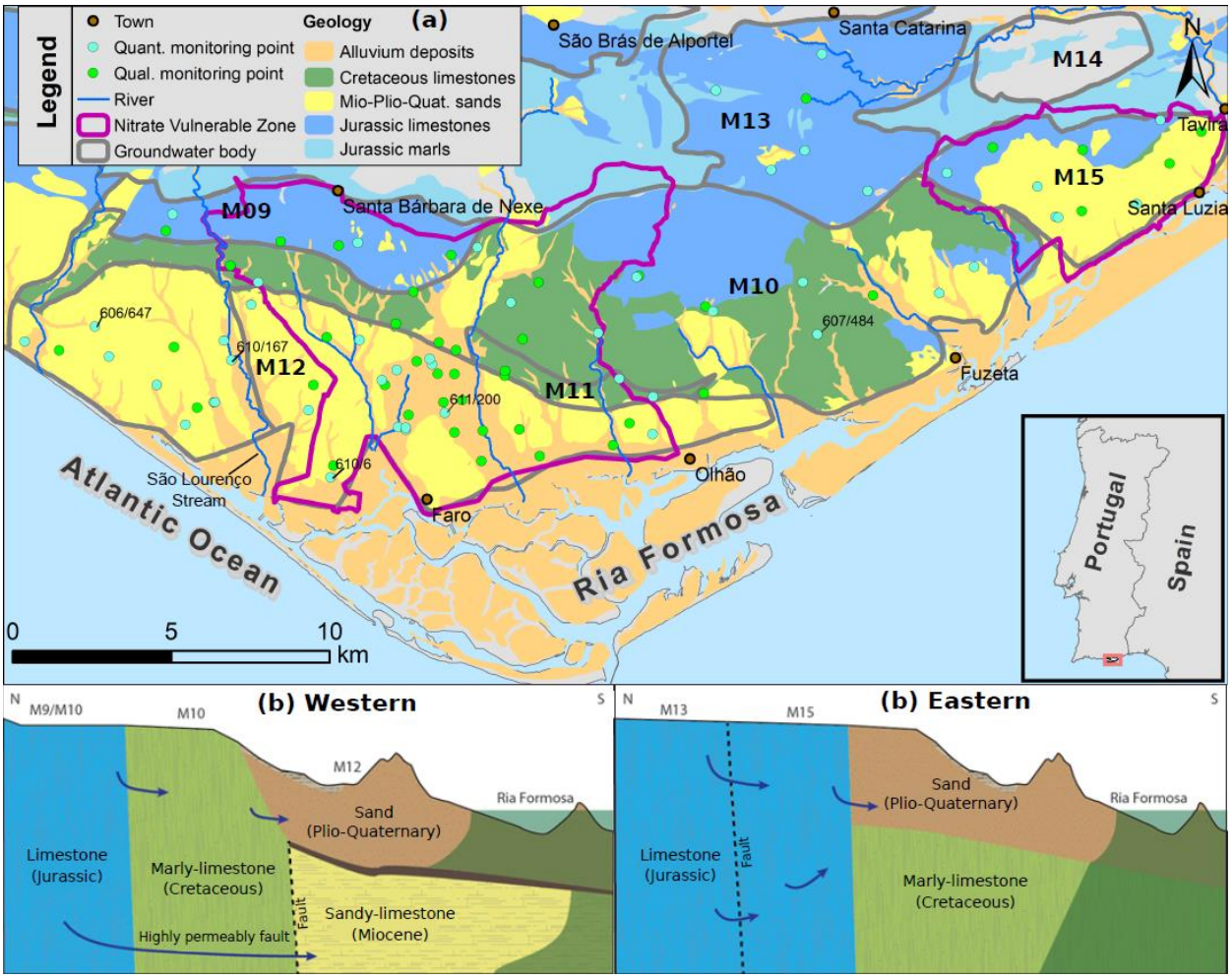

Figure 5.1 – **(a)** Location of the study area, simplified geology, groundwater bodies, official monitoring network and nitrate vulnerable zones. **(b)** Conceptual models of the western and eastern sectors of the study area; not to scale

The catchment includes two areas of low permeability: the Palaeozoic schists and greywackes to the north (not shown) and outcrops of marls from the upper Jurassic. The detailed overview of each system is provided by Almeida et al. (2000a) and further detail for specific systems can be found in Silva (1988), Stigter (2005), Roseiro (2009) and Hugman (2017).For the purposes of this modelling exercise, only the aquifer systems within the catchment area that are directly interconnected (M9-M13 and M15) were considered. An additional three aquifer systems are within the catchment (M8, M14 and M16 - not shown), however these are geographically separated by outcrops of M0 and are thus not considered to function as a unit. It is unclear

whether M8 and M14 provide discharge to the lagoon, streams or deep flow towards the Atlantic Ocean (Stigter 2005; Stigter et al. 2007; Malta et al. 2017).

5.2.1 Groundwater and nitrogen (N) budget

The spatial distribution of rainfall (Nicolau 2002) and recharge ratios according to outcropping lithology (Almeida et al. 2000) were cross-referenced to estimate total available groundwater recharge. Current groundwater use in the area is mostly for agricultural purposes, although a considerable use is attributed to public supply and golf course irrigation. Irrigation water demand was estimated based on land use mapping for 2007 provided by the regional environmental agency (APA-ARH Algarve) and average crop water demands presented in the first generation of the River Basin Management Plan (RBMP) (RBMP 2012) by crop type and occupied area. Net loss to irrigation is calculated taking into account the irrigation efficiency in the same report (76.5%) and irrigation return flow (estimated to be 15% for drip irrigation systems used in the area (Beltrão 1985; Keller and Bliesner 1990)). Calculated groundwater budgets for the selected groundwater units are presented in Table 5.1.

Table 5.1 Calculated groundwater budget for the selected groundwater bodies

Groundwater body		**Aquifer area $x10^6 m^2$**	**Rainfall mm/a**	**Rainfall $x10^6 m^3/a$**	**Recharge ratio**	**Recharge $x10^6 m^3/a$**	**Irrigation (net loss) $x10^6 m^3/a$**	**Budget $x10^6 m^3/a$**
M9	Almansil-Medronhal	23.35	617	14.4	0.50	7.2	-1.8	5.4
M10	S. João da Venda-Quelfes	113.31	631	71.5	0.20	14.3	-14.5	-0.2
M11	Chão Cevada-Qta João Ourem	5.34	618	3.3	0.50	1.7	-1.5	0.3

Groundwater body		Aquifer area $x10^6 m^2$	Rainfall mm/a	Rainfall $x10^6 m^3/a$	Recharge ratio	Recharge $x10^6 m^3/a$	Irrigation (net loss) $x10^6 m^3/a$	Budget $x10^6 m^3/a$
M12	Campina de Faro	86.39	568	49.1	0.20	9.8	-10.2	-0.4
M13	Peral-Moncarapacho	44.07	708	31.2	0.40	12.5	-0.9	11.6
M15	Luz-Tavira	27.72	606	16.8	0.25	4.2	1.6	5.8
Total study area		300.18	-	192.2	-	49.7	-27.3	22.4

Annual N requirements for the crops grown in the area are in the order of 200-300 kg/ha. An average N loss of 20% to the groundwater, suggested by previous authors (Stigter et al. 2007), is applied to land use data to estimate the total N load to groundwater. Leaching of domestic effluents from septic tanks is an important point source of nitrogen in areas not connected to the sewerage network (c.a. 20% of the population), which is clearly revealed by the microbiological contamination observed in many groundwater wells (Stigter et al. 2007). The total N load from septic tanks was estimated assuming the same values as previous authors (Stigter et al. 2007) (average population density in the Ria Formosa basin of 165 hab/km^2, water use per capita of 150 l/day, 70 mg/l N concentrations in wastewater and N removal efficiency of the treatment system of 25%). The contribution from atmospheric deposition was calculated based on the spatial distribution of rainfall (Nicolau 2002) and average concentration of N in rainwater (20 µmol/l) measured in the area(Stigter et al. 2007; Malta et al. 2017).

Table 5.2 presents calculated values of abstraction, return flow and agricultural contribution to nitrogen load for the selected aquifer systems. Input from domestic effluents was estimated at 31.1 ton/a for the model area and atmospheric deposition at 63.8 ton/a. A total N load of 255 ton/a is estimated for the agriculture N input for the whole area, which accounts for 73% of

total load, and domestic effluent and atmospheric deposition for the remaining 9% and 18% respectively.

Table 5.2 Calculated current abstraction, return flow and N load from agriculture for the aquifer systems in the study area

Aquifer System	**Unit**	**Irrigated area (km^2)**	**Return-flow ($x10^6$ m^3/a)**	**Abstraction ($x10^6$ m^3/a)**	**N (ton/a)**
S. João da Venda - Quelfes	M10	19.7	2.5	17	98.3
Chão de Cevada - Quinta João de Ourem	M11	1.9	0.25	1.7	9.4
Campina de Faro	M12	11.9	1.8	12	59.5
Malhão	M13	1.4	0.17	1.1	7.2
Luz - Tavira	M15	14.0	1.6	-	70.1
Almancil - Medronhal	M9	2.2	0.32	2.1	10.8
Total study area		51.1	6.6	33.9	255.3

5.2.2 Groundwater levels

The study area comprises a complex hydrogeology and stratigraphy, with hydraulic connections, which are currently not well established, particularly for the case of M12. In fact, groundwater abstractions from M12 are higher than the average annual recharge (Almeida et al. 2000), but long-term decreasing trends in groundwater levels are generally not observed, which is a suggestion that this aquifer must be in hydraulic connection with other aquifers located more to the north, a phenomenon that has not been properly assessed so far.

For the purpose of management, M12 was divided in Western and Eastern sectors by the water authority, within the second generation of the RBMP (APA 2016), spanning from 2016 to 2021, with the border being defined along the São Lourenço stream. Additionally, the vertical stratigraphy of M12 is composed of a phreatic aquifer layer and a semi-confined aquifer layer separated by an aquitard (Figure 5.1, cross sections (b) Western).

It is important to state that the majority of the contaminated area in the study area is reflected in the eastern sector of M12, in the phreatic aquifer layer.

Figure 5.2 shows the average annual evolution of hydraulic head collected from observation points located at the Eastern and Western sectors of M12, for both the confined and unconfined aquifer layers, as well as an observation point location in the upstream system M10.

The confined and unconfined aquifers do appear to have somewhat independent flow. In general, the confined aquifer layers of the M12 system appear to have a similar behavior and amplitude to the upstream M10 system, whereas the phreatic aquifer layer does present smoother amplitudes. Additionally, observation point M10 - 608/286 shows a better relation with levels registered in the Eastern sector (M12 – East conf 611/200). This suggests that the confined formations may be in hydraulic connection with the upstream systems, particularly in the eastern sector of M12, as previously suggested by other studies (Almeida 1985; Almeida et al. 2000; Hugman 2017).

From Figure 5.2 it can also be noted that there are two steep groundwater level decreases (606/647), one in the 1980s, and one in the early 1990s, which is typical for the confined aquifer layer in the western sector of M12. These accentuated groundwater level decreases are not verified in the eastern sector of M12. In fact, according to the second generation of the RBMP, the western sector of M12 is currently assessed as not achieving good quantity status due to this depression, while the eastern sector of this aquifer is assessed as good quantity status. On the other hand, the western sector of this aquifer is assessed with good quality status, while the eastern sector is assessed as not reaching good quality status due to the aforementioned nitrate contamination.

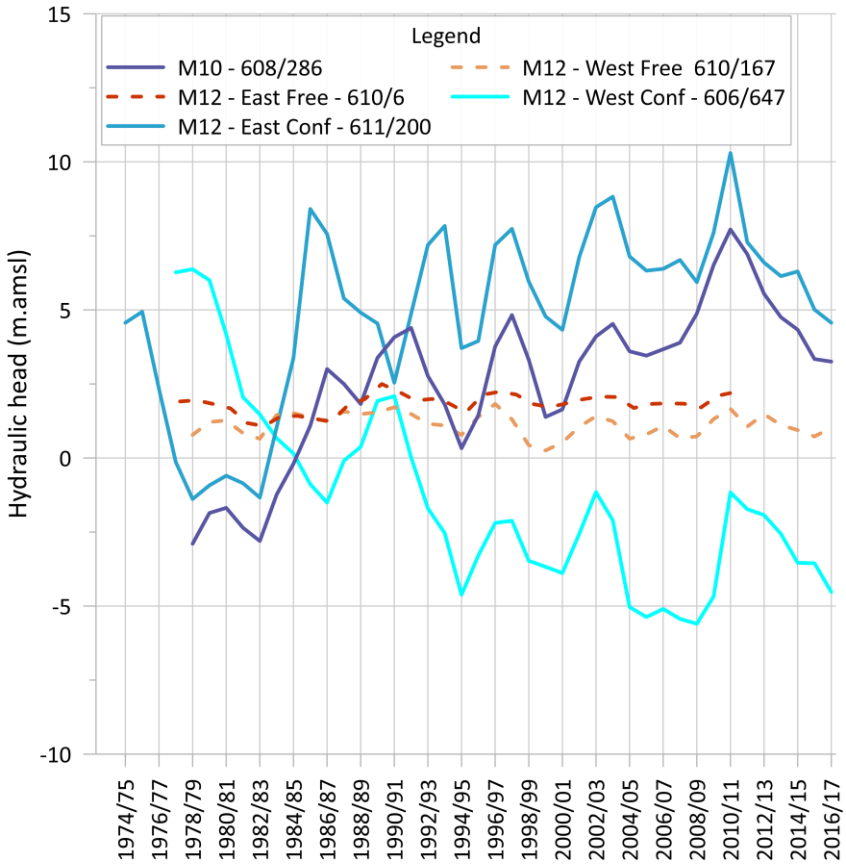

Figure 5.2 -Temporal evolution of average yearly hydraulic head at piezometers from M12 and M10. At M12, both the eastern and western sectors are represented as well as the confined aquifer (Conf) and phreatic (Free) aquifer

5.3 Numerical model

5.3.1 Model setup

A three-dimensional flow and transport model of the aquifer systems that discharge directly into the Ria Formosa was developed using finite element code FEFLOW (Diersch 2014). The geometry of the groundwater management units, geological outcrops and main hydrogeological features (streams, fault and boreholes) were used to generate a triangular prism finite element mesh with 633,048 elements and 428,904 nodes distributed equally across

four slices and three layers. The mesh was refined within the NVZs. The resulting model domain has a total area of 3.32 $x10^8$ m^2 and a volume of 3.88 $x10^{10}$ m^3. Elevation of the top of the model domain was set equal to the surface elevation obtained from a digital elevation model. The remaining slices were distributed equally to obtain a uniform model thickness of 100 m, with the exception of the Campina de Faro (M12) aquifer. This system is a multi-layered aquifer with phreatic and confined layers separated by a clay aquitard. Elevation of the bottom of the confined aquifer and top and bottom of the clay layer were sourced from prior studies (Hugman 2017), and imposed on the respective model slices. Elements were deactivated along the northern boundary of the Campina de Faro (M12) in contact with outcropping Cretaceous formation. Nonetheless, where the permeable fault intersects the system and Miocene, Plio-Quaternary or alluvium sediments outcrop near the border with M12, flow from northern aquifers may occur, bringing in lateral recharge.

Recharge was assigned according to the spatial distribution of rainfall (Nicolau 2002) and recharge ratios according to outcropping lithology (Almeida et al. 2000). Constant head BC equal to 0 m above mean sea level were imposed along the coastline and channels of the coastal lagoon to simulate the outflow of the model to the coastal lagoon. Seasonal streams that cross the model domain were assigned as seepage faces (i.e. constant head BC, with constraints to only allow flow out of the model and not in). Well boundary conditions were assigned to nodes slice within irrigated areas not supplied by surface water dams. Abstraction rates were spatially distributed according to calculated water demand and irrigation efficiency for each specific plot of agricultural land in areas not supplied by surface water dams. Wells abstracting for golf courses were included within the area of the Campina de Faro (M12). When simulating periods prior to the year 2000, average annual public supply abstraction rates were assigned to nodes in the vicinity of municipal well fields. Additionally, irrigation return flow was added to recharge over agricultural areas as 15% of the calculated abstraction rate for all irrigated areas (including surface water) as 2^{nd} type (Neuman) constant flow rate BC. A spatially uniform return-flow rate was set, as the model discretization does not follow the spatial distribution of land use patterns. Therefore, total return flow ($6.5x10^6$ m^3/a) was divided by the total area of the BC, which does lead to some artificial spatial re-distribution of water.

Mass-transfer BCs (3rd type Cauchy) were assigned to the same nodes as used for return-flow to represent excess N from fertilizer application, with values equal to the calculated concentration in return-flow and transfer rate equal to the imposed fluid flux rates. Total mass calculated for the model domain is distributed uniformly across the BC area, similar to return-flow. Time-steps were defined as automatic time-step control with a forward Euler/backward Euler time integration scheme and an initial time-step length of 0.001 days.

5.3.2 Hydraulic parameters

Spatial distribution of hydraulic conductivity (*K*) was estimated by inverse modelling under steady-state conditions for the period prior to 1999, using the Gauss-Marquardt-Levenberg method as implemented in the nonlinear parameter estimation software PEST (Doherty 2002). Uniform hydraulic property zones were considered for all aquifers except the Campina de Faro (M12), São João da Venda-Quelfes (M10) and Luz-Tavira (M15). The latter two aquifers were divided into zones according to outcropping geology from the Jurassic, Cretaceous and Miocene. The Campina de Faro (M12) was subdivided into three vertical layers with distinct parameter zones for the phreatic and semi-confined aquifer layers; the aquitard was set as an internal no-flow boundary, which although physically inaccurate, was necessary to avoid vertical transport of contamination due to an artificially high value of dispersivity. An additional parameter zone was set along the elements adjacent to the permeable fault. During the calibration process it was found that groundwater flow from Jurassic limestones in M10 and M9 towards the fault was being hindered by the lower-permeability Cretaceous limestone of M10, forcing the calibration towards unrealistic parameter values. Therefore, the parameter zone representing the Jurassic limestone was extended between the outcrop in M10 and the M9 aquifer, solely in the bottom layer. Horizontal *K* was assumed isotropic (K_x=K_y) and an order of magnitude greater than vertical ($K_x = K_y = 10K_z$).

As can be seen in Figure 5.3 (a), the model provides a good fit between observed and simulated head, with the optimal parameter values presented in Table 5.3. Error has a normal distribution (Figure 5.3 (b)), although larger residuals tend to be located in the eastern sectors, as can be

seen from the spatial distribution of the error presented in Figure 5.4. This is likely due to a mixture of a higher density of observation points in the west providing a greater weight during the calibration process and the lack of structural detail in the east oversimplifying the model in this area.

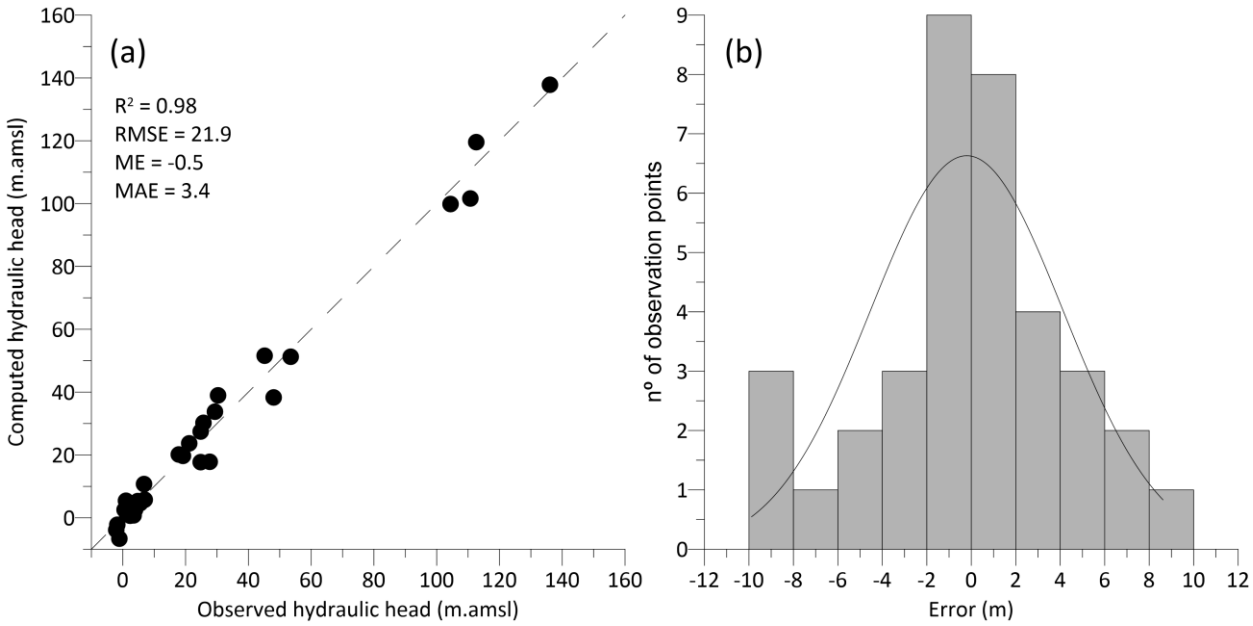

Figure 5.3 - Comparison between observed and simulated values of hydraulic head and associated summary statistics [correlation coefficient (R2), root mean square error (RMSE), mean error (ME) and mean absolute error (MAE)] and b histogram of difference between observed and simulated hydraulic head with calibrated parameters

Table 5.3 Summary of calibrated model parameters and sensitivity statistics

Groundwater body	**Parameter zone**	**Hydraulic conductivity (*K*) [m/d]**	**Sensitivity coefficient (*y*) [-]**	**Effective Porosity (n_e) [-]**
M9	Jurassic	25.8	0.42	0.2
M10	Cretaceous	1.8	1.84	0.2
	Jurassic	43.2	0.68	0.3
M11	Cretaceous	35.0	* 0.01	0.2
M12	Phreatic (PQ)	4.5	0.48	0.1

Groundwater body	Parameter zone	Hydraulic conductivity (*K*) [m/d]	Sensitivity coefficient (*y*) [-]	Effective Porosity (n_e) [-]
	Semi-confined (M)	6.0	0.41	0.1
M13	Jurassic	3.5	2.01	0.1
M15	Cretaceous	$4x10^{-4}$	* 0.01	0.05
	Miocene	43.2	0.44	0.01
	Jurassic	2.9	0.35	0.1
Fault	-	1000.0	0.56	0.2

*insensitive parameter

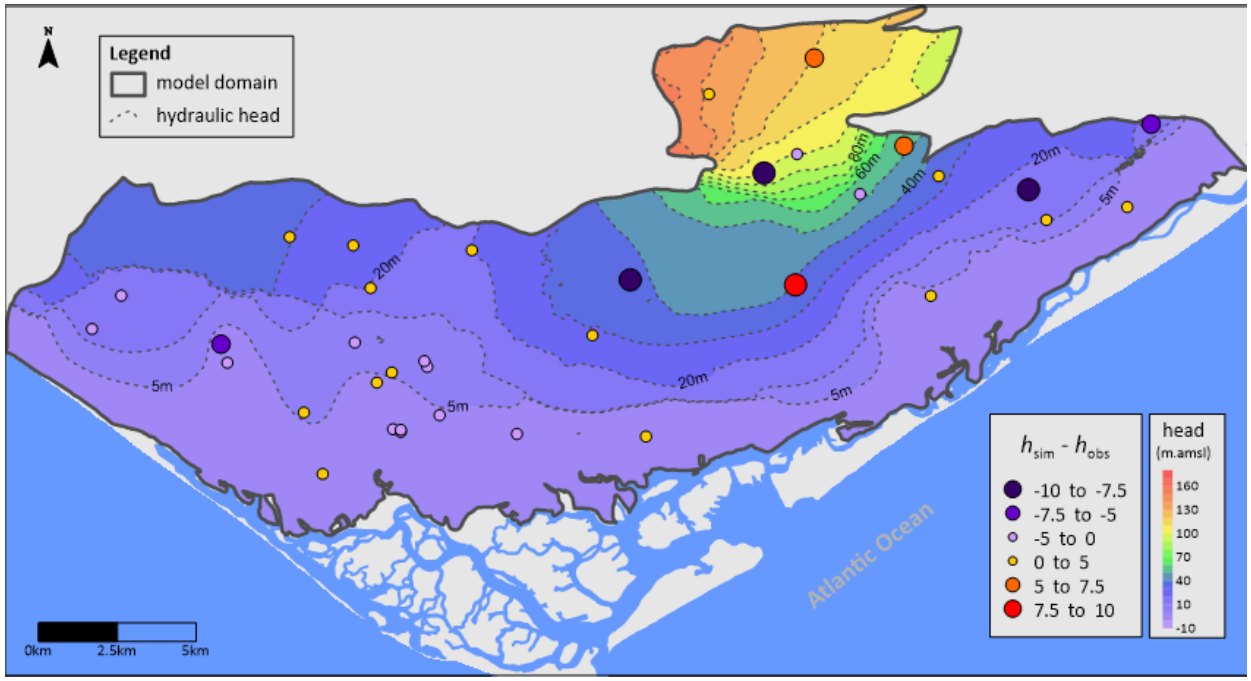

Figure 5.4 - Simulated hydraulic head under pre-2000 conditions and spatial distribution of error between observed and simulated hydraulic head at observation points with calibrated parameters

5.3.3 Transport parameters

Zones of uniform effective porosity (n_e) matching those of K were assumed and values were manually calibrated by trial and error for a 17-year simulation between 1995/96 and 2012/13, to obtain the best fit with average observed nitrate concentrations in 2012/13. Initial conditions were interpolated from average observed values during 1995/96. Calibrated values for n_e are presented in Table 5.3. Uniform values of longitudinal and transverse dispersivity were assumed as 50 m and 5 m respectively as a compromise between numerical stability and realistic parameter values according to the literature (Gelhar et al. 1992; Roseiro 2009). These are likely overestimated for the sandy aquifers, however there is insufficient data to constrain the model parameter.

Overall the model is able to simulate changes in nitrate concertation between 1995/96 and 2012/13, replicating trends across the system and with a relatively uniform distribution of error, with one notable exception (Figure 5.5 and Figure 5.6).

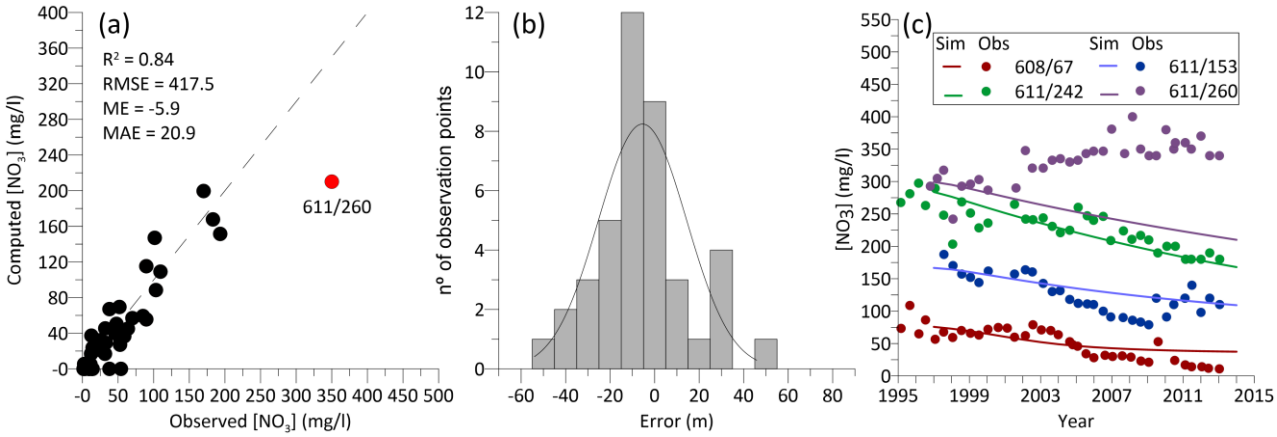

Figure 5.5 – (a) Comparison between observed and simulated values of NO3 concentration and associated summary statistics [correlation coefficient (R2), root mean square error (RMSE), mean error (ME) and mean absolute lute error (MAE)], (b) histogram of difference between observed and simulated nitrate concentration with calibrated parameters, and (c) time series of nitrate concentration at selected well

Observed values at well 611/260 increased during the considered period, which the model is unable to replicate. The observed increase is believed to be caused by increasing nitrogen loads in the southern area of the aquifer, which is most likely caused by leaching of excess

fertilizer and the slow migration of groundwater with higher NO_3 concentrations toward the south (Stigter et al. 2011). However, as the initial conditions used in the model are based on interpolated values from 1995/96, the point of highest concertation at that time is already found on well 611/260, which then flows away as the model is run forward. In practice, higher concentrations may have been further up gradient, flowing toward the well and causing the observed increase. On the other hand, it may be that there are other factors or sources that are not accounted for in the model.

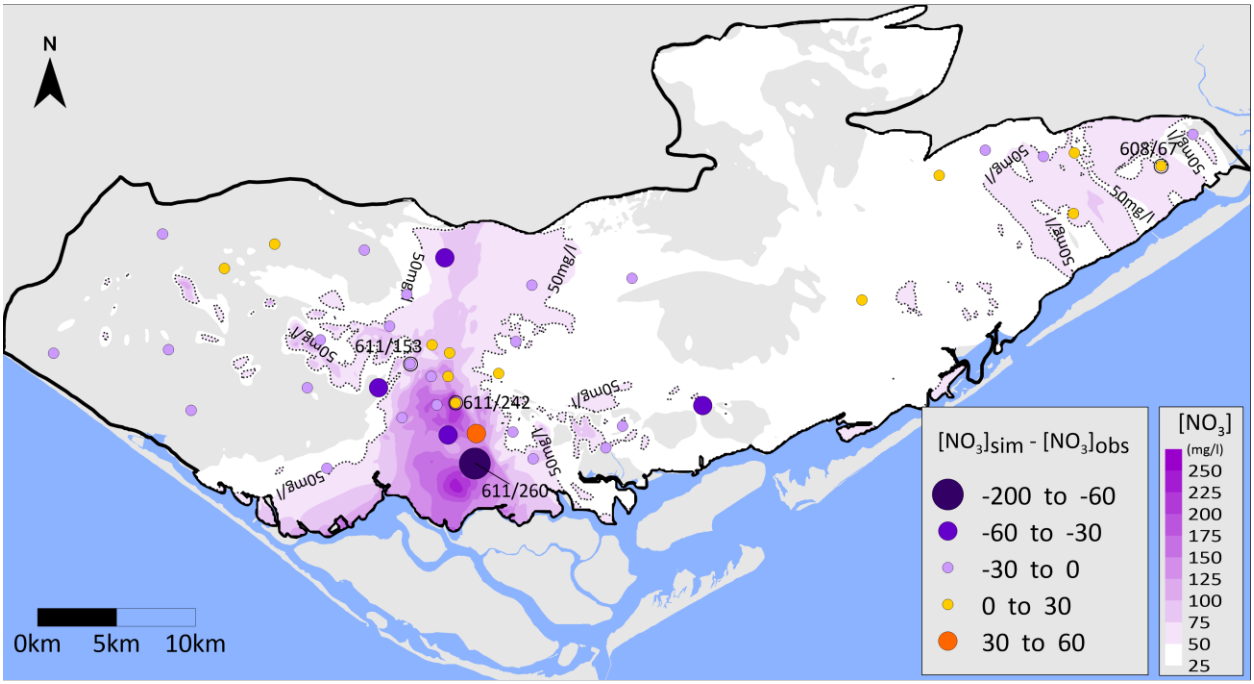

Figure 5.6 - Simulated distribution of nitrate concentration in 2013 and spatial distribution of error between observed and simulated values at observation points with calibrated parameters

5.3.4 Return-flow

This section is describing a model run that is distinct from the calibration run, since the calculated nitrate loads do not account for the high concentrations measured in groundwater in the study area, with the exception of the M15 Luz-Tavira (however, this is likely an artefact of the model as discussed above). A 30-year simulation shows that nitrate concentrations should not exceed 150 mg/l and fail to match observed values at observation wells. Prior research has

shown that the high values of nitrate observed in the field is most likely caused by irrigation return flow iteratively concentrating the contaminant (Stigter 2005; Stigter et al. 2015). In fact, by the end of the simulated period, 56% of the nitrate load is being captured by abstraction wells and only 23% is reaching the coast. To test this hypothesis, a subsequent 30-year simulation was run, distinct from the calibration run, in which abstracted mass was reapplied as an additional nitrate load every five years. While the calibration run starts with initial concentrations interpolated from observation registered in 1995/96, the simulated described in this section starts with zero nitrate concentration in order to attempt reaching observed values within 30 years, by 1995/96.

As can be seen in Figure 5.7 recycling does account for a significant increase in the areas identified as NVZs, yet still does not reach observed values in the M12 Campina de Faro aquifer. This can be attributed to either simplifications in the model leading to unaccounted sources or historically higher nitrate loads than the ones considered in this modelling exercise. Thus, although the model at this stage cannot definitively demonstrate that return flow has caused current levels of contamination, it does contribute to the growing amount of evidence to support the hypothesis.

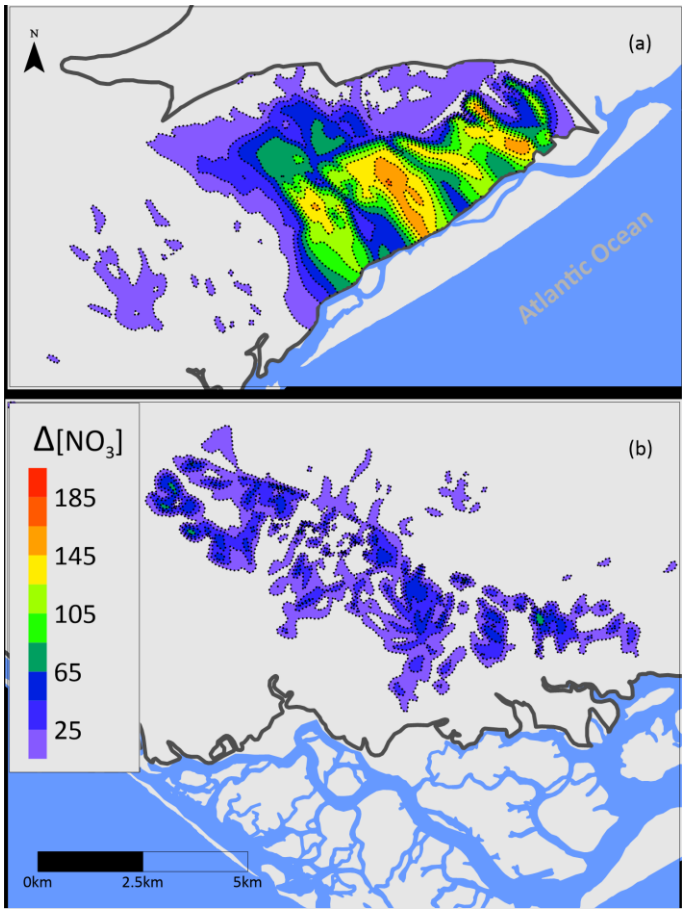

Figure 5.7 - Simulated impact of recycling on nitrate concentrations after 30 years in the (a) Luz-Tavira and (b) Campina de Faro NVZs. Δ[NO3]stands for the difference between nitrate concentration calculated by the model with and without recycling

5.3.5 Mitigation scenarios

As per the Action Plan for the NVZs implemented in 2010, current maximum allowed nitrogen loads are 3.5 kg/ha/a for temporary crops, although the predominant land-use is for permanent crops with a maximum permitted load of 1.89 kg/ha/a. Monitoring of agricultural practices has shown a 100% compliance. Thus, to simulate a 'worst case' scenario of current agricultural practices (*business as usual* (BAU)) a constant rate of 3.5 kg/ha/a was applied to irrigated areas. To highlight the impact of current practices a second scenario is considered with no nitrogen loading whatsoever.

Besides the previous two scenarios, the impact of three mitigation measures are assessed: a switch to surface water supply for irrigation, and two previously proposed managed aquifer recharge (MAR) schemes. Two MAR schemes have previously been proposed for the M12 Campina de Faro area: (1) increased infiltration along the Rio Seco stream (Roseiro 2009), and (2) injection of rainwater harvested from greenhouse run-off, into large diameter wells in the *Campina de Faro* (M12) (Costa et al. 2015b, 2020). Locations of the selected MAR sites are shown in Figure 5.8. Roseiro (2009) estimated available average stream flow for infiltration at $2x10^6$ m/a, though the infrastructure to infiltrate this water would have to be installed. Costa et al. (2015) calculated available average annual rainfall occurring over selected greenhouses on the *Campina de Faro* (M12) at 1.63 $x10^6$ m^3/a, although in practice this value may be slightly lower due to technical issues related to rainwater collection and transfer to the injection wells.

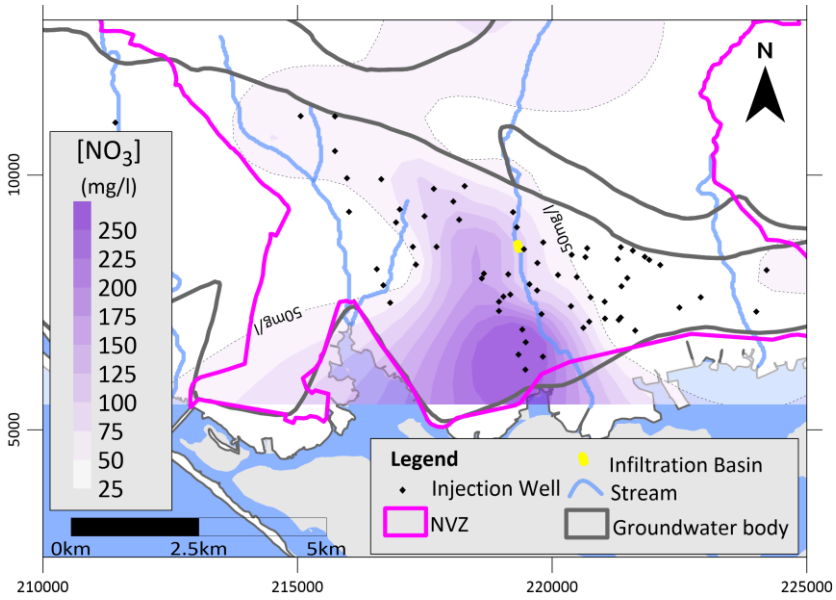

Figure 5.8 - Location of proposed managed aquifer recharge (MAR) schemes and interpolated nitrate concentration in 2013

5.3.6 Climate scenarios

An ensemble of scenarios for recharge and crop water demand was sourced from the study by Stigter et al. (2014). These authors obtained temperature and rainfall data from scenarios from the ENSEMBLES project (van der Linden and Mitchell 2009), that result from the combination of

a Regional Climate Model (RCM) and a Global Circulation Model (GCM), with a 25x25 km resolution and a balanced CO_2 emission scenario A1b. Three climate models cover the study area and period up to 2100: CNRM-RM5, C4IRCA3 and ICTP-REGCM3, for which they bias corrected using a control period from 1980 to 2010. Bias-corrected values were then applied to develop total and net (taking into account crop water demand) groundwater recharge scenarios, using the soil water budget. An in-depth description of the development and results from these climate and recharge scenarios can be found in Stigter et al. (2014).

The 'worst' and 'best' case scenarios in terms of reduction in recharge and increase in crop water demand were simulated to assess the range of potential impact from climate change. As the model applied in the current study is not calibrated for transient flow conditions, average annual values for two distinct periods were applied under steady-state flow conditions (and transient mass). Stigter et al. (2014) provide values for average decrease/increase in recharge/crop demand for two periods: 2020-2050 and 2070-2100 (Table 5.4). To account for the gap from 2050 to 2070, values from the initial period were maintained until 2065. Climate change simulations were run under BAU conditions, assuming no change in water management or mitigation measures.

Table 5.4 Estimated relative changes in recharge and crop water demand from climate change (adapted from Stigter et al. (2014))

Parameter	**2020-2050**		**2070-2100**	
	worst	**best**	**worst**	**best**
Recharge	-27%	23%	-48%	-21%
Crop water demand	31%	0%	42%	18%

5.4 Results

5.4.1 Mitigation scenarios

Simulated scenarios are compared at two monitoring points, 211/242 and 211/260 (Figure 5.9), which have the highest registered nitrate concentrations in the area. Monitoring point 211/242

is in the midst of the Campina de Faro NVZ, with 211/260 downgradient and close to the coastline. Results show that under BAU, nitrate concentrations at all monitoring stations will not drop below 50 mg/l before 2080, and even in the best-case scenario not before 2060. As previously described, the model underestimates values at 211/260 by about 100 mg/l; therefore, time until compliance may be significantly longer in practice. A very rough and rudimentary offset of the 211/260 time-series by 100 mg/l suggests that compliance at this point would only be reached sometime after 2100. However, values at 211/242 reach 50 mg/l much earlier, around the year 2050. There is a need to clarify the cause of elevated values at 211/260, and identify whether these are due to an unidentified point source or the downgradient movement of the contamination plume.

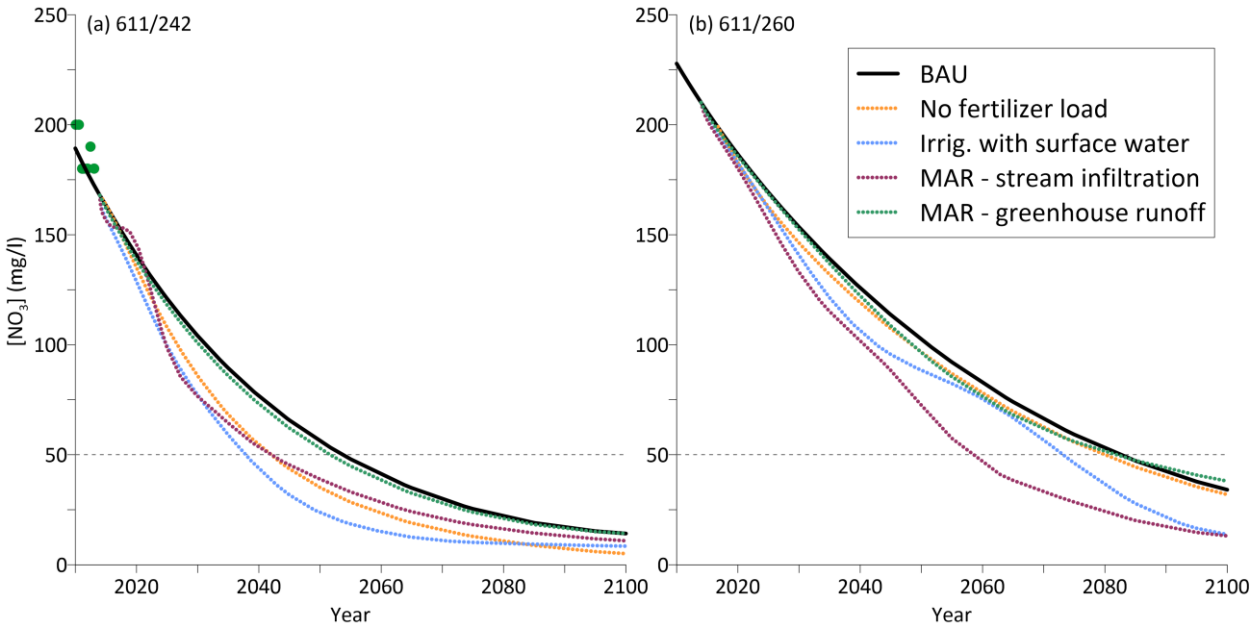

Figure 5.9 - Simulated impact of water use and mitigation measure scenarios on nitrate concentrations at monitoring wells: (a) 611/242 and (b) 611/260

Comparing the BAU scenario to that with no fertilizer load highlights the impact of current agricultural practices. The effect of removing additional nitrate loading is most evident up-gradient at 211/242, as the monitoring point is surrounded by agricultural land, reducing time to compliance by about ten years. However, further down-gradient the impact on 211/260 is negligible, suggesting that the effects are localized. Observing the difference in discharge rates

to the coastal lagoon (Figure 5.10) corroborates this, as the impact of current agricultural practices has little effect.

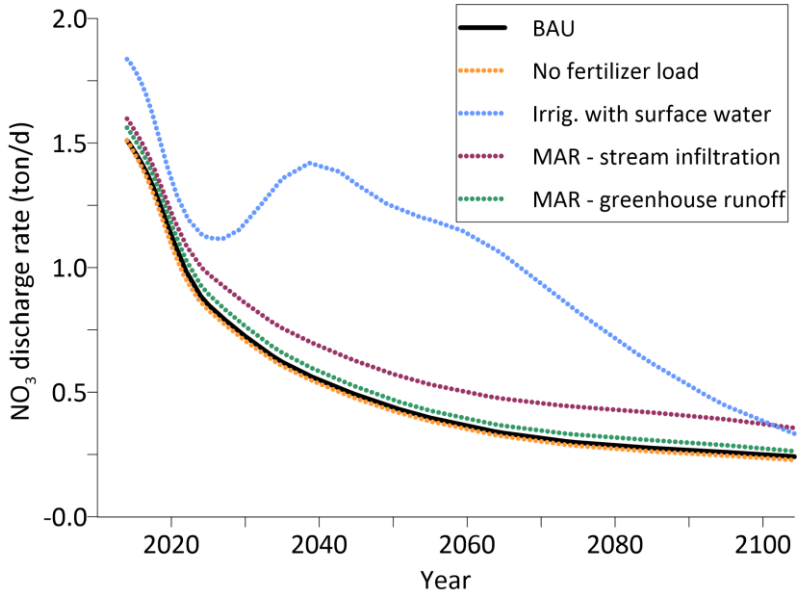

Figure 5.10 - Simulated nitrate discharge rates to the Ria Formosa coastal lagoon

Switching to surface water supply for agricultural irrigation has a dual effect: (1) reduced abstraction rates increase hydraulic heads, and thus flow rates towards the coast, and (2) nitrate is no longer captured by abstraction. The increased flow rates enhance the 'flushing' of the system, similar to what has already happened in the M15 Luz-Tavira system during the early 2000s. This causes the most rapid decline in observed nitrate concentrations at 211/242. At 211/260 values decrease rapidly until 2050, with a decline in the rate of reduction between 2050 and 2060 caused by the existing nitrate in the system being 'pushed' towards the coast, with a subsequent decline to full compliance around 2075. Although this scenario leads to one of the fastest declines in observed nitrate concentrations, the impact on mass discharge to the coastal lagoon is significantly higher than any of the others. It must be considered that absolute discharge rate values may not be realistic, as they are accounting for by interpolated quantities of mass imposed on the model as initial conditions, and should therefore only be used comparatively. Switching to surface water for irrigation leads to discharge rates three times higher than any other scenario, as mass is no longer being captured by abstraction. Algal

blooms associated to elevated concentrations of nitrate in the coastal lagoon are already a concern, and groundwater has been identified as one of the main sources (Stigter et al. 2007; Malta et al. 2017). Reducing nitrate discharge rates would likely be beneficial to water quality in the Ria Formosa. On the other hand, future mass discharge rates for the surface water for irrigation scenario are similar to current simulated mass discharge rates, suggesting that at least the *status quo* could be maintained.

Of the two MAR schemes, the injection of greenhouse run-off has the least effect with very slight reductions in nitrate concentrations at both observation points and slight increase in mass discharge rates to the lagoon. As the additional infiltration is spread out over the Campina de Faro NVZ, impacts are localized and the change in water budget is insufficient to create significant increases in hydraulic gradient. Enhancing stream infiltration on the other hand has significant impact, reducing time to compliance at 611/242 and 611/260 by 10 and 20 years respectively; however, this effect is more impactful in wells near the river, whereas wells further away are less impacted. Mass discharge rates to the lagoon increase by about 10% in comparison with the BAU scenario. As additional recharge is concentrated in a smaller area, the impact on flow rates is greater. The location within the center of the Campina de Faro NVZ has a triple effect of acting as a hydraulic barrier (enhancing capture to wells upgradient), 'pushing' the contaminant plume sideways (also enhancing capture to wells) and diluting the plume where it is the most concentrated.

5.4.2 Climate scenarios

The uncertainty regarding climate change within the short to mid-term (i.e. 2050) is evident in the range of results presented in Figure 5.11. Nitrate concentrations at observation point 611/242 reach 50 mg/l almost 45 years later in the 'worst' case scenario than in the 'best'. However even in the best case, acceptable nitrate concentrations at 611/242 and 611/260 will only be reached by 2045 and 2075 respectively, if BAU is maintained. In the worst case, elevated nitrate concentrations can be expected to last into the next century.

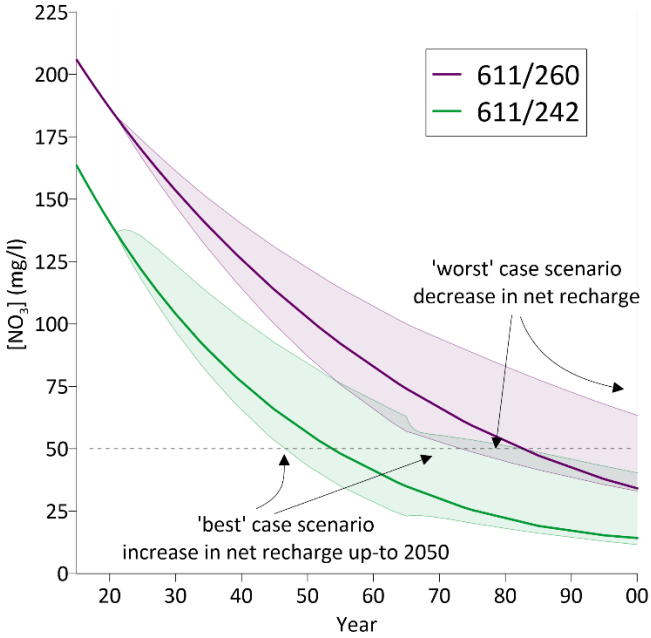

Figure 5.11 - Simulated impact of climate change uncertainty on nitrate concentration at monitoring points 611/242 and 611/260

The impact of the ‘best’ case scenario on discharge rates to the coastal lagoon is minor, with a slight increase associated to higher hydraulic gradients from extra recharge up to 2050, as seen for the mitigation scenarios. From 2050 onwards, as well as for the ‘worst’ case scenario, mass discharge rates are lower than for the BAU simulation. Less recharge and higher abstraction rates cause hydraulic heads to lower across the entire system, in some cases inverting the hydraulic gradient. This reduces flow rates towards the coast, and by association, the mass discharge rate (Figure 5.12).

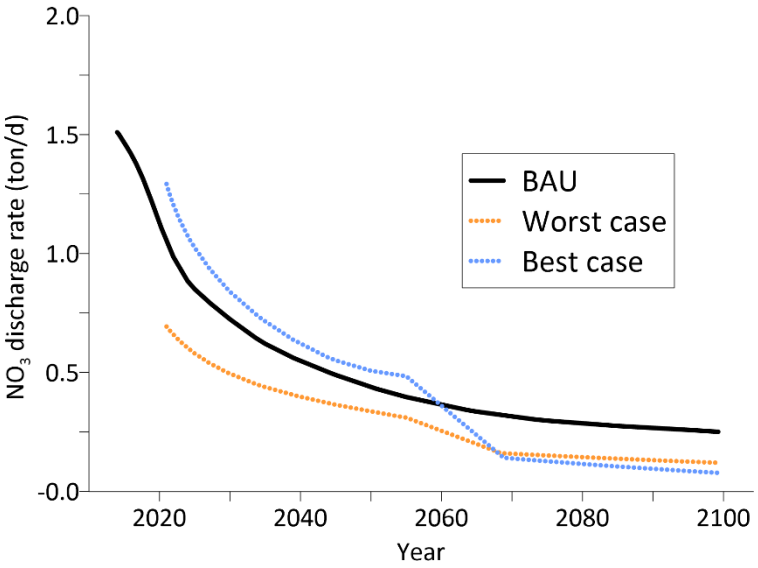

Figure 5.12 – Impact of climate scenarios on nitrate discharge to the Ria Formosa

By 'trapping' contaminant for longer, the amount that is captured through pumping also increases (Figure 5.13. However, despite the increase in abstraction rate being greater than the reduction in discharge rate, this does not lead to faster decrease in observed concentrations.

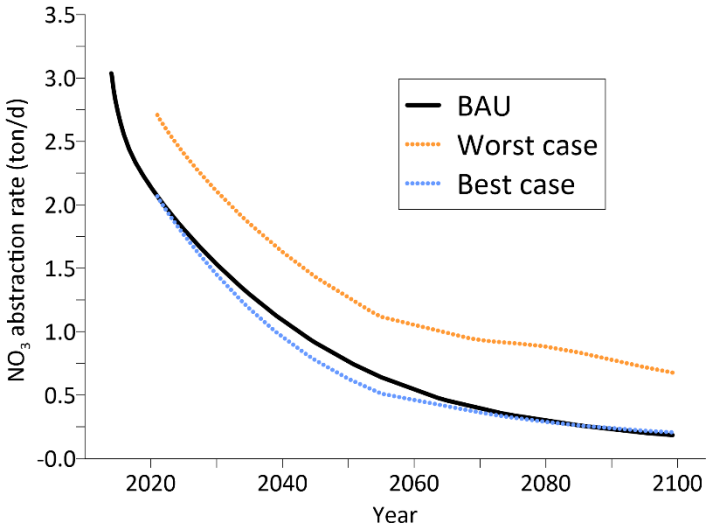

Figure 5.13 - Impact of climate scenarios on nitrate abstraction rate from pumping

The predicted climate changes may have significant impacts on groundwater level, however, this is a subject out of the scope of the current work. Nonetheless, it is important to infer that large drawdowns and hydraulic inversion would, without a doubt, cause seawater intrusion, making groundwater unfit for use. Although any reduction in discharge to the coast will cause the fresh-saltwater interface to move inland, how far it would reach inland cannot be accurately determined based on a flow model that does not account for the effects of density contrasts between fresh water and seawater. Predicting seawater intrusion risk with any degree of accuracy would require a fully density-coupled flow and transport model, with the necessary model simplifications capable of decreasing the computational weight in order to run simulations at the scale of the problem.

5.5 Discussion

Results demonstrate that the compliance with EU policy cannot be met within the set deadlines, despite the 100% compliance with good agricultural practices in the area. Observed nitrate concentration in groundwater does not reflect current land-use but, instead, is the remnant of past nitrate loading – which cannot be significantly reduced by changing agricultural practices. This highlights the disconnect between hydrogeological and policy time-scales, with the latter not reflecting the reality of the 'slow' movement of water and mass within the subsurface. Jackson et al. (2008) demonstrated similar issues for Chalk catchments in the United Kingdom (UK), where retardation in the unsaturated zone of the porous matrix will prevent control of nitrogen levels being achieved within the timescales demanded by European and UK legislation. Similarly, Musacchio et al. (2020), shows the same issue in the Lombardy plain in Italy, aggravated by local governance issues.

So far, the discussion of mitigation measures has focused on decreasing nitrate levels in groundwater, with little thought towards the impact of increasing nutrient loads to the coastal lagoon. Recent work by Malta et al. (2017) has shown that, on an annual basis, nutrient input to the Ria Formosa is dominated by waste water treatment plant discharge and groundwater outflow. They also found that extreme events, such as strong rainfall and oceanic upwelling,

strongly disrupt the lagoon's nutrient exchange pattern from a nutrient export to import. Thus, if the frequency of these events will increase, as predicted under global climate change, this will have great consequences on the annual nutrient budget and consequently on the ecological functioning of Ria Formosa lagoon. Understanding the long-term impacts of groundwater's contribution to the lagoon's nutrient load may be important to maintaining the ecological wellbeing of this important ecosystem. Any discussion of how to manage water and land in the catchment should take into account current and future impacts on the lagoon. Considering the model results when switching to surface water for irrigation, one would expect a decrease in discharge of nitrate to the Ria Formosa, due to the dilution effect as shown in the past (Stigter et al. 2011). However, results show an increase of groundwater nitrate discharge to Ria Formosa for such a scenario. This is likely because changing to surface water in the model means an interruption of irrigation wells, which, when extracting groundwater, were also removing NO_3 and acting as a sink for this contaminant. What the model shows is the fact that the values of N discharge to Ria Formosa end up being higher, since the output of N from the models created by the wells is no longer there.

The numerical model used in the current work does not take into account processes in the unsaturated zone, nor the impact of seasonal variability. All simulations for the future assume that nitrate rates reaching the saturated zone reflect current loading, however this may not be the case. There are currently no available data to characterize the transport processes through the unsaturated zone in the study area. However, work in other areas (i.e Jackson et al. (2008)) has shown that the unsaturated zone plays an important role in retarding nitrate reaching groundwater. Denitrification is the dominant nitrate attenuation process in the subsurface system; and although conditions conducive to denitrification may not be encountered in many unconfined aquifers (i.e. Wang et al. 2016), long residence times mean that improved understanding of even low rates is required as these may still partially alleviate nitrate problems (Rivett et al. 2008). It is possible that the applied model overestimates concentrations in the long-term due to not accounting for such effects.

Furthermore, predicted increases in the variability of rainfall and recharge for the coming century may also increase leaching and dilution processes. The effect of fluctuating water table

on solute concentrations can be the dominant control on solute concentration in mobile groundwater (Fretwell et al. 2000). Jackson et al. (2008) suggest that it is important to establish whether the effects of this fluctuating region on solute transfer have significant consequences for future time-scales of trend reversal or absolute magnitudes of concentrations reached. In fact, observing fluctuations in nitrate concentrations within the Ria Formosa catchment, a peak can be seen at most monitoring points associated to the high rainfall (and high groundwater level) year wet season of 2009/2010. Given that predicted climate change in the short to mid-term indicates an increase in seasonal and inter-annual variability of rainfall, similar occurrences can be expected to become more frequent. There is a need for further work to address the impacts of these inter-linked issues for greater confidence in predicting attenuation times and designing mitigation measures.

The uncertainty associated with the hydrological processes of climate change scenarios is a matter that must be considered when simulating future scenarios. Her et al. (2019) attempted to include some climate uncertainty in their results by considering a worst- and best-case scenario in terms of recharge and increase in crop water demand and simulated climate change scenarios under BAU conditions. The results between the worst- and best-case scenarios on the evolution of the nitrate contamination show there could be a time lag of 50 years or more between each, to achieve compliance with the EU Directive, i.e., 50 mg/l.

Regarding the development of the model, two main sources of uncertainty can be highlighted, one related to the parameterization and the other to the conceptual model in what refers to the hydraulic connections between the different aquifers modelled. Regarding the parameterization, it must be considered that parameters such as effective porosity were calibrated manually by best-fit trial and error, leading to physically unrealistic values. The fact that they are unrealistic suggests they are compensating for model structural inadequacies. This means that there are issues with the model construction/setup that really should be explored further. Another source of uncertainty of the developed model relies on the hydraulic connections between the different aquifer formations in the study area, in particular with the case of M12 and the upstream aquifers. Since the aquifers in Algarve are considered independent groundwater management units, mitigation measures are applied at the individual

scale of such systems. Yet, as mentioned before, water balance analysis of M12 suggests there are groundwater contributions to this system from the upstream aquifers (Almeida et al. 2000), although, how and where these occur, and what volumes are involved, is a matter not well understood and there is need for further research. The results of the large-scale model presented demonstrate that land use practices in one aquifer system can influence groundwater quality in other aquifer systems, in particular for the case of M12. This reflects the importance of managing these units as a whole, instead of individual systems. A better assessment of such contributions is a crucial step in order to provide a more robust model that can better represent not only the distribution of groundwater flow in M12, but the dispersion and evolution of the nitrate plume as well. Although some attempt to address the impact of parameter uncertainty on predictive uncertainty has been made here, the applied parameterization approach (using zones) does not allow for an exploration of the system's hydraulic property heterogeneity, nor the variability in pressure (such as abstraction or recharge). As shown by Moore and Doherty (2005), this heterogeneity can play an important role in controlling the simulated evolution of nitrate contamination in both the past and future. The large-scale (and consequently, relatively long run-times) of the model, precluded the ability to use a large number of parameters during history-matching and predictive uncertainty analysis. In future work, when exploring remediation and/or resource management interventions, it will be necessary to explore options to simplify model construction in order to characterize and quantify the influence of model parameters on predictive uncertainty.

Regarding the quality status of the aquifer, in particular, the nitrate contamination, there are several options for remediation, removal and attenuation (e.g. Rivett et al. 2008; King et al. 2012; Huno et al. 2018). These options can rely on natural and engineered processes, *in-situ* and *ex-situ*. Engineered *ex-situ* solutions rely mostly on pump-and-treat methods, which are often costly and difficult to apply, with beneficial results usually lasting a reasonable time frame, whereas *in-situ* approaches rely mostly on the enhancement of natural degradation of the contaminant into less harmful products (King et al. 2012). The *in-situ* approach is not appropriate for contaminants that are spread over large regions or are recalcitrant to degradation (King et al. 2012), which is the case of diffuse nitrate contamination at the M12

NVZ, spreading over an area of nearly 100 km^2. While natural attenuation processes result in small amounts of nitrate removal from groundwater, engineered processes are able to achieve significantly higher nitrate removal from groundwater; however, the challenges of secondary pollution need to be addressed in adopting these technologies for groundwater treatment for potable use (Huno et al. 2018). Both *ex-situ* and *in-situ* methods are typically accompanied by removal or reduction of the sources of contamination, which are particularly important for successful long-term solutions to the nitrate problem at larger or basin scale problems (King et al. 2012).

5.6 Final remarks

Despite the implementation of the European Nitrates Directive almost 30 years ago, groundwater nitrate contamination is still a serious threat to ecosystems and human health. This is the case for Campina de faro aquifer system in southern Portugal, which has been within a NVZ since 1997.

Considering the NVZ at Luz-Tavira aquifer, nitrate concentration has shown consistent decrease to values below or close to the legal limits, and it is expected that EU compliance for this groundwater body will be achieved within the EU deadlines. It is likely that the change of irrigation water source from groundwater to surface water has had an important contribution for this. On the other hand, it is highly improbable that good quality status will be attained in the Campina de Faro NVZ within the deadlines imposed by the EU. Despite the beneficial effects of reducing fertilizer use, current high levels of nitrate do not reflect the good agricultural practices that are in place, nor will these have significant short to mid-term effects on concentrations in groundwater. Even if large-scale mitigation measures are put into practice, model results suggest that it will be decades before nitrate concentrations drop below target levels. The hydrogeological properties and elevated residence time within the system mean that contaminants will always take a long time to be 'flushed' out. Results from simulated mitigation measures suggest that the most effective solution is to enhance stream infiltration along the Rio Seco, as this both dilutes the plume and enhances capture by abstraction;

however, even so, decades are needed until compliance can be met. Efforts to demonstrate the feasibility of such a MAR scheme were carried out by the FP7 funded MARSOL project - FP7/2007-2013 GA619120 (Leitão et al. 2017). This MAR scheme would have the added benefit of enhancing water security by storing surface water which is otherwise discharged to the lagoon. Whether reduced surface runoff to the lagoon has a detrimental impact is unknown.

Groundwater remediation is one of the most difficult tasks in environmental clean-up, especially when it comes to large areas. Therefore an ensemble of solutions, some local, some more regional, including land management measures, should be considered in order to attain a significant reduction of time in achieving good quality status of groundwater bodies.

Despite the simplifications inherent to the approach, this large-scale model supplies an important first assessment of the nitrate transport in groundwater within the saturated zone within the Ria Formosa catchment, as well as discharge rates to the coastal lagoon. Significant improvements in the characterization of the current three-dimensional distribution of nitrate in groundwater might improve estimates of nutrient discharge rates to the lagoon. However, obtaining representative measurements of groundwater discharge and associated contaminant concentration is complicated given the highly heterogeneous nature of the groundwater system, with large variability along the coastline; thus, numerical modelling likely provides the most reasonable approach to understanding the spatiotemporal distribution of nutrient loads reaching the lagoon via groundwater.

Aquifers in the Algarve are classified as “groundwater management units”, following the systematic classification by Almeida et al. (2000a), which has led to most resource assessments and management policies being applied at the scale of individual units. The connections between them and the existence of underlying water-bearing layers is often ignored or not well understood. The simplified large-scale model of the aquifer systems that discharge into the Ria Formosa highlights that these systems should not be considered as individual groundwater bodies, as water and land use practices associated to one system can cause impacts on others. The approach applied here should be extended to understand how uncertainty in aquifer connectivity, parameters and water budget components affect the predictive uncertainty.

The results presented in the current work show evidence that solutions for nitrate contaminated groundwater bodies should rely in a set of measures, some local, some more regional, in order to significantly reduce the needed time to achieve compliance with EU directives in regards to the quality status of groundwater bodies.

Chapter 6: Climatic teleconnections with groundwater levels in the Algarve

The current chapter refers to the description and characterisation of the groundwater levels at Central Algarve aquifers, and how these are controlled by climate. In order to do so, two case-studies with different analysis have been considered, namely: case-study a) karst aquifer Querença-Silves (Q;S) and case-study b) the aquifers in connection with the ria Formosa.

Regarding case-study a) Querença-Silves karst aquifer, the study focus on the quantification of the effect of the large-scale atmospheric and oceanic circulation pattern NAO and the geological effect on groundwater levels and is based on the congress presentation (Costa et al. 2015d) and the peer reviewed paper Neves et al. (2016).

As for case-study b) Central Algarve aquifers in connection with Ria-Formosa, the analysis focus more on the effect of the different atmospheric teleconnections patterns on the natural groundwater fluctuations and is based on the works Neves et al. (2019a) and Malmgren et al. (submitted) of which, the author of this dissertation is a co-author.

- Costa L, Neves MC, Monteiro JP (2015b) "Efeito Conjugado da Geologia e do Clima na Piezometria do Aquífero Querença-Silves – Combined Geological and Climatic Forcings on the Querença-Silves Piezometry". 9º Simpósio de Meteorologia e Geofísica da Asosciação Portuguesa de Meteorologia e Climatologia – APMG2015. Hotel Vila Galé Albacora, 16 a 18 de Março, Tavira. Disponível em http://www.apmg.pt/?p=933

- Neves MC, Costa L, Monteiro JP (2016) Climatic and geologic controls on the piezometry of the Querença-Silves karst aquifer, Algarve (Portugal). Hydrogeol J 24:. https://doi.org/10.1007/s10040-015-1359-6

- Neves MC, Costa L, Hugman R, Monteiro JP (2019a) The impact of atmospheric teleconnections on the coastal aquifers of Ria Formosa (Algarve, Portugal). Hydrogeol J 27:2775–2787. https://doi.org/10.1007/s10040-019-02052-6

- Malmgren K, Neves MC, Gurdak J, Costa L, Monteiro JP (submitted) Mediterranean groundwater response to climate variability coupling in California and Portugal. Hydrogeology Journal. Manuscript Number: HYJO-D-21-00129R1

6.1 Introduction

The impact of climate variability on groundwater systems is central to the successful management and sustainability of water resources. The issue is even more important in semi-arid regions like the Algarve (Portugal), where climate models predict a progressive reduction in water availability during the 21st century, due to diminished precipitation and increased potential evapotranspiration (Santos and Miranda 2006).

Aquifers have been buffers against climate variability in the past, especially in semi-arid regions like the Algarve, the southernmost province of Portugal. Rainfall projections for the end of the twenty-first century in Portugal are alarming, particularly in the south of the country where decrease in precipitation may reach 20% to 50% (Soares et al. 2017). Increases in temperature, with maximum increments of 8 °C in some areas inland, may further exacerbate droughts and water shortages (Cardoso et al. 2018). Coastal aquifers are particularly sensitive owing to the threats of overexploitation and saltwater intrusion. In fact, a reduction in aquifer recharge of ~25 % is expected towards the end of the century in Mediterranean semi-arid areas, as shown by Stigter et al. (2014) for case studies in south Portugal, Spain and Morocco.

Atmospheric teleconnections, also known as climate patterns, are a major driver of natural long-term fluctuations in aquifer levels. They can be regarded as seesaw-like oscillations of large-scale dipoles of atmospheric pressure, and are designated that way for their long-distance impact (Bridgman and Oliver 2006). The influence of teleconnections on aquifers is evident in several parts of the world (Dong et al. 2015; Velasco et al. 2017; Zhang et al. 2017). In India and East Africa, for example, groundwater storage is strongly dependent on monsoon rainfall, which is mainly driven by the Indian Ocean Dipole (Taylor et al. 2013b; Asoka et al. 2017). Low-frequency oscillations in groundwater levels across North America, in turn, are synchronized

with patterns such as the El Niño Southern Oscillation (ENSO) and the Pacific Decadal Oscillation (Tremblay et al. 2011; Kuss and Gurdak 2014). In Europe, although earlier studies focused primarily on NAO (North Atlantic Oscillation), there is growing awareness that NAO acts in conjunction with SCA (Scandinavian pattern), EA (East Atlantic pattern) and EA/WR (East Atlantic/West Russia pattern) to control the surface water and the groundwater flow (Holman et al. 2011; Kalimeris et al. 2017; Steirou et al. 2017).

A recent nationwide study in Portugal has shown that NAO and EA together are responsible for most (80%) of the inter-annual variability of groundwater levels (Neves et al. 2019b). Despite their large spatial extent, atmospheric patterns undergo regional interactions resulting in distinctive areas of influence, even at relatively small scales. This is what happens in Portugal, where the contribution of EA to the groundwater level variability is much larger in the north (40%) than in the south (20%) of the country (Neves et al. 2019b). Furthermore, the response to climate-induced fluctuations is highly affected by local hydrogeological conditions and by human activities like irrigation and pumping, even within the same aquifer (Ferguson and Gleeson 2012b; Gurdak 2017; Corona et al. 2018). This highlights the need to improve understanding on the response of groundwater systems to atmospheric drivers at both regional and local scales.

Climate-induced variability is obviously affected by local geological conditions, particularly in karst aquifers like the Querença-Silves (QS), characterized by spatially heterogeneous geomorphologic and hydrogeologic properties (Monteiro et al. 2006b; Hugman et al. 2012). The contribution of internal (geologic) forcings to the spatio-temporal variability of piezometric levels in karst aquifers has been previously quantified in the Upper Normandy (France) (Slimani et al. 2009; El Janyani et al. 2012). As pointed out in those studies, a common feature of karst aquifers is the co-existence of a dual flow system, assisted by the fissured matrix (responsible for the capacitive function) and the conduit drainage network (responsible for the transmissivity function).

The primary goal of the current chapter is to quantify investigate the impact of climatic patterns NAO and EA on the Algarve aquifer systems and assess the contribution of the geology and the

climate to the groundwater level oscillation in the Algarve. In order to do so, two case-studies have been selected, a) the karst aquifer system Querença-Silves (QS) and b) the set of aquifers in connection with the Ria Formosa coastal lagoon.

For the case-study a) Querença-Silves karst aquifer, The primary goal of this study is to quantify the relative contributions of climate and geology to the spatial and temporal variance of the groundwater levels in this aquifer. These contributions are identified and evaluated by applying wavelet transform methods and singular spectral analysis to the groundwater time series.

For the case-study b) central Algarve aquifers in connection with the Ria Formosa coastal lagoon, the study aims to investigate the impact of NAO and EA on the coastal aquifer systems that discharge to the Ria Formosa coastal lagoon. In order to do so, the first part of the work provides a description of the main components of the long-term (30 years) groundwater level fluctuations at key locations within this coastal system. To achieve these goals, the study uses wavelet transform methods and singular spectral analysis. The ultimate aim is to understand the spatial heterogeneity in response to climate patterns and identify the anthropogenic and natural factors behind them.

6.2 Climate and geological controls of groundwater oscillation in Querença-Silves karst aquifer

6.2.1 Site description: Querença-Silves karst aquifer system

The QS aquifer system (Figure 6.1a) is the largest (324 km^2) and most important groundwater reservoir in the Algarve region (south Portugal). This region has a temperate climate with dry summer (Csa Köppen classification), monthly average temperatures between 12°C and 24°C and a total annual rainfall of about 500 mm/yr (1981-2010 climate normal). Most of the annual precipitation occurs during the 3-month winter season, while the summer months (June to August) are extremely dry, contributing to only 6% of the annual precipitation (Miranda, P., Coelho, F.E.S., Tomé, A.R., Valente 2002). As typically observed in southern Iberia, the

precipitation in the study area is characterized by large values of inter-annual variability, with large disparities between wet and dry years (Santos and Miranda 2006).

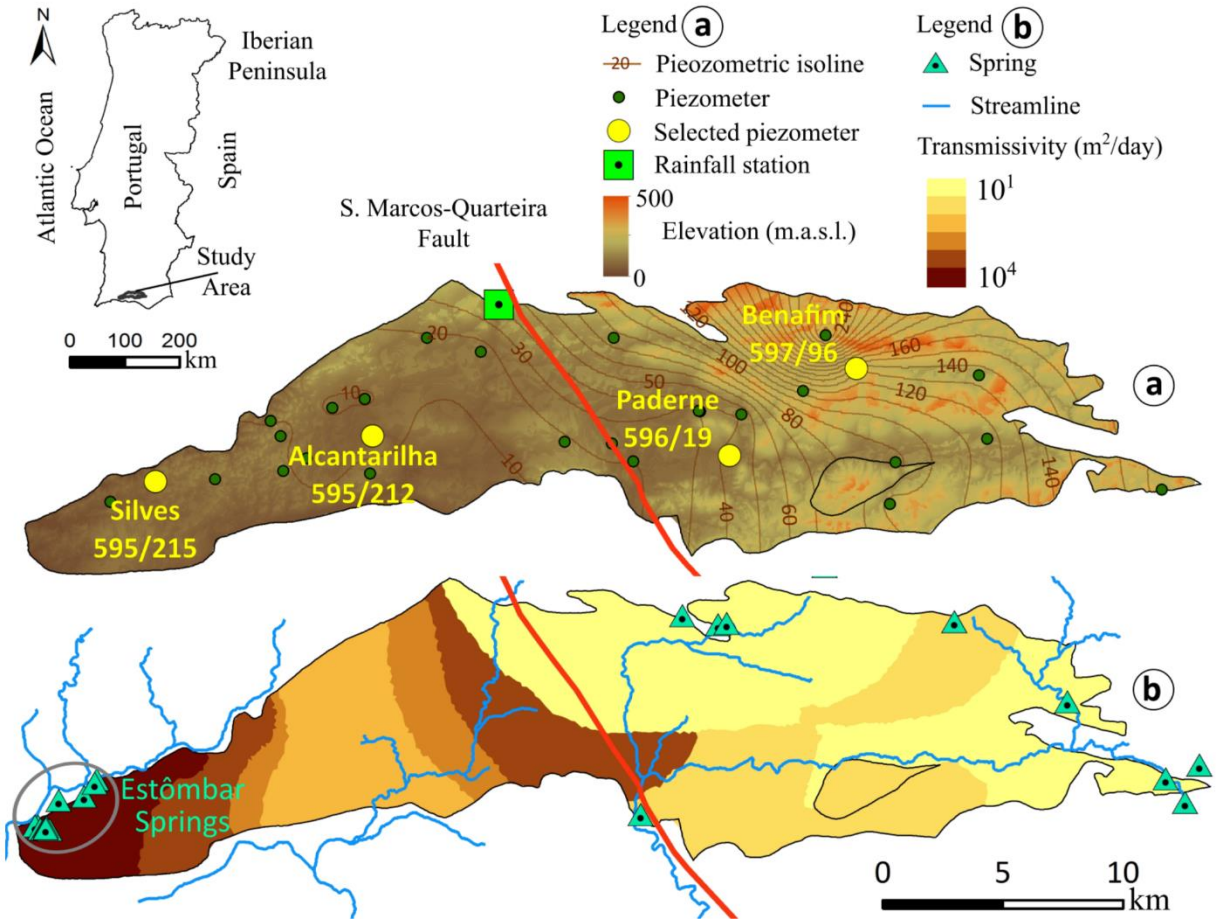

Figure 6.1 - Location of the Querença-Silves aquifer and the S. Marcos-Quarteira fault (red line) which divides the aquifer into two sectors. (a) Location of the four piezometers selected for analysis and the terrain elevation. The average piezometric isolines are computed from the average hydraulic head observed at the total 28 piezometers using the krigging linear method of interpolation. (b) Location of the Estômbar springs, among others, the stream network and the equivalent transmissivity distribution of the aquifer as calculated by Hugman et al. (2012)

The QS aquifer is formed mostly by Early and Middle Jurassic (Lias-Dogger) carbonate sedimentary rocks, which span from the Arade river estuary (to the west) to the village of Querença (to the East). It is limited to the north by the Triassic-Hettangian rocks and to the south by the Algibre thrust, a major thrust in the Algarve Basin separating the lower and upper Jurassic formations (Terrinha 1998; Monteiro et al. 2006b, 2007b). The stratigraphy of the Lias-

Dogger formation shows that the aquifer thickness increases from north to south, reaching average values of around 600 m (Manuppella et al. 1993). The most important fault in the QS aquifer is the S. Marcos-Quarteira fault (Figure 6.1), which is a major regional structure inherited from the Variscan Orogeny. This NNW-SSE fault controlled the evolution of the Algarve basin during the Mesozoic, separating it into two blocks that evolved differently (Dias 2001). This fault also plays an important role on the regional groundwater circulation, as it apparently divides the QS aquifer into two compartments with distinct hydrogeological behaviour. The compartments can be identified from the spatial distribution of the piezometric isolines (Figure 6.1a). The region to the east of the fault is characterized by closely spaced isolines, corresponding to relatively high (~15%) hydraulic gradients (Almeida 1985), with an irregular contour pattern that is largely controlled by the topography. This pattern determines spatially varying groundwater flow directions, which are mainly directed towards the west. In contrast, the compartment to the west of the fault is characterized by small (~1.5%) hydraulic gradients, smooth piezometric isolines and a predominant E-W flow direction. Given the evidence, the S. Marcos-Quarteira fault has been suggested to act as a low-permeability hydraulic barrier (Andrade 1989; Almeida et al. 2000).

The aquifer water balance has been thoroughly studied by several authors (Almeida 1985; Almeida et al. 2000; Vieira and Monteiro 2003). The most recent studies obtained a detailed spatial distribution of recharge and estimated that the average annual recharge is 45% (100 $hm^3.yr^{-1}$) of the rainfall (Oliveira et al. 2008, 2011).

As a result of several monitoring and modelling studies, mainly carried out at the University of Algarve, the groundwater flow pattern of the QS is reasonably well known (e.g. Monteiro et al. 2003; Vieira and Monteiro 2003). Groundwater abstraction in the region has strongly decreased since the 1990s, due to the implementation of a multi-municipal system of urban water supply based on dams. However, the historical piezometric records obtained by the available monitoring system do not display any important changes in the regional flow pattern, as inferred from the spatial distribution and temporal evolution of the observed hydraulic heads.

This suggests that, in this aquifer, the impact of anthropogenic processes on groundwater level fluctuations has not been significant. The numerical groundwater flow model presented by Monteiro et al. (2006b) was the first to focus on the calibration of the hydraulic parameters, in particular of the transmissivity (corresponding to an equivalent porous media of a karst system). Stigter et al. (2009) performed simulations of hypothetical extraction scenarios in order to optimize a regional groundwater/surface-water integrated supply system, in which the distribution of the irrigation wells was refined according to their location. Attempts to synthetize the hydraulic behavior of the QS aquifer lead to the definition of 23 transmissivity zones (Figure 6.1b) estimated by inverse modelling(Hugman et al. 2012, 2013). For each of these zones, a reasonable fitting of field data is obtained using a single value of transmissivity. The discharge occurs mainly through a small number of large springs, called the Estômbar springs, located at the border of the aquifer with the Arade River (Figure 6.1b).

The different hydrogeological behavior in the east and west side of the S. Marcos-Quarteira fault becomes evident when the hydraulic head variations are plotted as a function of longitudinal distance (Figure 6.2) considering all the 28 piezometers in the area. The hydraulic head variations are not only larger as they are much more heterogeneous in the eastern sector of the aquifer. These observations provide a qualitative measure of the spatial variability of the system which is indeed much larger in the compartment to the east of the S. Marcos-Quarteira fault.

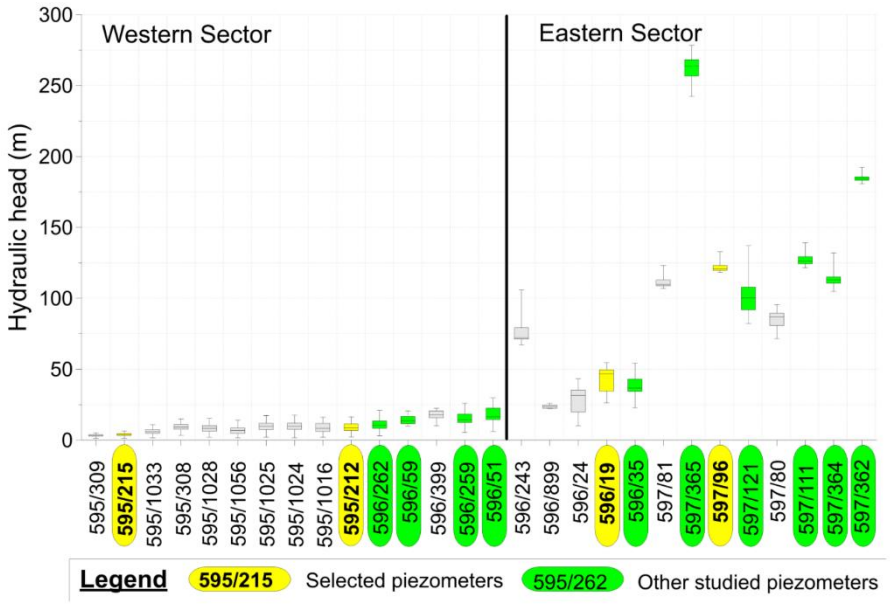

Figure 6.2 - Box and whisker plot of the available piezometric level (m a.s.l.) data between 1985 and 2010. The 28 piezometers on the x-axis are arranged according to their longitudinal distance to the westernmost observation point (Estômbar spring). The black vertical thick line represents the location of the S. Marcos-Quarteira fault. The edges of the boxes are the 25th and 75th percentiles, and the whiskers extend to the minimum and maximum observed groundwater levels

6.2.2 Data and methods

6.2.2.1 Time series data

In order to assess the climate forcing, the groundwater level records need to be long enough to capture inter-annual and inter-decadal fluctuations. The QS aquifer has few long-term records that fulfil this requirement, being 1984 the starting year of the most complete (up to 2013) datasets. The piezometer selection criteria was primarily based on the length and completeness of the water level records, and only secondly determined by their spatial location: two piezometers lie on the west side of the Quarteira fault (Alcantarilha and Silves) and other two on the east side (Benafim and Paderne). The locations are meant to represent the two kinds of hydrogeological conditions found in the QS aquifer. The monthly groundwater level time series span from January 1985 to December 2010 (26 yr long) and were obtained from the Portuguese National System for Water Resources Information SNIRH site (Sistema Nacional de Informação de Recursos Hídricos (Nacional Information System of Water Resources). Although outside the

main scope of this analysis, the relation between precipitation and groundwater level is succinctly explored using one rainfall station (Messines). Monthly precipitation data for this station were also obtained from the SNIRH site, but the available data only spans from January 1985 to December 2009.

6.2.2.2 Time series analysis

The groundwater time series were investigated using several analytical techniques in order to characterize the temporal structure and the periodic components of their signal. The applied methods were: (1) computation of autocorrelation functions, (2) simple spectral analysis, (3) continuous wavelet transform and (4) singular spectral analysis. Each technique has its own purpose and advantages, and their combination provides a more robust estimate of the statistical properties of the aquifer regarding its groundwater level variability. Typical pre-processing steps such as searching for outliers, interpolation for estimating missing values, detrending and normalization by standard deviations were carried out before the analysis.

(1) Autocorrelation functions represent the linear dependence of an event on the subsequent values of the time series, and thereby are usually computed to quantify the memory effect. The auto-correlogram is the plot of the correlation of a time series with itself after being shifted by increasingly larger time intervals (lags). The time lag corresponding to an autocorrelation coefficient of 0.2 is referred as the memory effect (Mangin 1984).

(2) Simple spectral analysis is classically used to obtain the energy spectrum, a plot of the variance of a time series as a function of wavenumber or frequency. It is calculated from the Fourier transform of the autocorrelation function normally using a windowing function to reduce spectral leakage. One of the advantages of simple Fourier spectral analysis is that it allows to visualize the global statistics of the time series in terms of scale invariants regimes (eg. Mandelbrot 1982; Lovejoy and Schertzer 2013) . Multifractal behavior can be identified when the log-log plot of the energy spectrum can be broken in more than one interval (range of frequencies), each interval being fitted by a straight line with a different slope (power law exponent). There is a growing body of evidence showing that groundwater levels may show

scale-invariant, or fractal, behavior over a wide range of time scales (Bloomfield and Marchant 2013; Liang and Zhang 2013). Given the time scale of this study it seems appropriate to investigate if there is one scaling regime in the low frequencies, representing the response to long-term climate variations, and another on the high frequencies, representing the short-term response to the meteorological conditions.

(3) A comprehensive review of the applications of the wavelet transform in hydrology time series has recently been made by (Sang 2013). This study uses the continuous wavelet transform (CWT) in order to further explore the temporal structure of the groundwater level records. In contrast with classical Fourier analysis, which implicitly assumes that the underlying physical processes are stationary, the CWT is suited to the analysis of signals that have temporal variations in both amplitude and frequency. Its main advantage over classical spectral methods is that it is able to reveal the time evolution of the dominant modes of variability, being as such specially tailored for the detection of localized or intermittent events. The CWT is defined as the convolution of the signal with a scaled and translated version of the wavelet function (Daubechies 1990). The method is implemented using the Morlet wavelet and the algorithm described in Torrence and Compo (1998). In the case of the Morlet wavelet the scale and the equivalent Fourier period are practically identical, so the two terms are used synonymously. The wavelet spectrum, defined as the absolute value squared of the wavelet transform, is constructed to display the distribution of the variance of the time series at each scale, as a function of time. A clear picture of the net changes in variance over the whole recording period is provided by the global wavelet spectrum, which is a time average of the wavelet spectrum.

(4) The singular spectral analysis (SSA) is a form of principal component analysis that is used to detect periodic signals and extract the dominant frequencies in short and noisy time series. Following the methods outlined by Dettinger et al. (1995) and Hanson et al. (2004) this technique is applied to decompose the detrended and normalized groundwater level records into principal components (eigenvalues) that represent the projection of the original time series onto empirical orthogonal functions (eigenvectors). The calculations are carried out by diagonalizing a lagged covariance matrix (Vautard et al. 1992; Ghil et al. 2002). The main

advantage of SSA is that it allows the reconstruction of the original record using a linear combination of the most statistically significant oscillations. Hanson et al. (2004) showed that the variability in most hydrological time series can be described in terms of the first 10 reconstructed components (RCs). In this study the Chi-square significant test is applied to isolate the most significant reconstructed components of the variability modes, and then compute their relative contribution to the total variance of the time series.

The relation between groundwater level and monthly precipitation in the QS area is examined using both linear regression, with a two-tailed significant *t* test at the 95 percent confidence level, and lag correlation analysis. First, the monthly precipitation times series needs to be transformed into cumulative departures, detrended and normalized using the methods described by Hanson et al. (2004). The lag correlation analysis, which gives the correlation coefficient as a function of the lag between the two time series, allows identifying the lag of maximum correlation between the causal process (precipitation) and the system response (groundwater level).

6.2.3 Results

The four raw piezometric time series are displayed in Figure 6.3 and their main statistical parameters are summarized in Table 6.1. All piezometers show annual fluctuation superimposed on multi-year periods of high and low groundwater level stands. On the long-term (over 26 yr) all piezometers show slight negative tendencies on the mean groundwater level, the most significant (-0.018 m/month) being found in Alcantarilha and Paderne. This long-term trend is in agreement with an important, but not statistically significant, decrease in the regional average total precipitation observed in Portugal in the period 1976−2007 (de Lima et al. 2014). The most striking observation is the clearly distinct oscillatory pattern in the western and eastern sectors of the aquifer. Alcantarilha and Silves, in the western sector, present similar regular fluctuations with smoother piezometric variations, while Benafim and Paderne, in the eastern sector, display relatively heterogeneous and sharp head variations, with fast rise and

recession events. The eastern compartment of the QS aquifer is thus characterized by a relatively higher temporal and spatial variability than its western counterpart.

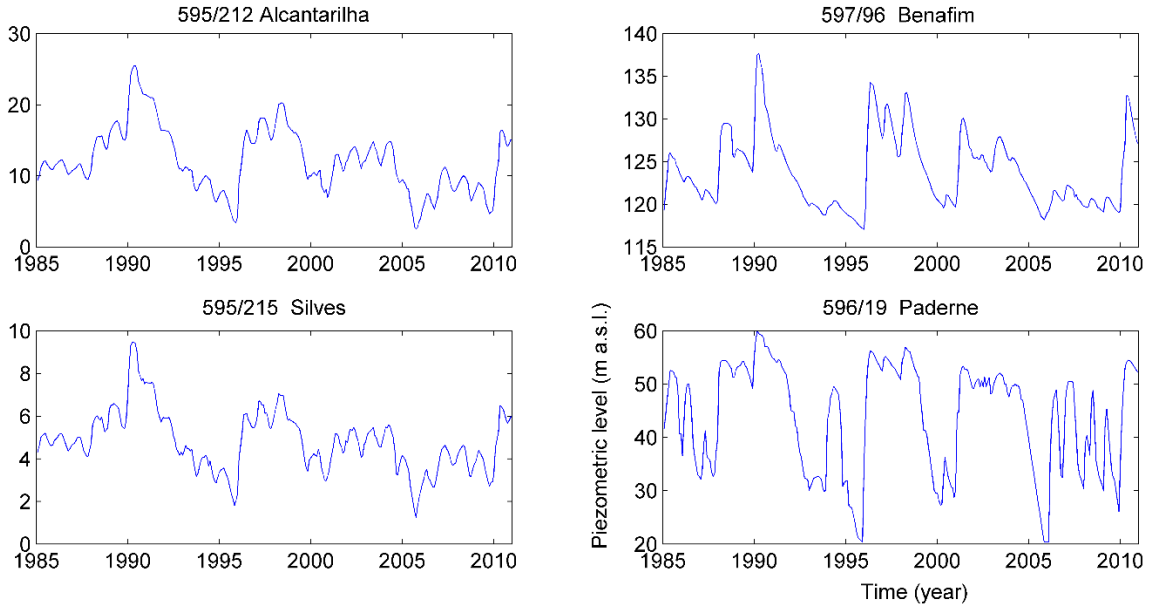

Figure 6.3 - Monthly groundwater levels at four piezometers from the two main sectors of the Querença-Silves aquifer: Alcantarilha and Silves (western sector) and Benafim and Paderne (eastern sector)

Table 6.1 - Summary of hydrologic and statistical parameters of the data (1985-2010)

Piezometer	**Topographic elevation (m a.s.l.)**	**Mean piezometric level (m)**	**Range of water-level fluctuations (m)**	**Memory effect (months)**	**Scaling exponent (β)**
Alcantarilha (595/212)	47.02	12.16	2.50 – 25.55	16	2.6
Silves (595/215)	63.76	4.82	1.22 – 9.46	15	2.4
Benafim (597/96)	182.52	123.91	117.04 – 137.69	13	1.7 & 3.8
Paderne (596/19)	75.34	43.83	20.34 – 59.94	11	1.8 & 2.1

Figure 6.4a shows the raw monthly precipitation data recorded at the Messines rainfall station, which lies exactly in between the two sectors. After transforming the raw precipitation data into monthly cumulative departures (Cdep) the linear regression analysis between Cdep and the groundwater level time series (truncated for the 1985-2009 period) was performed for each one of the four selected piezometers. The obtained linear regression coefficients vary between 0.6 and 0.75 revealing that, despite the local geological complexities and other potential perturbing factors, there is a strong positive correlation between the groundwater levels and the rainfall in the two sectors of the aquifer. The results of the lag correlation analysis indicate that the time lag of maximum correlation is 1 month in both sectors (Figure 6.4b).

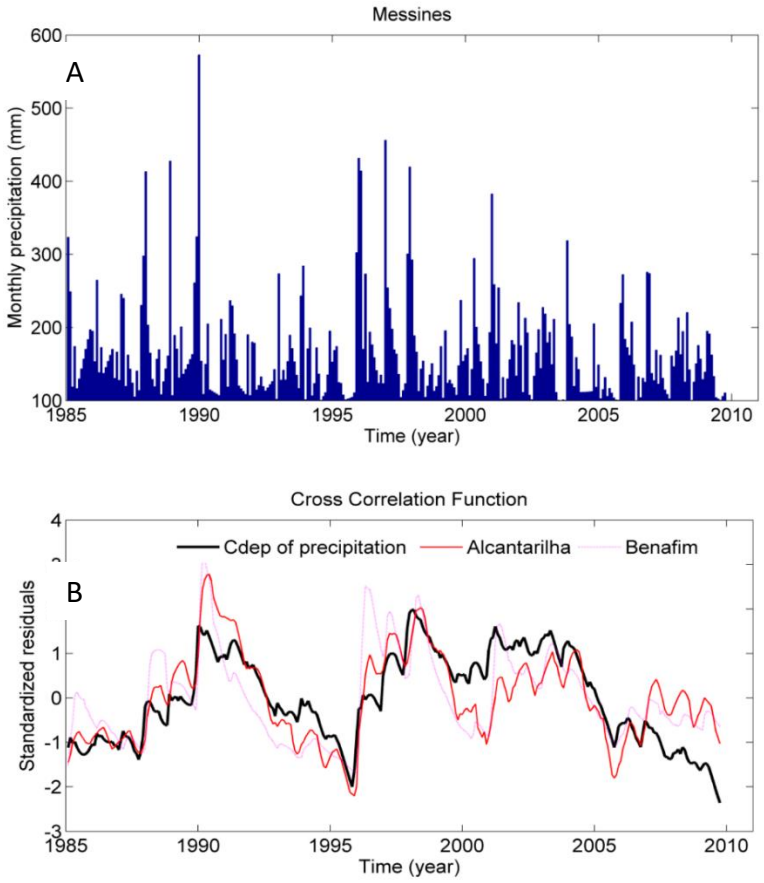

Figure 6.4 - Relation between precipitation and groundwater levels. (a) The monthly precipitation at the Messines rainfall station. (b) The monthly values of normalized residuals of cumulative departure of precipitation and the normalized residuals of groundwater level at Alcantarilha and Benafim lagged 1 month

The east-west split in hydrogeological behavior of the QS aquifer is confirmed in quantitative terms in several ways. A first quantitative estimate of the timescale of the natural attenuation, or filtering properties of the aquifer, is provided by the autocorrelograms (Figure 6.5).

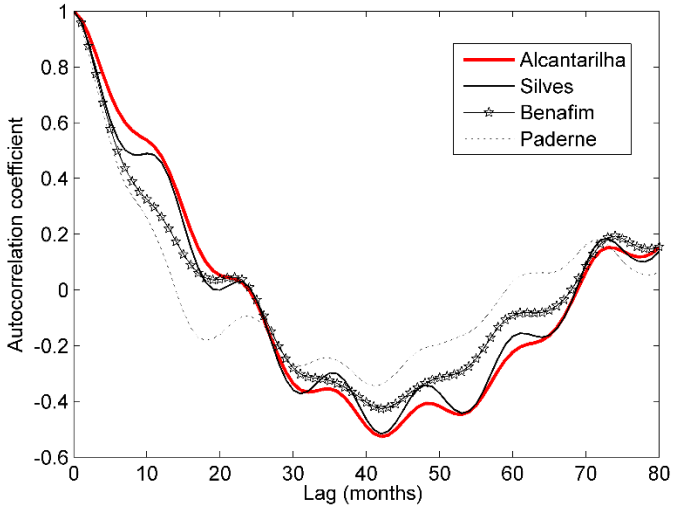

Figure 6.5 - Autocorrelation functions of the four piezometric time-series (total window of 312 months and lag step of 1 month) truncated in the 0-80 lag range

The so-called memory effect obtained using this method is 15-16 months in the western sector (Alcantarilha and Silves) and 11-13 months in the eastern sector (Benafim and Paderne). The longer memory effect that characterizes Alcantarilha and Silves is consistent with the smoother variations of the hydraulic head observed in Figure 6.3. Longer memory effects, which denote high inertia to changes and low-pass filtering properties, often reflect thick surficial formations (longer times of recharge) or significant amounts of water storage/volume in the karst network. In the QS aquifer the longer memory effects in the western compartment are mainly attributed to larger water storage capacities that have been recognized in this sector in previous studies (e.g. Hugman et al. 2012).

The simple spectral analysis of the four piezometric records (Figure 6.6) reveals relatively consistent peak frequencies corresponding to cycles of 1, 4.3 and 6.5 yr. In the eastern sector there is also a peak at 2.5 yr, which is not observed in the west. The peaks in the spectrum

indicate that a significant amount of the variance of the groundwater level record is contained in these frequencies. The sharpest peak is associated with the annual precipitation cycle (1/12-month frequency). The multi-annual periodicities are related to low-frequency climate signals and will also emerge from the continuous wavelet transform and singular spectrum analysis methods. Their association with large-scale climate teleconnections patterns have already been recognized in other Mediterranean aquifers (Andreo et al. 2006; Massei et al. 2007; Luque-Espinar et al. 2008; Slimani et al. 2009) and will be analyzed in more detail in the next section.

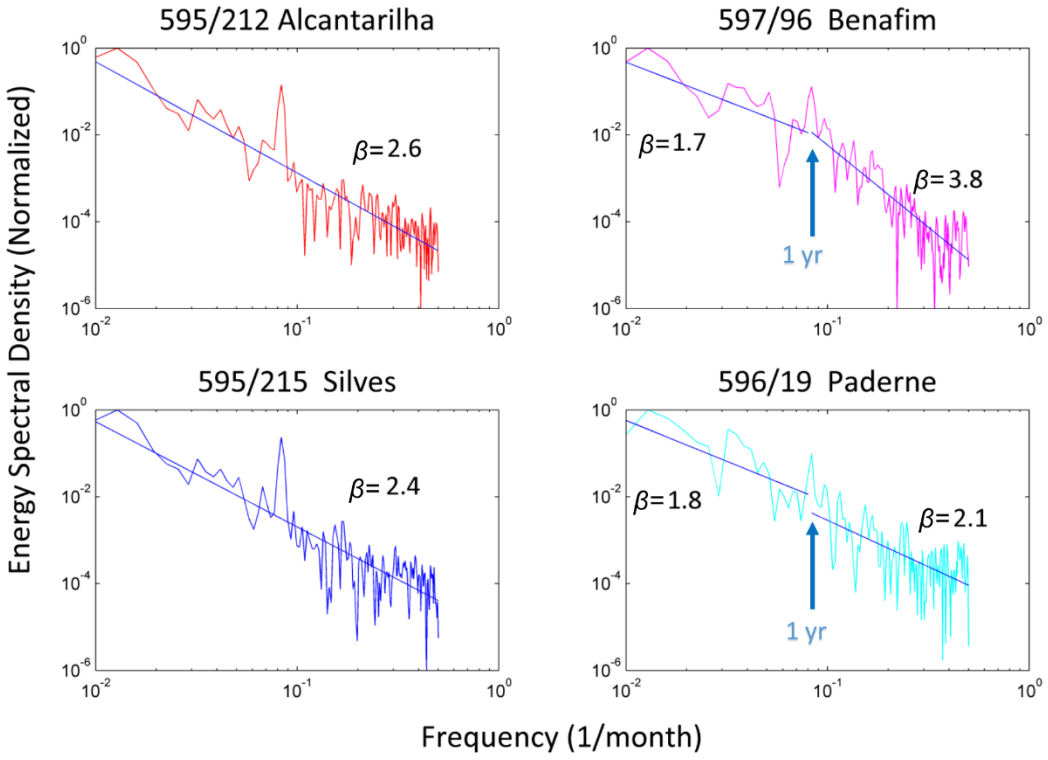

Figure 6.6 - Energy (power) spectra of the four groundwater level records in a log-log plot. The slopes of the lines, computed from linear regression, correspond to estimates of the empirical *β* exponents defining scaling regimes

Figure 6.6 also enables the definition of scaling regimes by fitting the energy power spectra with an empirical power law with exponents *β*. In Alcantarilha and Silves the spectral slope remains unchanged on both sides of the annual peak, that is, there is only one scaling regime, with *β*=2.4−2.6. In general, the lower the magnitude of the spectral exponent, the higher the variability in the data. As the magnitude of the β exponent is similar in these two piezometers

these results quantitatively demonstrate that a similar amount of variability is present in Alcantarilha and Silves. In contrast, in Benafim it is possible to detect two scaling regimes, with the break occurring at the 1/12 month frequency. In this case it is possible to separate the short-term response to intermittent meteorological conditions from the low frequency response to multi-annual climate variations. The scaling behavior of Paderne is not clear. It is similar to Benafim in the long-term range, but in the short-term, like the two piezometers in the western sector, it lacks a distinctive response to high-frequency variations. The difference between the energy power spectra of Benafim and Paderne, despite being in the same sector, reflects the compartmentalized structure of this part of the Aquifer. Benafim, at relatively high elevation (182 meters above sea level (m a.s.l.)) is an upstream site, whereas Paderne (44 m a.s.l.) is close to a spring outlet that defines one of the downstream boundaries of the groundwater basin. The eastern sector is indeed subdivided into a large number of more or less independent units, which result from limitations on flow paths generated by stratigraphic and lithologic factors and a less developed karst when compared with the western sector.

The normalized wavelet power spectra of the groundwater levels, computed using the continuous wavelet transform method, are displayed in Figure 6.7. Each diagram depicts the temporal distribution of the power (variance) of the time series as a function of period, over the 26 yrs of analysis, in a color scale that goes from blue (minimum) to brown (maximum). The 5% significant levels, computed using a Chi-square test against a red noise spectrum as the null hypothesis, are displayed as white contours. Also shown is the cone of influence (black parabolic lines) which delimits the regions where the edge effects, due to zero padding, make the results less reliable. The comparison of the four spectra immediately exposes the east-west division of the aquifer. The most remarkable difference between the two sectors occurs in the 2-4 yr band. These modes of variability are intermittently quite important in the east, the most extreme example being the peak at ~2.5 yr located in Paderne and centered on 1996. The presence of these modes of variability in the east, but not in the west, is discussed in the next section.

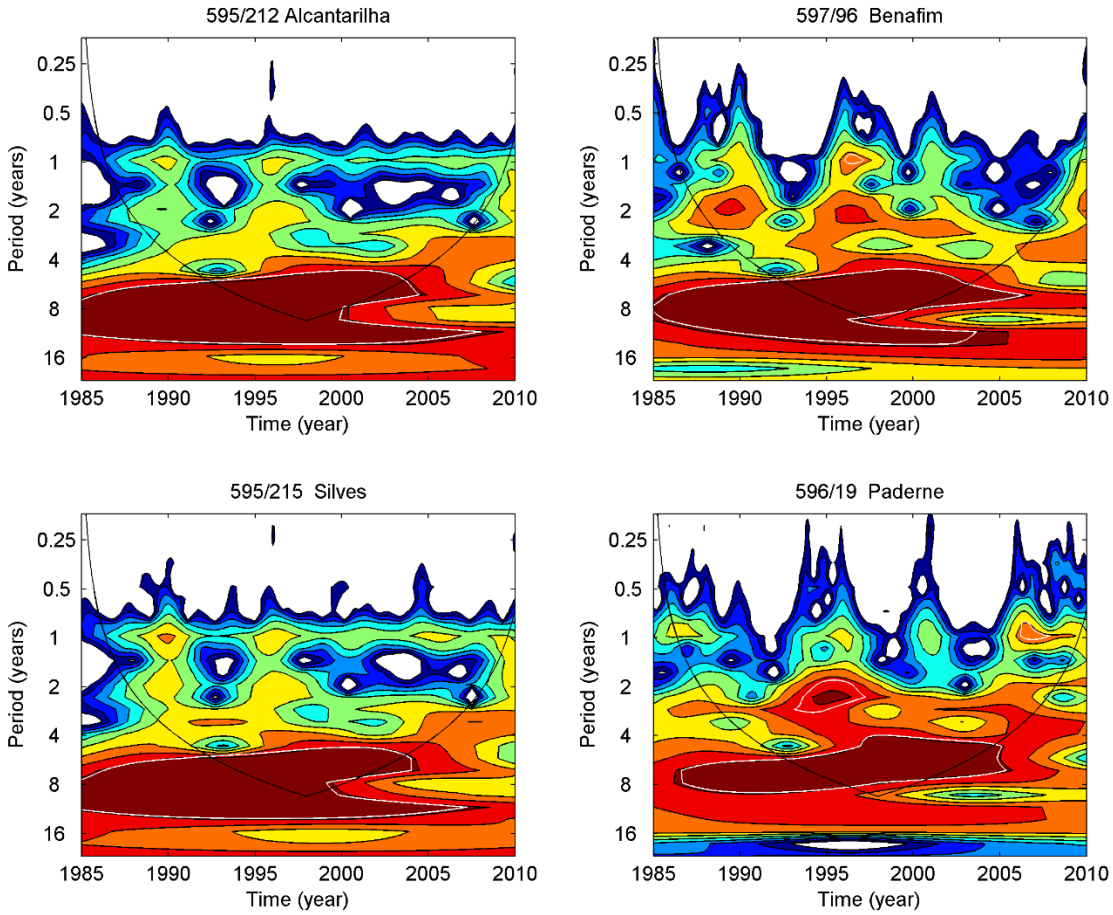

Figure 6.7 - Local wavelet power spectrum of the four time-series computed using a Morlet wavelet and normalized by $1/\sigma^2$. The white contours enclose regions of greater than 95% confidence levels. The black lines delimit the cone of influence, where zero padding has reduced the variance

Despite the local differences, the most important aspect that emerges from Figure 6.7 is the power concentration in the 5-13 yr band, within the 95% confidence interval, present at all sites. The 5-13 yr variance can be mainly attributed the North Atlantic Oscillation (NAO) which is the dominant mode of atmospheric variability at mid-latitudes in the North Atlantic. The spectrum of the winter (December-March) NAO index, is indeed characterized by a slightly enhanced power in the 6-10 yr band, particularly on the last quarter of the 20th century (Hurrell and Van Loon 1997; Hurrell et al. 2003). At smaller scales, with less amounts of energy, one can observe several scattered peaks at periods of 1 yr. The strongest patches occur in 1990, 1996 and 2000, which were anomalously wet years (Miranda, P., Coelho, F.E.S., Tomé, A.R., Valente

2002). It is also interesting to note the strong attenuation of power, or lack of variance, in the 1-2 yr band centered on 2004, but extending for almost a decade in the western sector. This anomaly is attributed to the outstanding drought that affected the Iberian Peninsula in 2004–2005 (García-Herrera et al. 2007).

Figure 6.8 displays the time-averaged wavelet spectrum over the whole period (26 yr) of record, the so-called global wavelet spectrum, computed using the method described in (Torrence and Compo 1998). When averaged over time only two variability modes have enough persistence and amplitude to remain statistically significant. The first and more conspicuous has a period of 6.5 yr. The second, with a period of 11-13 yr, is also statistically significant at the 5% level at three (Alcantarilha, Silves and Benafim) of the four sites.

These are enough to represent the western and eastern sector of the aquifer, respectively, since the EOFs of Silves and Paderne (not shown) are the same. EOFs 1 and 2, as well as EOFs 5 and 6 in Alcantarilha, and EOF 4 and 5 in Benafim, are in quadrature. The most robust result is the persistence of the first EOF pair, corresponding to the 6.5 yr periodicity, over the whole aquifer. The other leading scales of variability correspond to a set of oscillations with associated periods of 4.3 yr (EOF 3), 3.2 yr (EOF 4) and 1 yr (EOFs 5-6) in Alcantarilha, and 13 yr (EOF 3), 2.6 yr (EOFs 4-5) and 2 yr (EOF 6) in Benafim.

Overall, these results are in agreement with those found using the simple spectral analysis and the continuous wavelet transform. The amount of variance attributed to the 6.5 yr mode of variability (EOFs 1-2) is approximately 70% in the western sector (73% in Alcantarilha and 68% and Silves). In the eastern sector, the same components explain approximately 55% of the total variance (59% in Benafim and 52% in Paderne). The contribution of the annual cycle component to the total variance is approximately 7% in both sectors (EOFs 8-9 in Benafim, not shown).

The reconstruction of a set of significant components, the reconstructed components (RCs), is carried out by linearly combining the EOFs and the principal components.

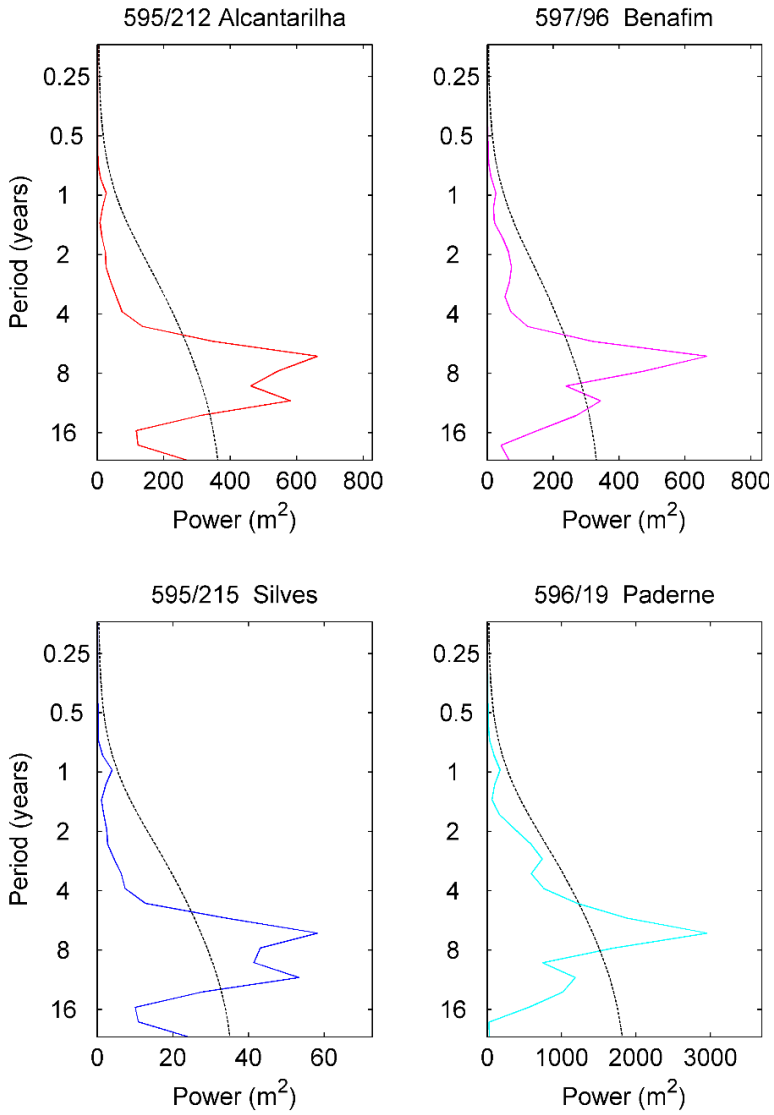

Figure 6.8 - Global (or time averaged) wavelet spectrum of the groundwater level records (solid line) as a function of period. The dashed line is the 5% significance level, assuming a corresponding red noise process. The power amplitude (σ^2) is proportional to the amplitude of the hydraulic head variations in each piezometer

The RCs have the property of capturing the phase of the time series and can be superimposed with the original data on the same timescale. Here, only the most important EOF pairs in each one of the piezometers are used: 1-2 and 5-6 in Alcantarilha, and 1-2 and 4-5 in Benafim, (Fig. 9). In the terminology of Ghil et al. (2002) each of these two RCs form the robust skeleton of the Lorenz attractor. The composite of selected RCs contain 80% and 70% of the total variance of the groundwater level record, in Alcantarilha and Benafim, respectively. The low frequency

components (RCs 1-2 and RCs 4-5) show substantial amplitude modulation. The amplitude of the 6.5 yr oscillation progressively decreases towards the end of the recording period (after year 2000). The amplitude of the 2.6 yr component, in Benafim, is much more irregular but also slightly decreases after year 2000. This result is consistent with the wavelet power spectra (Figure 6.7) which clearly shows that the power concentration in the 5-13 yr band is much weaker in the 21th century than before. Although this band is inside the cone of influence after year 2005, the SSA analysis confirms that these low frequency periodic oscillations have been losing strength in recent years. These results also demonstrate the complementarity of the SSA and continuous wavelet transform methods.

6.2.4 Discussion

6.2.4.1 Climate forcing

The North Atlantic Oscillation (NAO) is the main large-scale phenomenon controlling winter precipitation over the western Iberian Peninsula (Hurrell and Van Loon 1997; Trigo et al. 2004). Its impact on river flow regimes, with obvious consequences for all water resources in the region, has been thoroughly assessed in previous years (eg. Trigo et al. 2004; Gámiz-Fortis et al. 2008; Lorenzo-Lacruz et al. 2011; Jerez and Trigo 2013). A singular spectral analysis carried out to isolate the main oscillatory components of the streamflow series of the main Iberian Peninsula international rivers (Douro, Tejo, and Guadiana) revealed modulated amplitude oscillations with associated periods in the bands 2–3, 4–5, and 6–8 yr (Gámiz-Fortis et al. 2008). The winter Guadiana series (south Portugal), in particular, was found to be represented by a model containing a decadal variability with a set of oscillations with associated periods of 2 yr, 4.5 yr, 6.5 yr, and 3.4 yr, which are remarkably similar to the periods found during this study in the QS aquifer. However, caution is required in analyzing these results as the relation between the NAO and the surface climate has been shown to be non-stationary (Vicente-Serrano and López-Moreno 2008).

The NAO index, on the other hand, can be broken down into some modulated amplitude oscillations with periods around 4.8 yr, 7.7 yr, and 2.4 yr, along with nonlinear trends (Gámiz-

Fortis et al. 2002). When trying to match the NAO index and the streamflow main modes of variability in Iberia, previous studies found common oscillations at 7.7 yr and 4.8 yr, but suggested that the overall relationship between the NAO and streamflow is complex and nonstationary (Gámiz-Fortis et al. 2008). The complexity was attributed to the role played by other climate variables, such as temperature and wind, which have a direct effect on evapotranspiration but are not so clearly related to the NAO. Moreover, it has been recognized that the average monthly and seasonal precipitation in the Iberian Peninsula, although mainly influenced by the NAO, also depends on other teleconnections such as the Scandinavian and Eastern Atlantic patterns (Trigo et al. 2008; Espírito Santo et al. 2014).

Groundwater levels have a more complex relation to precipitation than river flow. For example, models of time-varying climate controls on groundwater recharge have shown that groundwater responds more strongly to the comparatively slow trends associated with low frequency climate fluctuations than to isolated climate extremes (Dickinson et al. 2004).The relationship between groundwater level fluctuations and low frequency (inter-annual to multi-decadal) atmospheric circulation systems has been intensively investigated in recent years (Gurdak et al. 2009; Tremblay et al. 2011; Kuss and Gurdak 2014). In the south of the Iberian Peninsula, periodicities of 2.5 yr and 5 yr were reported in a study that focused on the relation between rainfall, temperature and outflow of a karst spring from the Sierra de las Cabras carbonate aquifer, near Gibraltar (Andreo et al. 2006). Spectral methods applied to a set of 53 piezometer time series from the Vega de Granada alluvial aquifer, along with rainfall, temperature and river flow data, also identified cycles of 8-11 yr and 3.2 yr (Luque-Espinar et al. 2008). In both cases, the authors argued for a clear correlation between the NAO index and the low frequency hydraulic head variations. Another study in a karst aquifer, this time in the Upper Normandy (France), detected the same frequencies, 2-3 yr and 6-7 yr, in piezometric levels (Slimani et al. 2009). The results from this study, especially the wavelet power spectra (Fig. 7), are remarkably similar to the results of Slimani et al. (2009)most likely because this study analyzed a similar time span (in the Slimani et al. (2009) case, 1985-2005). The evidence thus suggests that the 3.2 yr, 4.3 yr, 6.5 yr, and 2.6 yr oscillations identified in the QS aquifer are

driven by natural recharge rates associated with the NAO climate cycle. The full demonstration of this relation is nonetheless outside the scope of this study.

6.2.4.2 Geologic forcing

Once the climate forcing has been identified, the question now is to determine the extent to which the geologic factors filter the climate-induced oscillations in the groundwater levels. This section aims to explain the distinct behavior of the piezometers in the face of a common climatic input, focusing on the differences between the eastern and western sector of the aquifer. According to the results, the most important differences between the two sectors are: (1) in the western sector the groundwater level response is spatially homogenous, the memory effects are larger, the high-frequency content is filtered out and there is only one scaling regime, meaning there is no distinctive response to short-term variations; (2) in the eastern sector there is greater spatial variability in hydraulic head variations, and there is, at least in some piezometers, two scaling regimes, implying that there is a noticeable response to short-term meteorological conditions. There is also a 2.6 yr mode of variability in the eastern sector, probably related to the frequency of depressions and frontal systems affecting western Iberia in connection with the NAO, which was not detected in the western sector.

All these observations are consistent with the regional flow pattern model developed for the QS aquifer (Monteiro et al. 2006b, 2007b; Hugman et al. 2012, 2013). The spatial distribution of the porous-karst media equivalent transmissivity in the aquifer has been obtained in previous studies using inverse calibration of finite element model predictions against piezometric and discharge data (Hugman et al. 2012), and considering both autogenic and allogenic recharge (Salvador et al. 2012). In the western sector, the models show a regular distribution of high transmissivity values, indicative of a well-developed karst conduit network that supports high rates of water flow. The main region of water storage, with relatively large storage coefficients, also occurs in the western sector of the aquifer (Hugman et al. 2012). Together, these two properties (high transmissivity and large storage capacity) make the western sector more resilient to short-term climate-induced variations. In contrast, the eastern sector of the aquifer

is characterized by comparatively less efficient water storage and water transport, owing to the less developed and discontinuous nature of the karst conduit network. This explains why the eastern sector is less sensitive to the long-term climate oscillations and more reactive to the short-term meteorological conditions. Thus, it becomes apparent that the 2.6 yr periodic oscillations, which are probably related to stormy episodes, have not enough amplitude to affect the western sector (with large volumes of stored water) but are sufficient to impact the relatively depleted eastern sector of the aquifer.

A quantitative measure of internal variability due to geological filtering can be obtained by comparing the contribution of the different modes of variability to the total variance of the groundwater levels (Table 6.2). For instance, comparing Alcantarilha and Benafim, there a difference of 14% in the contribution of the 6.5 yr mode of variability. The difference in the 2.6 yr mode contribution is also of that order of magnitude (12 %).

Table 6.2 - Comparative results of the SSA in the western/eastern sectors of the aquifer

EOF	(595/212) Alcantarilha (west)		(597/96) Benafim (east)	
	Period (yr)	Variability (%)	Period (yr)	Variability (%)
1	6.5	43	6.5	34
2	6.5	30	6.5	25
3	4.3	8	13	7
4	3.2	5	2.6	6
5	12	4	2.6	6
6	12	3	2	5

In order to further assess the spatial distribution of the geological filtering, the SSA analysis was extended to another ten piezometers in this aquifer (Table 6.3 for western sector and Table 6.4 for the eastern sector).

Table 6.3 - Main mode of variability and contribution to the total variance (VAR) for an extended set of piezometers at the western sector of QS aquifer. Measure of geological variability relative to the Alcantarilha record

	Piezometer	Time (yr range)	Period (yr)	VAR	Difference with Alcantarilha 595/212
Western sector	595/215 Silves	1985-2010	6.5	68%	5%
	596/262	1988-2010	6.5	69%	3%
	596/259	1985-2010	6.5	73%	0%
	596/51	1985-2010	6.5	72%	1%
	596/59	1985-2010	6.5	76%	3%

Table 6.4 - Main mode of variability and contribution to the total variance (VAR) for an extended set of piezometers at the Eastern sector of QS aquifer. Measure of geological variability relative to the Alcantarilha record

	Piezometer	Time (yr range)	Period (yr)	VAR	Difference with Alcantarilha 595/212
Eastern sector	596/19 Paderne	1985-2010	6.5	52%	21%
	597/96 Benafim	1985-2010	6.5	59%	14%
	597/111*	1987-2010	6.5	58%	14%
	597/362*	1996-2010	5	17%	41%

	Piezometer	Time (yr range)	Period (yr)	VAR	Difference with Alcantarilha 595/212
	597/364*	1996-2010	5	25%	33%
	597/365*	1996-2010	5	24%	34%
	596/35*	1996-2010	5	37%	21%
	597/121*	1996-2010	5	30%	28%

* - analyzed period is restricted to the 1996-2010 due to lack of data

Only five of the piezometers have records in the time span analyzed so far (1985-2010), and in this subset the 6.5 yr periodic component is also significant. The difference in variability with respect to the Alcantarilha piezometer, taken as the reference and considering the same time interval, emphasizes the uniformity of the response in the western sector. It also confirms the existence of a systematic difference of 15%-20%, that can be attributed to geological filtering, between the eastern and western sectors of the aquifer. The analysis in the remaining five piezometers (in light grey shading) is restricted to the 1996-2010 interval and to the eastern sector. In this time interval the SSA indicates a shorter periodic component (5 yr) and an even larger spatial variability due to geologic factors.

6.3 Climate patterns and atmospheric teleconnections with groundwater levels in Central Algarve aquifers

The aquifers considered in this study are located in the area of the Ria Formosa mesotidal lagoon, considered a wildlife reservoir of high ecological value (Hugman et al. 2017b). There is still no evidence of saltwater intrusion in the Ria Formosa basin, but groundwater abstraction in the area of Quinta do Lago (Figure 6.9) has lowered hydraulic heads below sea level, and numerical models suggest that current groundwater use is unsustainable in the long term (Hugman 2017). A better understanding of the natural fluctuations in aquifer levels will help to

evaluate potential risks and serve as the basis for improved modelling and more informed management decisions in the region.

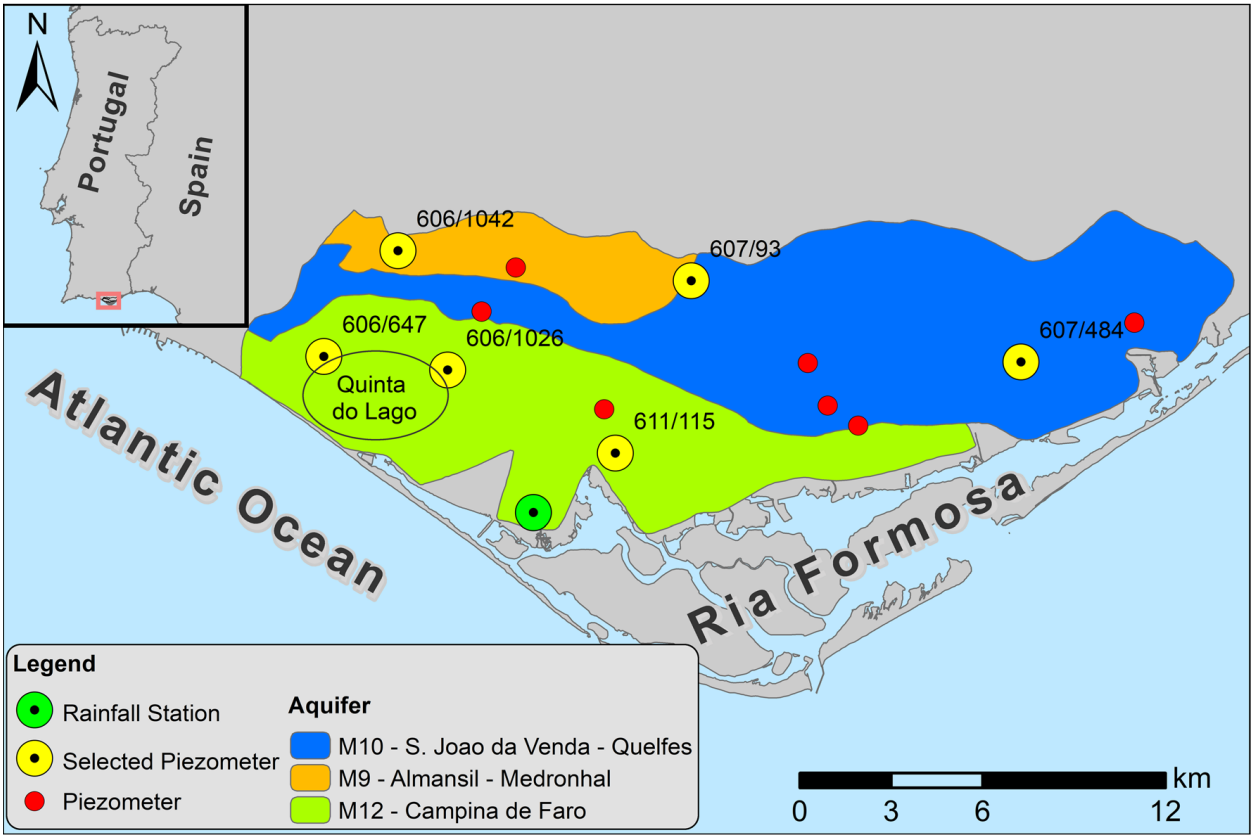

Figure 6.9 - Aquifer systems in the study area: S. João da Venda-Quelfes (M10), Almansil-Medronhal (M9) and Campina de Faro (M12). Location of the 13 piezometers used to compute the average hydraulic head and of the rainfall station. A subset of six piezometers is selected for analysis

6.3.1 Data and methods

6.3.1.1 Site description: Central Algarve aquifers in connection with Ria Formosa coastal lagoon

The Ria Formosa is a complex system of coastal saltwater lagoons and barrier islands. Composed of extensive saltmarshes, mudflats and sand banks, the site has been recognized as both a Ramsar wetland of international importance and as a “Nature 2000” protected area. The Ria Formosa is connected to a group of aquifers that discharge groundwater to the lagoon,

amongst which are the Campina de Faro (M12), São João da Venda-Quelfes (M10) and Almansil-Medronhal (M9), which define the case study area (Figure 6.9).

The area is located to the south of the Caldeirão mountain range, which is one of the major mountains ranges in the Algarve region and a natural barrier to atmospheric circulation. The northern part of aquifers M9 and M10 have significant relief and lie near the slopes that are most exposed to wet southerly fluxes coming from the sea (Figure 6.10A). In comparison, topography of the Campina de Faro (M12) is rather flat. The boundaries of the aquifers can almost be delineated from the surface geology map (Figure 6.10C) (Manuppella et al. 1993; Almeida et al. 2000). System M9 is a karst aquifer mainly composed of dolomites and limestones of Upper Jurassic age, forming sequences that dip (20°-40°) towards the south. Aquifer M10 is mainly composed of detritic sediments (silt and sand) overlying a thick marly limestone sequence, both of Cretaceous age. These two sub-units have similar hydraulic productivities and are considered a single system. Aquifer M12 presents a multilayered structure comprised of three units (Stigter et al. 2006c). The deepest unit is formed by marls and limestone of Cretaceous age. These formations outcrop in the NW area of M12 and dip towards the south. The overlying sub-aquifer is composed of Miocene sediments deposited in a grabben-like structure, bounded by N-S trending faults. Although Miocene outcrops are scarce and small, the Miocene formations are relatively thick, exceeding 200 m near the coast. Finally, the third shallowest unit is made of Plio-Quaternary sands and gravels which constitute the predominant lithologies at surface. There is some evidence for the existence of a confining layer, composed of silt and clay, between the Miocene and Plio-Quaternary units of M12, with variable thickness and some lateral discontinuity.

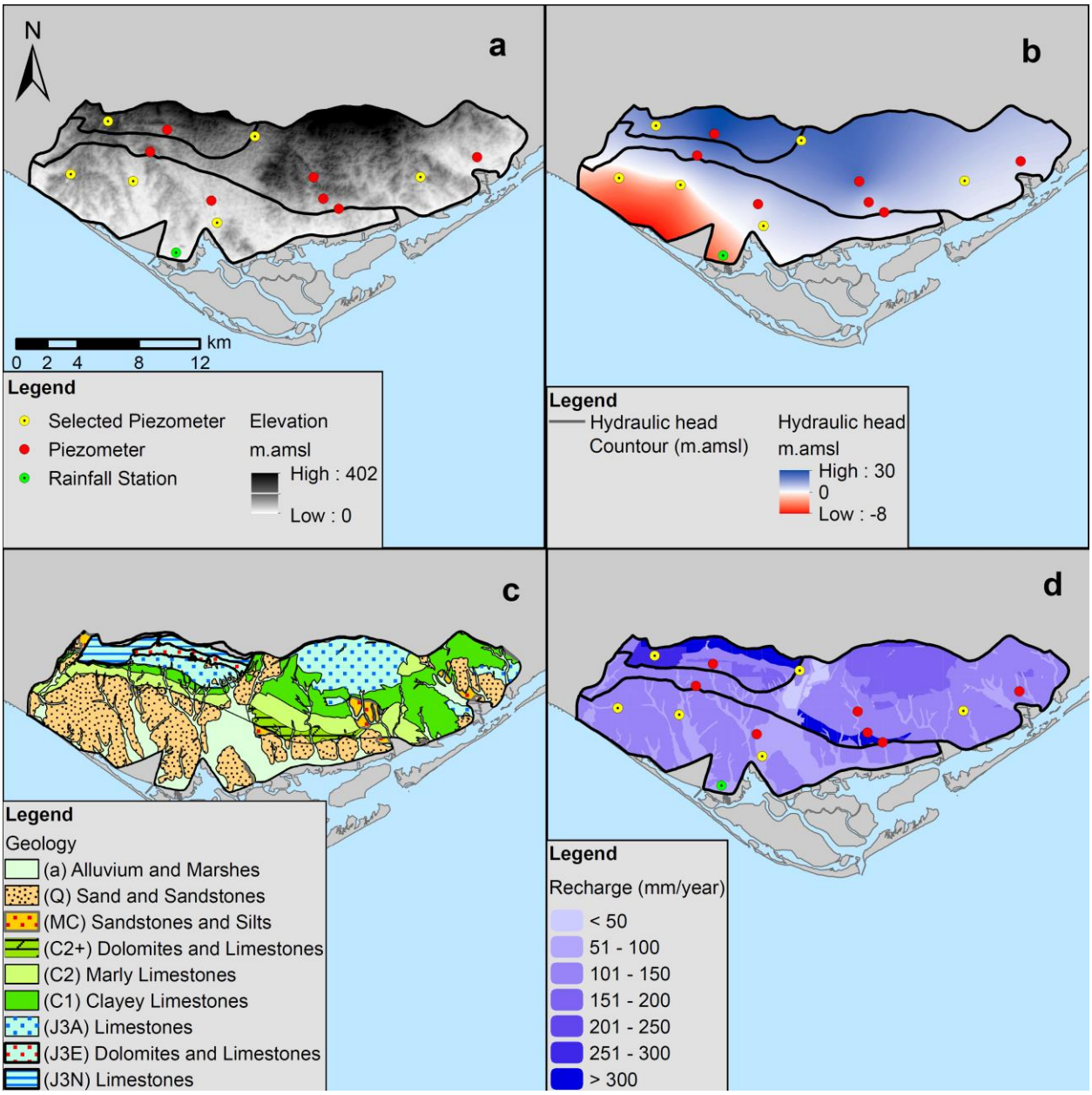

Figure 6.10 - Hydrogeological characterization of the study area. a Terrain elevation based on data obtained from ASTER satellite imagery (Team US/Japan 2009). b Hydraulic head distribution calculated based on in- verse distance weighting interpolation of mean monthly piezometric levels from a total of 13 piezometers. c Geologic map at the scale of 1:100000 adapted from Manuppella et al. (1993). d Recharge distribution calculated based on infiltration rates of outcropping lithology and average annual rainfall (Nicolau 2002)

The climate in the Algarve region is temperate with hot and dry summers (Mediterranean of type Csa in the classification of Köppen-Geiger). The monthly average temperature ranges

between 12 and 24°C and the total annual rainfall is about 500 mm/year (1981-2010 climate normal) (IPMA, 2019). On average, about 42% of the annual precipitation falls during the 3-month winter season (Miranda, P., Coelho, F.E.S., Tomé, A.R., Valente 2002). Due to the orography, the precipitation decreases substantially from north to south, with coastal areas receiving on average less 70% of precipitation than northern areas. Mean recharge values are therefore more intense in the northern part of aquifers M9 and M10 (Figure 6.10d). The recharge calculation is based on the average annual rainfall distribution proposed by Nicolau (2002) and infiltration rates of outcropping lithology. The recharge of aquifers M9 and M10 comes predominantly from direct infiltration of rainfall (Almeida et al. 2000). In contrast, the deeper units of aquifer M12 are mainly fed by groundwater flowing in from the aquifer systems to the north. A significant source of this indirect recharge is provided by N-S trending faults in the central part of the study area, forming preferential flow paths that have been inferred from hydrogeochemistry surveys and geophysical campaigns (Stigter et al. 1998). On average 34% of the annual natural recharge is consumed for irrigation, mainly in the western sector of aquifer M12 (Stigter et al. 2006c). This largely reduces the coastal groundwater discharge to the Ria Formosa lagoon. The severe reduction in groundwater discharge along the coastline originates long residence times that promote groundwater salinization and nitrate contamination (Stigter et al. 2006c).

6.3.1.2 Hydrological data

The selection of the groundwater level data is based on a compromise between the length and completeness of the records and a distributed geographic location sampling the three aquifers. Only six piezometers in the study area (Figure 6.9) have records satisfying the requirement of being continuous for at least 30 years, which is the classical period for the definition of average weather patterns. From this subset, some have been affected by abstraction, namely, piezometers 606/1042 and 607/93 (these two mainly before 1993) and 606/647 (until present-day). Despite these limitations, the selected piezometers represent the range of observed hydrogeological conditions in aquifers M9, M10 and M12 (Table 6.5). It is worth mentioning that in the multilayered aquifer M12 the wells are screened within the Miocene formation.

Table 6.5 - Summary of hydrologeologic and statistical parameters of piezometric data (1987-2016)

Aquifer	Main lithology	Piezometer	Topographic elevation (m a.s.l.)	Mean piezometric level (m)	Variance	Correlation with Precipitation (1993-2016)
M12	Limestone, Sand	606/647	27.47	-2.58	5.96	0.7
M12	Limestone, Sand	606/1026	6.83	-1.96	6.89	0.7
M12	Limestone, Sand	611/115	5.91	3.23	2.43	0.9
M9	Limestone, Dolomite	606/1042	74.21	16.64	31.08	0.8
M10	Sand, Limestone, Marl	607/93	51.61	20.63	8.05	0.8
M10	Sand, Limestone, Marl	607/484	34.98	6.14	6.01	0.8

Monthly groundwater level time series were obtained from the Portuguese National System for Water Resources Information SNIRH site (SNIRH 2021). The data for six selected piezometers (Figure 6.9) span from January 1987 to December 2016. The data for the remaining 7 piezometers (red dots in Figure 6.9 used to compute the spatial distribution of hydraulic head in Figure 6.10b) includes only nine hydrologic years (2008-2016). Monthly precipitation data was collected from one weather station located in Faro and operated by the Portuguese

Meteorological and Ocean Office (IPMA 2019). This station, located near the discharge area of the Campinas de Faro (M12) aquifer, is the only one in the region with continuous records in the 1987-2016 time span.

6.3.1.3 Climate indices

The NAO is a meridional dipole of the pressure field, located between Iceland and the Azores, which presents considerable inter-annual and decadal oscillations (Hurrell and Van Loon 1997; Goodess and Jones 2002). In its positive phase (NAO+) high pressures dominate over the Azores and low pressures over Iceland, promoting colder and drier (warmer and wetter) winters across southern (northern) Europe, the reverse occurring in the opposite phase (NAO-) (Trigo et al. 2008). Its impact on surface climate is non-stationary (Vicente-Serrano and López-Moreno 2008) mainly because NAO is affected by the concomitant phases of other atmospheric teleconnections such as EA (Moore et al. 2013). The EA pattern has also a dipole configuration but is displaced to the southeast when compared to the NAO dipole. During its positive phase (EA+) it is associated with low pressures in the North Atlantic at approximately 50°–55° North (to the west of the United Kingdom) which cause above than average precipitation over northern Europe.

The NAO and EA indices used in this study were retrieved from NOAA's Climate Prediction Center (NOAA 2019) at monthly temporal resolution, spanning from 1987 to 2016. Figure 6.11 shows their winter aggregates (monthly index values averaged from December to March) as solid lines. Positive and negative phases are defined by winter (DJFM) index values above the 3rd and below the 1st terciles, respectively. Years corresponding to these phases are marked with symbols.

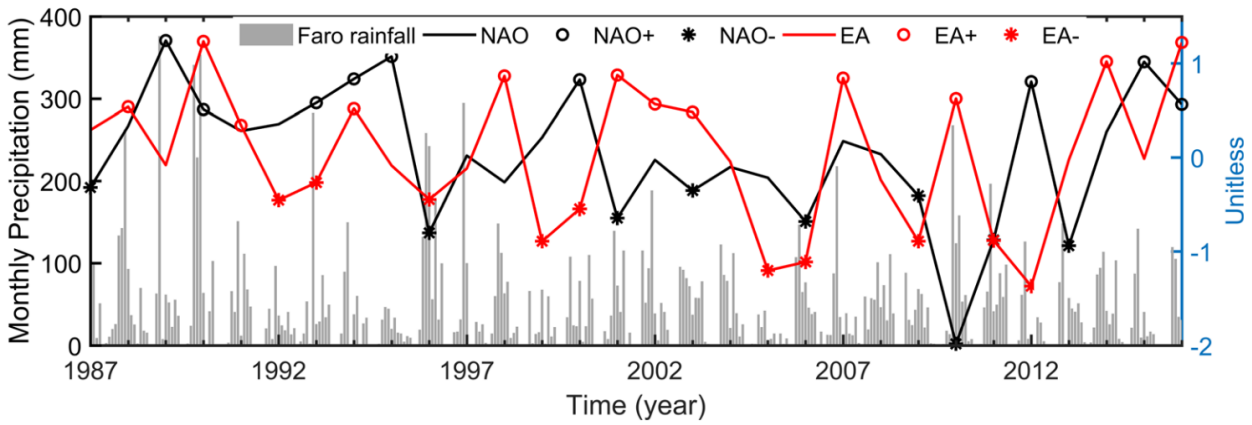

Figure 6.11 - Standardized winter (average from December through March) NAO and EA indices. Years of positive and negative phases (marked by symbols) correspond to winter NAO and EA indices above the third and below the first terciles, respectively. The bar plot shows the monthly precipitation at the Faro rainfall station between 1987 and 2016

6.3.1.4 Methods of analysis

Typical pre-processing steps, such as searching for outliers and interpolation for estimating missing values, were carried out for all piezometric records. Groundwater levels represent cumulative departures of changes in groundwater storage. Therefore, in order to compare precipitation and groundwater levels, the monthly precipitation data needs first to be transformed into cumulative departures, detrended and normalized. Linear correlation coefficients between the cumulative departures of precipitation and groundwater levels were computed using a two-tailed significant t-test at the 95 percent confidence level.

In order to explore the temporal structure of the groundwater levels, two complementary methods are applied: Singular Spectral Analysis (SSA) and Continuous Wavelet Transform (CWT).

The SSA is a form of frequency analysis applied to decompose the piezometric records into periodic or quasi-periodic components (Dettinger et al. 1995). This study follows the methodology described by Hanson et al. (2004) to extract the first 10 reconstructed components (RCs) which take the form of almost-sinusoidal oscillations. The calculations are carried out by diagonalizing a lagged covariance matrix (Vautard et al. 1992; Ghil et al. 2002) using the US Geological Survey's Hydrologic and Climate Analysis Toolkit (Dickinson et al. 2004).

According to Vautard et al. (1992), a window length of 60 months is used, which is less than one-fifth of the total number of points in the time series (360 months). The most significant periodic components are then associated with either NAO or EA in order to estimate their relative contribution to the total variance of the groundwater levels.

The CWT is a powerful method of time series analysis especially suited to analyze non-stationary signals that have temporal variations in both amplitude and frequency. The method has been widely applied in hydrology in order to examine how the dominant modes of variability change over time, to detect localized or intermittent events or to reduce noise in chaotic time series. This study uses the MATLAB implementation of the method based on the algorithm described in Torrence and Compo (1998). The base wavelet function is the Morlet wavelet for which the scale is almost equal to the Fourier period. The local wavelet power spectrum, defined as the absolute value squared of the wavelet transform, displays the distribution of the variance of the time series as a function of time. The cone of influence (black parabolic lines) delimits the region where the edge effects make the results less reliable. The statistical significance tests of the wavelet power spectra are estimated using the Monte Carlo method. The global wavelet spectrum is an average in time of the wavelet spectrum and displays the net changes of variance over the entire recording period.

Finally, the wavelet coherence method has the purpose of identifying time-localized common oscillatory behavior between the climate indices (NAO and EA) and the groundwater level time series. Its definition is similar to a localized correlation coefficient between two continuous wavelet transforms in time-frequency space (Torrence and Webster 1998). The wavelet coherence is computed at the 95% confidence level using the algorithm described in Grinsted et al. (2004). The phase of the wavelet cross-spectrum, shown by the orientation of arrows, is indicative of the relative lag between coherent components. When the correlation between two time series is positive and in phase the arrows point right, and point left when they are in antiphase and their correlation is negative (Fu et al. 2012). Regions in time-frequency space with large common power and consistent phase relationship are likely to possess a causality between the time series.

6.3.2 Results

Figure 6.11 shows the climate indices and the monthly precipitation recorded at Faro rainfall station. Some of the most extreme precipitation events occurred in years of negative NAO phase (1996, 2010). However, the connection between the indices and precipitation is not straightforward. Typically, the precipitation during the winter months determines the availability of water in subsequent months. Fig. 4 illustrates the groundwater level time series using data from three piezometers (one example per aquifer). Annual and multi-year fluctuations in groundwater levels are closely related to peaks in precipitation (note the agreement in precipitation peaks and the fast rise of groundwater levels in 1996 and 2010 for example). However, linear regression analysis between precipitation and groundwater levels yields rather poor correlation coefficients (varying between 0.3 and 0.5) when computed over the entire period of analysis. Correlation coefficients rise to 0.7-0.9 when the time span is restricted to 1993-2016 (Table 6.5). This can either be due to improvements in water management since the late 1990s, when public supply switched to a system based on surface water dams, or to an improved quality control of the rainfall station data. Piezometers located in aquifer M12 (606/647) show small amplitude fluctuations and little variance (Figure 6.12 and Table 6.5). In contrast, boreholes located further inland, in aquifers M9 and M10 (606/1042 and 607/93), show much larger hydraulic head variations. Negative long-term trends in both groundwater levels and precipitation (not shown) suggest a drying tendency in the region. The groundwater levels decrease towards the ocean attaining minimum values (below sea level) in the western sector of aquifer M12 (Figure 6.10B). Extreme low hydraulic heads are observed in the area of Quinta do Lago at piezometer 606/647 (Figure 6.9).

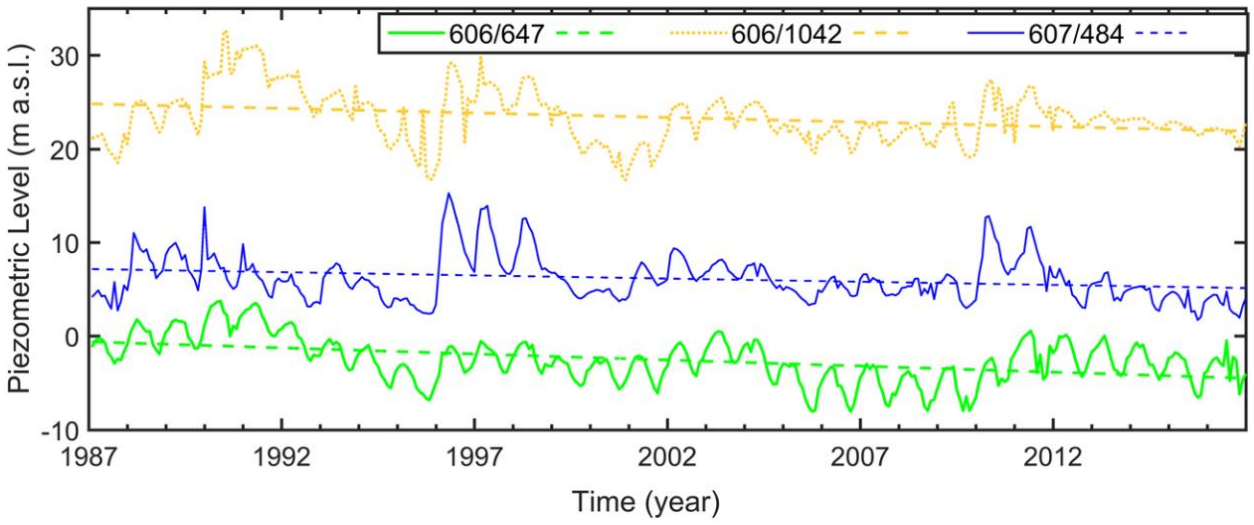

Figure 6.12 - Monthly groundwater levels at three selected piezometers, one for each aquifer: 606/647 fromM12, 607/484 from M10 and 606/1042 from M9. All sites show negative long-term trends (dashed lines)

Figure 6.13 shows the impact of NAO and EA on the seasonal variations of hydraulic head. The graphs display monthly groundwater levels averaged over years of positive and negative phases of the winter indices (years marked with symbols in Figure 6.11). In general, groundwater levels are consistently higher in years of negative NAO phase, and consistently lower in years of positive NAO phase (piezometers 611/115, 606/1042, 607/93 and 607/484). However, exceptions occur in M12 at sites near Quinta do Lago. In piezometer 606/647 the relation to NAO is even inverted, since it shows lower than average groundwater levels in wet years (NAO-). Interestingly, the response to the EA phase is neutral and almost equal to the mean level (dotted line) at all piezometers in the study area. This is in clear contrast with observations across other aquifers in mainland Portugal, where both the EA and NAO phase had a clear effect on hydrological extremes (Neves et al. 2019b).

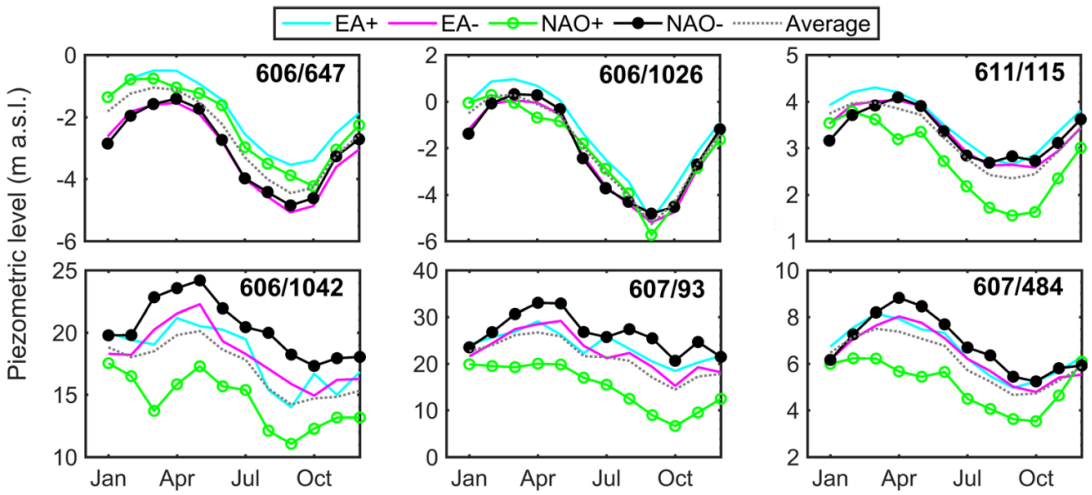

Figure 6.13 - Groundwater levels per month averaged over years of positive and negative winter NAO and EA phases. The dotted line is the average over the entire period of study (30 years). Piezometer 606/647 is the only site where groundwater levels are consistently higher during years of positive winter NAO phase

Figure 6.14 displays the normalized wavelet power spectra of the groundwater levels. The plots show the temporal distribution of power (variance) as a function of period, over the 30 years of record. Power concentrations within the 95% confidence level (within white contours) but lying outside the cone of influence are not considered, and hence the analysis is restricted to periods less than 10 years. There are noticeable differences amongst the three aquifers. Aquifer M12 is the one presenting the most systematic influence of the annual cycle. This influence is particularly strong in the Quinta do Lago piezometers 606/647 and 606/1026. In the remaining records, the 1-year peaks are more intermittent, coinciding with anomalously wet years (1990, 1996, 2000 and 2010). The spectra of records 606/647 and 606/1026 are also unique because they are characterized by a relative lack of power in the 2−8-year band whilst most of the variance is concentrated at longer periods (> 8 year). Apart from these two exceptions, all other sites are dominated by a concentration of power in the 4−8-year band, centered at year 2000 and extending for almost 10 years. A common feature to all records is the lack of power at 1−2-year periods focused in 2004, which is related to the severe drought that occurred in the Iberian Peninsula in 2004-2005 (García-Herrera et al. 2007).

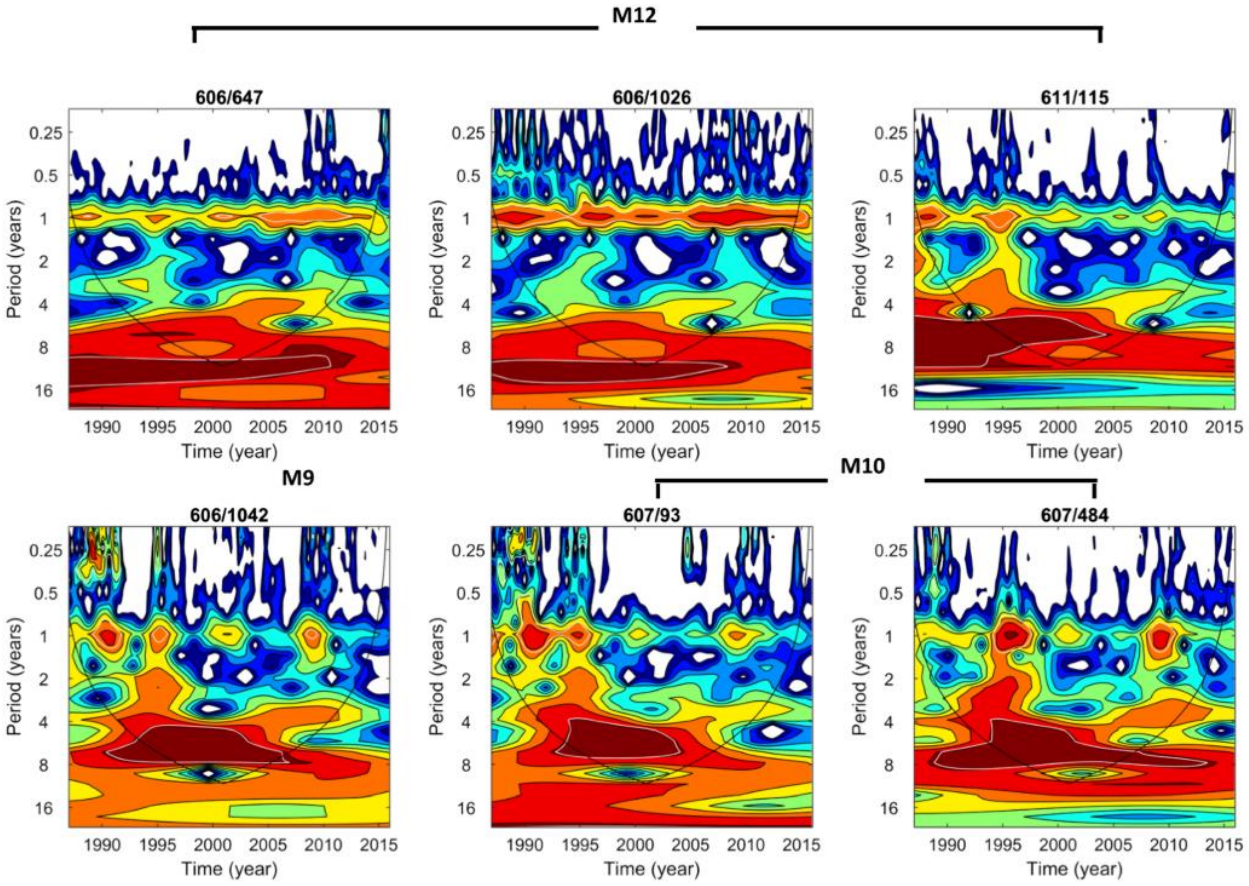

Figure 6.14 - Local wavelet power spectrum of groundwater level records using a Morlet wavelet and normalized by $1/\sigma^2$ where σ is the standard deviation. The white contours enclose regions of greater than 95% confidence levels. The black lines delimit the cone of influence, where zero padding has reduced the variance

The effect is more dramatic in aquifer M12 suggesting it may be less resilient to droughts. There is also an apparent declining strength of the long-term cycles and an increase in the 2−4-year periodicities towards the end of the recording period (after 2005). The global spectra allow a better identification of the peak periods of variance (Figure 6.15). The two most statistically significant set of oscillations peak at 10 years in the Quinta do Lago piezometers (606/647 and 606/1026) and at 6.5 years in the remaining sites (611/115, 606/1042, 606/93 and 607/484).

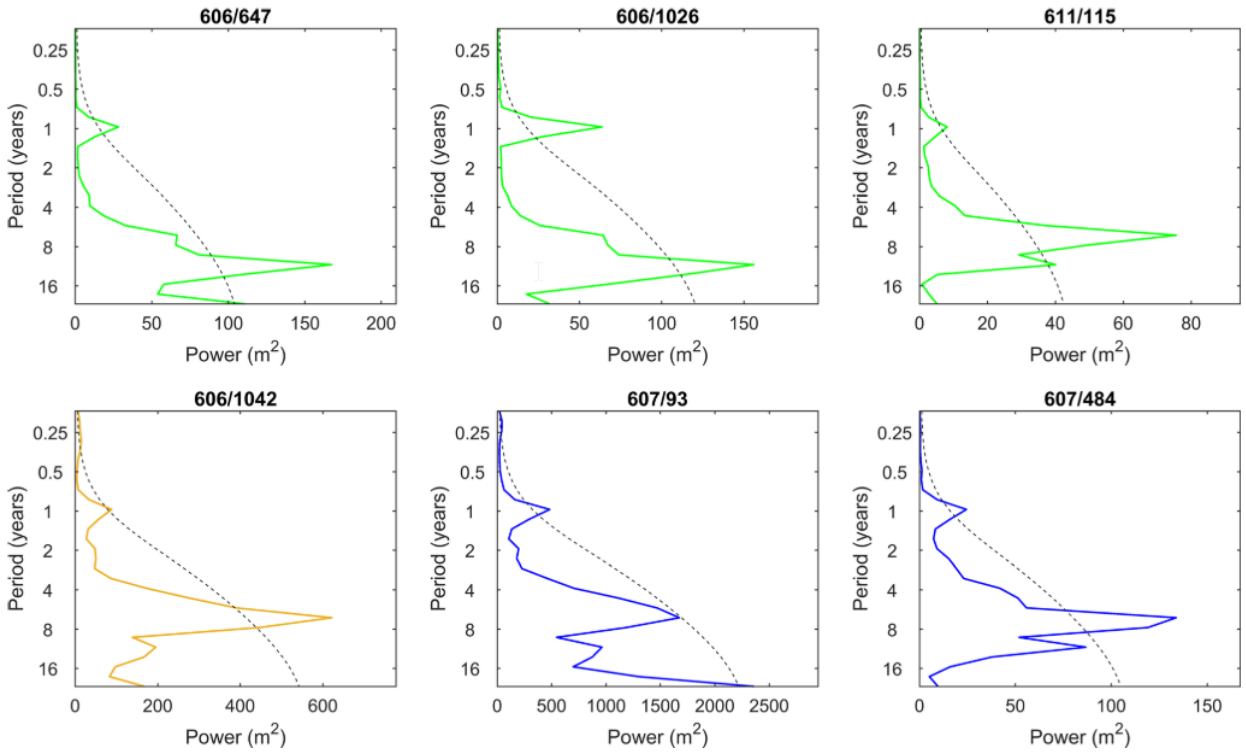

Figure 6.15 - Global wavelet spectrum, which is a time average (over 30 years) of the local wavelet spectrum. The dashed line is the 5% significance level, assuming a corresponding red noise process. The power amplitude (σ^2) is proportional to the amplitude of the hydraulic head variations in each piezometer

The wavelet coherence demonstrates the non-stationary effect of NAO and EA on the dynamics of groundwater levels (Figure 6.16 and Figure 6.17). Each diagram depicts the coherence as a function of period over the 30 years of analysis, in a color scale that goes from blue (minimum) to yellow (maximum). Statistically significant coherent patches (enclosed by thick black lines) indicate cause-effect relationship between the atmospheric teleconnections and the hydraulic head variations. The main driver of low-frequency variability is NAO as shown by the anti-phase locked behavior for periods in the 6−10-year band (Figure 6.16). Anti-phase relationships are in agreement with an inverse relationship between the amount of precipitation (recharge) and the NAO index sign. In comparison, the EA pattern exhibits more episodic and restricted phase-relationships (Figure 6.17). The most noteworthy episodes occur in the 2−4-year band after year 2005, but actually, these episodes are also coherent with NAO (Figure 6.16). Episodes of high coherence that are not attributed to a single index reveal synchronized influences, and

thus, are interpreted as a sign of coupling between NAO and EA. These results indicate that in the study area the impact of EA is manifest only in conjunction with NAO.

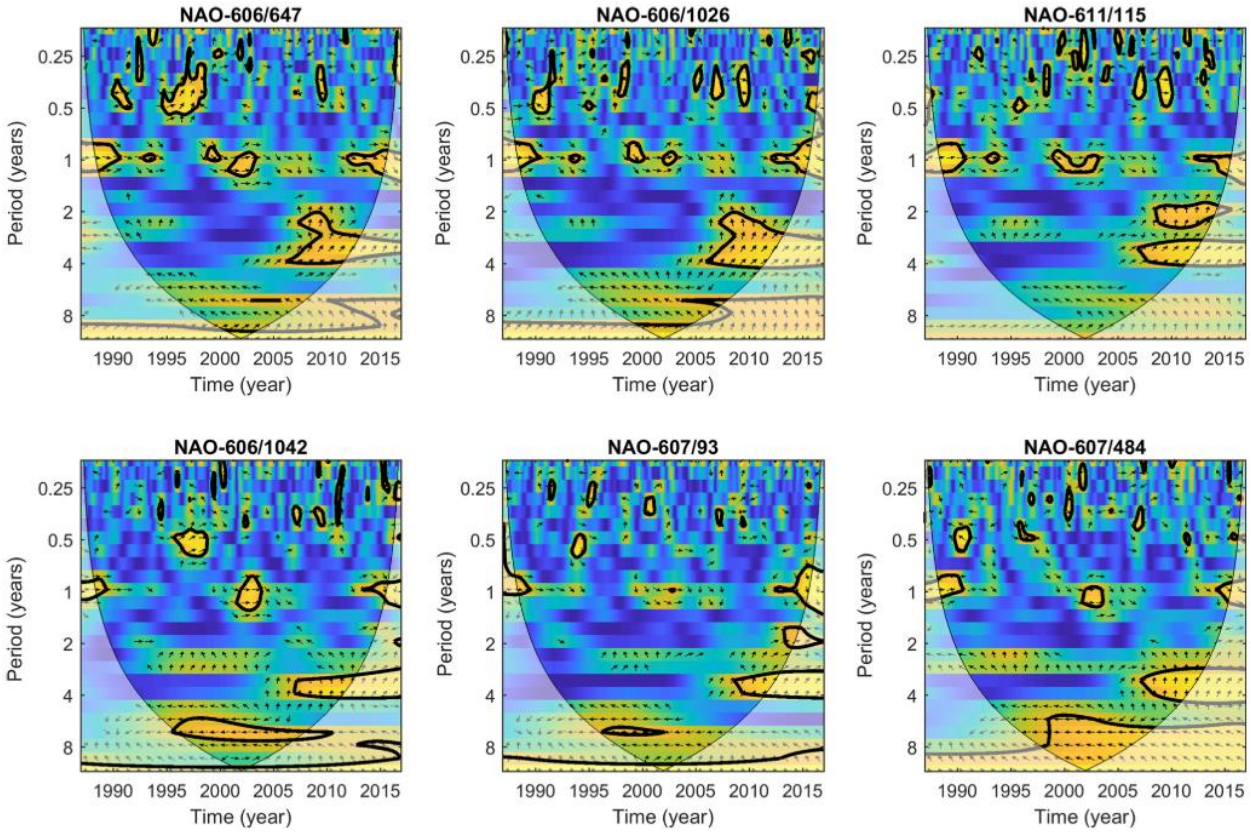

Figure 6.16 - Wavelet coherence between groundwater levels at the selected piezometers and NAO. The thick black lines are the 5% significance level and the less intense colours indicate the cone of influence. The phase-angle (black arrows) denote the phase difference between the data: horizontal right-pointing (left-pointing) arrows indicate the two time- series are in phase (anti-phase)

The percentage of explained variance derived from SSA helps to quantify the impact of the teleconnections on the studied aquifers (Table 6.6). The leading (among the first 10) oscillatory modes are grouped according to the period ranges of NAO (6−10 years) and coupled NAO and EA (2−4 years). The results at each aquifer are consistent, despite some amplitude modulation likely due to hydrogeological factors.

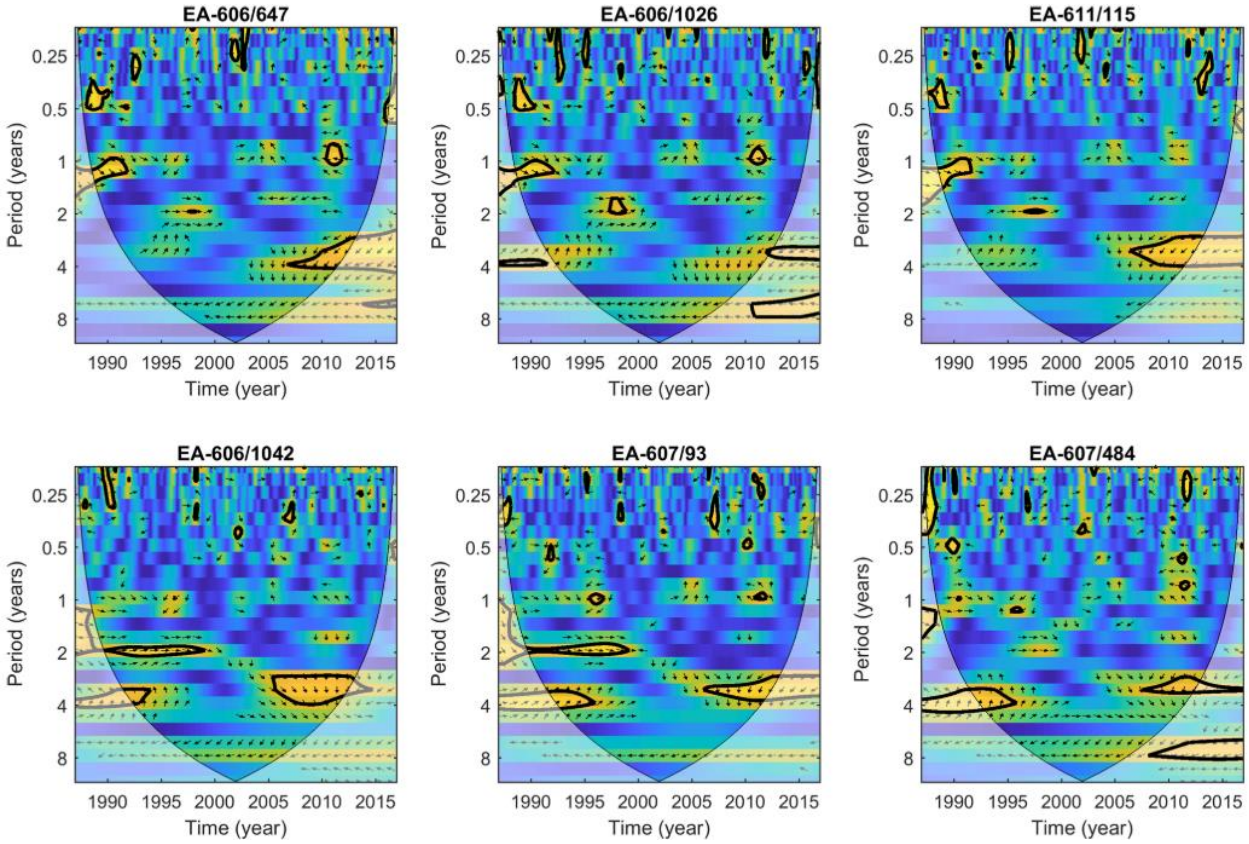

Figure 6.17 - Wavelet coherence between groundwater levels at the selected piezometers and EA (as Figure 6.16)

The low-frequency components of NAO and the annual cycle are the dominant components of variance. On average, NAO contributes to circa 50% of the groundwater level variability and the annual cycle to circa 25%. The climate driven fluctuations explain ~80% of the total groundwater level variability, with a larger fraction (90%) in Campinas de Faro (M12) than in aquifers M9 and M10 (70%). The impact of EA cannot be isolated and, even in association with NAO, has a rather limited impact at all sites (on average contributes to less than 5% to the total variance of groundwater levels).

Table 6.6 - Results from the SSA analysis. Contribution of the main oscillatory components to the total variance of groundwater levels

		Contribution of climate drivers to the total variance (%)						
Climate driver	**Period (year)**	**M12 606/647**	**M12 606/1026**	**M12 611/115**	**M9 606/1042**	**M10 607/93**	**M10 607/484**	**Average circa**
NAO	6-10	60	33	61	44	45	49	50%
NAO & EA	2 – 4	3	4	5	4	5	6	5%
Annual cycle	1	30	50	21	15	19	20	25%
Total variance (%)		93	87	87	63	69	75	80%

6.3.3 Discussion

At present, limited knowledge on the hydrogeological parameters and on the role of lateral inflow through fractures zones, hampers a more quantitative assessment of the spatial factors of variability in the studied area. From the previous section it becomes apparent that aquifers M9 and M10 have a relatively homogeneous response to climate cycles (Table 6.6). Groundwater levels in these aquifers are strongly dependent on NAO (45% of variance) with peak frequencies around 6.5 years (especially between 1995 and 2005). Frequencies in the 2−4-year band are less (but increasingly) important and occur in association with both NAO and EA. The same 6.5 and 2−4 year cycles have been recognized in the Querença-Silves aquifer also in the Algarve (Neves et al. 2016). In fact, the results of this study are broadly consistent with other studies addressing the effect of NAO over the southern Iberia Peninsula water resources (Trigo et al. 2004; Andreo et al. 2006; Luque-Espinar et al. 2008; Lorenzo-Lacruz et al. 2011). The small influence of EA (< 5% of variance) in the coastal system of Ria Formosa is perhaps the most surprisingly result. In the Querença-Silves aquifer, for instance, EA accounts for approximately 20% of the variance in groundwater levels. Moreover, hydrological extremes were found to be associated to opposite phases of NAO and EA (Neves et al. 2019b), whereas in

the current study area the piezometric levels are insensitive to the EA phase (Figure 6.13). The explanation for the observed differences relies on the amount of precipitation and on the precipitation regime, as the 2−4 year cycles are associated to stormy episodes that occur during the passage of frontal depressions. Less frequent storm tracks across the southern coast make this one of the most arid regions in Portugal. In contrast, the Querença-Silves aquifer is located at the foothills of the Caldeirão mountain range, one of the rainiest regions in the Algarve, where episodes of heavy rainfall are most frequent and torrential in character (Fragoso and Tildes Gomes 2008).

Aquifer M12 deserves particular attention because ongoing numerical modeling studies show it is at risk of seawater intrusion (Hugman 2017). Here, groundwater levels are characterized by small amplitude fluctuations, great sensitivity to the annual hydrological cycle and low-pass filtering properties in response to NAO (relative absence of 2−8-year periods as shown in Figure 6.16). A schematic cross-section cutting through M12 helps to understand these observations (Figure 6.18).

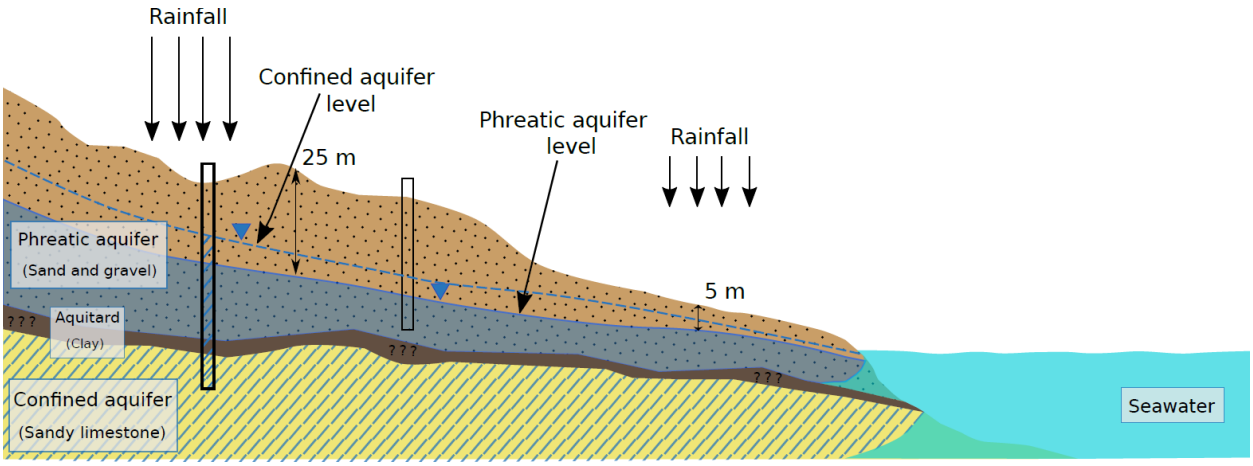

Figure 6.18 - Conceptual cross-section model of M12 representing the 2-layer aquifer system intercalated by an aquitard. The solid line above the shad- ow zone represents the water table of the free-surface phreatic aquifer The potential hydraulic head for the confined aquifer is represented by a dashed line. Question marks in the aquitard represent possible discontinuities

Small amplitude fluctuations are a common feature of hydraulic heads in coastal discharging areas due to the sea level boundary condition. In addition, the flat topography, small depth of

the water table and the permeable nature the sediment cover in M12, all facilitate the direct infiltration of rainfall and contribute to a strong annual cycle. More quantitative insights can be gained by comparing these observations with the damping depths of climate signals in the vadose zone (Corona et al. 2018). Assuming a mean recharge flux of 0.1-0.4 mm/day (consistent with a mean recharge of 50-150 mm/year in Figure 6.10D) the damping depth of periodic infiltration is located between 5-15 m for annual periods and between 20-100 m for periods in the 2-8 year range (Figure 6.12 in Corona et al. 2018). Since the thickness of the vadose zone (depth to the water table of the upper phreatic aquifer) decreases from 25 m to 5 m towards the sea (Figure 6.18) this depth-dependent damping can explain why the annual cycle is more prominent (not damped) near the coastline (where piezometers 606/647 and 606/1026 are located). Finally, the further distance to the main recharge zone in the north justifies the low-frequency content of M12 when compared to M9 or M10. That low-frequency content is usually the filtered response to regional recharge arising from rainfall integrated over the catchment area. This allows one to indirectly estimate that the NAO-induced regional recharge contributes to 40% − 60 % (on average) of the total variance of groundwater levels in M12. It is worth mentioning that the regional recharge in M12 is mainly transmitted to the lower confined aquifer through lateral flow coming from the M9 and M10 aquifers. Moreover, as water in the confined aquifer system is under pressure and the aquitard is likely to be spatially discontinuous, there may be some vertical flow from the lower to the upper aquifer (Figure 6.18).

Aquifer M12 is also the one presenting more heterogeneity in the response to climate patterns (Table 6.6). A major contributing factor may be the existence of semi-confining layers of silts and clays between the Miocene and the upper Plio-Quaternary sands in M12 (Figure 6.18). Pumping also causes heterogeneity in groundwater levels, as dispersed abstraction for agriculture, touristic activities, golf course irrigation and small scale private use may cause localized drawdown cones. Return flow from irrigation, which can explain the high concentrations of nitrate found in the vicinity of piezometer 611/115, is another source of perturbation in this aquifer by supplying an additional source of recharge during the dry season to the upper phreatic aquifer of the M12 (Hugman et al. 2017b).

Another peculiarity of aquifer M12 is the observation that in piezometer 606/647 the groundwater levels are lowest in wet (NAO-) years. Although the monthly sampling used in this study is unable to capture the effect of tides, a recent field campaign has shown that this piezometer is affected by semi-diurnal and fortnightly tidal cycles. Therefore, it is possible that the observed inversion is due to the "inverse barometric effect" of sea level height (inverse relationship between air pressure and water level) observed at analogous sites (Vallejos et al. 2014). Another hypothesis is that groundwater pumping at Quinta do Lago overshadows the NAO natural variability. Other studies show that in irrigated areas, especially in semi-arid regions, groundwater level changes may reflect climate-induced pumping variability rather than climate variability itself (Gurdak et al. 2007; Ferguson and Gleeson 2012b; Gurdak 2017; Russo and Lall 2017). The results of the present study highlight the need for additional research on the influence of climate-driven sea level height variations and on pumping patterns in the Ria Formosa aquifers, as well as on the critical implications of these factors for the shifts of the freshwater-seawater interface. As more data become available to calibrate the aquifer properties, underway numerical modelling will provide insights into these challenging problems.

6.4 Conclusions

The current task is work which was not foreseen in the work plan defined for the current thesis. Nonetheless, it was considered a necessary step, in order to provide a better insight on how climate and groundwater long term oscillations relate. This becomes more important in the current water management scenario in Algarve, since a long climatic drought period is affecting the region, raising an higher awareness for the analysis of water availability in the region.

The results derived from this task allowed provided soft knowledge for understanding how groundwater levels may behave in the towards different climatic scenarios, and what can be expected from the short to mid-term effects of drought in the Algarve region. In the following sub-chapters, conclusions for each case-study are presented.

6.4.1 Conclusions Querença-Silves aquifer

The analysis of groundwater time series from the Querença-Silves aquifer, using simple spectral analysis, continuous wavelet transform and singular spectral analysis, revealed the presence of consistent inter-annual periodicities. The main mode of variability having enough persistence and amplitude to remain statistically significant over the analyzed time interval (1985-2010) corresponds to a period of 6.5 yr. Other leading modes of variability correspond to oscillatory components with periods of 4.3 yr, 3.2 yr and 2.6 yr. A similar set of oscillations has been found in the surface flow of the Guadiana river time series in previous studies, suggesting that they have a common climatic origin related to the North Atlantic Oscillation. The differences in the temporal variability of hydraulic head variations are interpreted as a result of geologic forcing. The time series exhibit two distinctive types of modulation of the climate signals, showing that the aquifer is effectively divided in two distinct sectors by the S.Marcos-Quarteira fault. The region to the west of the fault is characterized by spatially homogenous periodic oscillations, larger memory effects and only one scaling regime. These properties are attributed to a better developed and connected flow network, which in conjunction with a greater water storage capacity make this part of the aquifer more resilient to short-term variations. The region to the east of the fault is more reactive to high frequency variations and shows a greater spatial and temporal variability in groundwater levels. The results are consistent with previous estimates of hydrogeologic properties (transmissivity and storage capacity) in the region. The 6.5 yr mode of variability contains ~70% (55%) of the total variance of the groundwater level in the western (eastern) sector of the aquifer. The geologic forcings then account to ~15% of the differential response among the two sectors.

6.4.2 Conclusions Ria Formosa aquifers

The impact of atmospheric teleconnections on the coastal aquifers of Ria Formosa is conspicuous. Groundwater level fluctuations in this region are dominated by low-frequency (6-10 year) components related to NAO, which on average contribute to 50% of the total variance.

The second most important component is the annual cycle, which on average explains around 25% of the total variance in groundwater levels. The power of the annual cycle increases towards the coastline with decreasing thickness of the vadose zone. Frequencies in the 2−4-year band are less important (< 5 % of variance) and occur in association with both NAO and EA. Compared to other regions in Portugal, the minor role of EA in the study region can be explained by less frequent and intense rainstorms in this part of the country. Aquifers M9 (Almasil-Medronhal) and M10 (S. João da Venda) present a relatively homogeneous response to climate cycles. The greater spatial heterogeneity observed in piezometric levels in aquifer M12 is in part due to its multilayered structure and in part due to localized abstraction. The effects of abstraction are particularly notorious in the western part of aquifer M12, in the Quinta do Lago region. There, the lack of intermediate periods (2−8 years) in the spectra of groundwater oscillations emphasizes the vulnerability of this region to droughts, especially those lasting for more than one hydrological year.

Chapter 7: Final considerations

The intention of this thesis was to provide an analysis of the hydrogeological problems affecting the groundwater management resources in the Algarve, with a particular look on the nitrate contamination occurring at the Nitrate Vulnerable Zone (NVZ) of Faro and eventual quantities problems at Querença-Silves (QS) that could lead to seawater intrusion.

Various types of assessment were performed throughout the thesis, with special incidence on numerical modelling of groundwater flow and mass-transport and statistical analysis of time-series. A hydrogeological and chemical characterization of the study areas has been performed based on available data and newly collected data, although these have not been described in detail the current thesis. Nonetheless, newly collected data had an important role in the characterization of the study areas and calibration of the implemented numerical models used.

The contributions of modelling presented in **chapter 3** were a result of the MARSOL FP7 Project (GA-2013-619120), which intended to show Managed Aquifer Recharge (MAR) as a sound and safe solution to increase groundwater security. The case study selected for this task was the QS which intended to assess the risk of seawater intrusion occurring from the Arade estuary. Under this scope, water availability for MAR was assessed, and a groundwater flow numerical model was a developed in order to analyze groundwater level response to different abstraction and MAR injection scenarios. Although this is a karst system, an equivalent porous media model was developed and results for the three-dimension model showed a good fit with the observed data. The analysis of the seawater interface performed in this task consisted of a post-processing analysis based on the Ghyben-Herzberg relation, since the development of a three-dimension density-driven model would be highly time-consuming and computationally demanding. The results obtained with the Ghyben-Herzberg relation provided a pedagogic understanding of the effect that MAR can have in the evolution of the fresh-saltwater interface. Nonetheless, these results can only be considered as a theoretical approach, due to the high limitations of the Ghyben-Herzberg relation.

Groundwater nitrate contamination assessment is extremely important under the scope of the Water Framework Directive (WFD) and Nitrate Directive (ND) and was subject of study on **chapters 4 and 5**. Whereas WFD establishes the framework for protection of all surface and groundwater bodies in European Union member countries, ND was implemented with the specific purpose of reducing the nutrient load of agriculture on surface and groundwater. Under this scope, **Chapter 4** relied on the analysis of different land-use scenarios impacts in the prosecution of the WFD and ND objectives in the NVZ Faro (with particular attention to the Campina de Faro aquifer (M12), as well as the analysis of a Managed Aquifer Recharge (MAR) mitigation measure based on rainwater harvesting in order to achieve compliance of nitrates in groundwater. The developed flow and mass-transport numerical allowed to understand that the nitrate contamination in the area is highly persistent, and compliance with the WFD cannot be achieved before the end of the simulated period (year 2040) in any of the analysed land-use scenarios. This analysis suggests achieving compliance with WFD in terms of nitrate contamination in the NVZ Faro would require significant impactful mitigation measures. Therefore, one scenario has also been assessed in chapter 4 which focuses on the use of harvested rainwater at greenhouses as a source of water to be injected in the aquifer, in order to dilute and flush the current nitrate contaminant mass, and hence reduce the concentration of nitrates in groundwater. This MAR scheme could result in a water availability for MAR corresponding to 10% of the average natural recharge of the M12 aquifer. Results of the numerical model simulation of the MAR scenario suggest this can decrease the time to achieve compliance in the majority of the NVZ, though high values are still observed by the year 2040. Although some issues can affect the potential benefit of such solution (such as well clogging of infiltration wells, quality concerns, among others), it can be considered that this could be a low-cost and local mitigation measure that could be easily implemented to contribute not only to improve the groundwater chemical status at NVZ Faro, in particular the Campina de Faro aquifer, as well as augment groundwater levels.

The task performed in chapter 4 allowed a better understanding on the evolution of nitrate contamination at the NVZ Faro in what respects to different land-use scenarios. Nonetheless, it was unclear on the effects of intrinsic aquifer processes, such as the connections between the

aquifers within the NVZ, the discharge of nitrate to the coastal lagoon Ria Formosa and the nitrate recycling resulting from the return flow of irrigation, which were some of the topics addressed on **chapter 5**. One important aspect of this chapter was to help understanding the evolution of nitrate contamination from the beginning of intense agricultural activities until the implementations of the NVZ, with the inclusion of the return flow and consequent nitrate recycling. In fact, by testing the impact of the nitrate recycling in the model based on known information, allowed to better describe the evolution of this contaminant and how it reached the values observed in the 90's. Simulated results showed that the inclusion of the recycling does explain the concentration of nitrates in the majority of the aquifers, except for a section of M12, where simulated results are still lower than what is observed. This supports the idea that either there are unaccounted sources of nitrate in the model or nitrate load in the past was higher than what the available data indicates or there could be local hydraulic barrier to mass-transport in this area. As for NVZ Tavira, aquifer Luz-Tavira (M15), the history-matching return-flow model run clearly describes the observed results by 1995/1996, showing that return-flow had a major role in causing the observed levels of contamination in the general area of the model.

Another important aspect addressed in chapter 5 focused on the analysis of mitigation and climate scenarios on groundwater nitrate concentration and discharge to coastal lagoon Ria Formosa. Mitigation scenarios included a no fertilizer load, similarly to what had been performed in chapter 4, a change of irrigation water source from groundwater to surface water and two MAR scenarios, one based on riverbed infiltration and one on rainwater harvesting at greenhouses. Similarly, to what happened in chapter 4, the best-case scenario showed that even without any nitrate load, EU compliance regarding nitrate concentration cannot be achieved, even with the implementation of good agricultural practices. This most likely happens because current nitrate concentrations are a reflex of nitrate loads in the past aggravated by the nitrate recycling from return flow, as well as the aquifer properties regarding the natural low gradients. The simulation of the remaining scenarios showed that they can have benefits in different parts of the study-area, with the change to surface water for irrigation scenario achieving the best results, but still, never before 2040. The analysis of the mitigation scenarios

showed that groundwater remediation is one of the most difficult tasks in environmental clean-up, especially when it comes to large areas. Therefore, an ensemble of solutions, some local, some more regional, including land management measures, should be considered in order to attain a significant reduction of time in achieving good quality status of groundwater bodies The simplified large-scale model of the aquifer systems that discharge into the Ria Formosa highlighted that these systems should not be considered as individual groundwater bodies, as water and land use practices associated with one system can cause impacts on others. The approach applied here should be extended to understand how uncertainty in aquifer connectivity, parameters and water budget components affect the predictive uncertainty.

The analysis of the time series performed in **chapter 6** was a necessary step in order to provide a better insight regarding the relations between climate patterns and groundwater oscillations. This becomes more important in the current water management scenario in Algarve, since a long climatic drought period is affecting the region, raising a higher awareness for the analysis of water availability in the region. Regarding the Querença-Silves aquifer, it was found that geology is an important forcing for the temporal variability of hydraulic head variations corresponding to approximately 15% of the groundwater oscillations differences observed in the both sectors of the aquifer. The time series exhibit two distinctive types of modulation of the climate signals, showing that the aquifer is effectively divided in two distinct sectors by the S.Marcos-Quarteira fault. This is already known from the observation of the groundwater levels, nonetheless, with this task, it was possible to assess that the region to the west of the fault is characterized by spatially homogenous periodic oscillations, larger memory effects and only one scaling regime, whereas the sector to the east of the fault is more reactive to high frequency variations and has a more heterogeneous in terms of spatial and temporal variability in groundwater levels. The results are consistent with previous estimates of hydrogeologic properties (transmissivity and storage capacity) in the region. The 6.5-year mode of variability contains ~70% (55%) of the total variance of the groundwater level in the western (eastern) sector of the aquifer. Regarding the impact of atmospheric teleconnections on the coastal aquifers of Ria Formosa, the current work showed that groundwater levels in the study area are mostly explained by the low-frequency (6-10 years) NAO pattern (accounting for 50% of the

total variance) and the annual cycle (25% of total variance), although the power of the annual cycle becomes more important towards the coastline. Additionally, aquifers located more upstream do have a more homogeneous response to climate cycles than those closer to the coastline. This is a result of the complex multi layered aquifer M12 and the high abstraction values occurring in this system. There, the lack of intermediate periods (2−8 years) in the spectra of groundwater oscillations emphasizes the vulnerability of this region to droughts, especially those lasting for more than one hydrological year.

The use of the numerical tools described in this thesis proved to be a powerful tool in the characterization of aquifers in central Algarve, which allowed to assess and analyse the main issues related to groundwater in the region. Not only did it allowed to perform an history-matching analysis, which helped understanding what were the past conditions that lead to the current status of groundwater, but also provided important insights regarding the expected evolution of the current conditions, under different scenarios of land-use, abstraction, mitigation actions and climate. This shows the role that numerical models can have under the scope of water resources management, and how they can, and should be, implemented to not only help the understanding of hydrogeological features of specific groundwater bodies or group of groundwater bodies, but also to provide a better insight and prediction on the outcomes of management decisions. Nonetheless, it is important to state groundwater numerical models are a simplified representation of the reality, in which input data or hydrological processes may be incorrect and therefore, lead to erroneous outcomes. In such way, particularly in predictive models, it is important to as far as possible, include uncertainty analysis regarding model parameterization and input data, to help decrease the unforeseen effects of a given scenario.

Chapter 8: References

Abdulla FA, Al-Shareef AW (2009) Roof rainwater harvesting systems for household water supply in Jordan. Desalination 243:195–207. https://doi.org/10.1016/j.desal.2008.05.013

Almeida C, Mendonça JJL, Jesus MR, Gomes AJ (2000) Sistema de aquíferos de Portugal continental. Lisbon: INAG.

Almeida CC (1985) Hidrogeologia do Algarve Central. PhD Dissertation, Faculdade de Ciências, Universidade Lisboa

Anderson M, Woessner W (1992) Applied Groundwater Modeling—Simulation of flow and advective transport. Academic Press, Inc., San Diego, Calif.

Andrade G (1989) Contribuição para o Estudo da Unidade Hidrogeológica Tôr-Silves (Contribution to the Study of Tôr-Silves Hidrogeologic Unit). PhD Thesis. Universidade de Lisboa, Portugal.

Andreo B, Jiménez P, Durán JJ, et al (2006) Climatic and hydrological variations during the last 117–166 years in the south of the Iberian Peninsula, from spectral and correlation analyses and continuous wavelet analyses. J Hydrol 324:24–39. https://doi.org/10.1016/j.jhydrol.2005.09.010

APA (2016) Plano de Gestão das Bacias Hidrograficas que Integram a Região Hidrográfica das Ribeiras do Algarve (RH8) 2016-2021 (River Basin Management Plan for the Hidrografic Region of the Algarve Streams(RH8) 2016-2021). Faro, Portugal

Appelo T, Postma D (2005) Geochemistry, Ground Water and Pollution, Second Edi. A.A. Balkema Publishers

Ashraful A, Islam M (2015) A Study on Rain Water Harvesting and Comparative Cost Analysis with Withdrawal of Underground Water around Gazipur City. J Environ Sci Nat Resour 8:91–94. https://doi.org/10.3329/jesnr.v8i1.24678

Asoka A, Gleeson T, Wada Y, Mishra V (2017) Relative contribution of monsoon precipitation and pumping to changes in groundwater storage in India. Nat Geosci 10:109–117. https://doi.org/10.1038/ngeo2869

Bear J (1979) Hydraulics of Groundwater. McGraw-Hill, Inc., New York, NY

Beckers B, Berking J, Schütt B (2013) Ancient Water Harvesting Methods in the Drylands of the Mediterranean and Western Asia. J Anc Stud 2:145–164

Beltrão (1985) Rega localizada (Localized irrigation). Faro, Portugal

Bloomfield JP, Marchant BP (2013) Analysis of groundwater drought building on the standardised precipitation index approach. Hydrol Earth Syst Sci 17:4769–4787. https://doi.org/DOI 10.5194/hess-17-4769-2013

Bouwer H (2002) Artificial recharge of groundwater: hydrogeology and engineering. Hydrogeol J

10:121–142. https://doi.org/10.1007/s10040-001-0182-4

Bridgman HA, Oliver JE (2006) The global climate system: Patterns, processes, and teleconnections

Cardoso RM, Soares PMM, Lima DCA, Miranda PMA (2018) Mean and extreme temperatures in a warming climate: EURO CORDEX and WRF regional climate high-resolution projections for Portugal. Clim Dyn 0:1–29. https://doi.org/10.1007/s00382-018-4124-4

Carvalho MR, Zeferino J, Silva C, et al (2017) Metodologia para avaliação da evolução da qualidade das massas de água subterrâneas nas zonas vulneráveis aos nitratos de origem agrícola no âmbito da diretiva nitratos e diretiva quadro da água - Relatório Final. Lisboa

Casanova J, Evau N, Pettenati M (2016) Managed Aquifer Recharge: An Overview of Issues and Options. In: Jakeman AJ, Barreteau O, Hunt RJ, et al. (eds) Integrated Groundwater Management., Integrated. Springer, Cham, pp 416–434

CCDR-Alg (2007) Population served by wastewater drainage and treatment facilities

Corona CR, Gurdak JJ, Dickinson JE, et al (2018) Climate variability and vadose zone controls on damping of transient recharge. J Hydrol 561:1094–1104. https://doi.org/10.1016/j.jhydrol.2017.08.028

Costa LRD da, Monteiro JPPG, Hugman RT (2020) Assessing the use of harvested greenhouse runoff for managed aquifer recharge to improve groundwater status in South Portugal. Environ Earth Sci 79:1–15. https://doi.org/10.1007/s12665-020-09003-5

Costa L, Monteiro J, Oliveira M, et al (2015a) Modelling Contributions of the Local and Regional Groundwater Flow of Managed Aquifer Recharge Activities at Querença-Silves Aquifer System. In: EGU General Assembly 2015. Vol. 17, EGU2015-146, poster presentation. Copernicus GmbH, Viena, Austria

Costa L, Monteiro JP, Leitão T, et al (2015b) Estimating harvested rainwater at greenhouses in south Portugal aquifer Campina de Faro for potential infiltration in Managed Aquifer Recharge . In: EGU General Assembly 2015. Copernicus GmbH, Vienna, Austria, p 10415

Costa L, Monteiro JP, Oliveira MM, et al (2015c) Interpretation of an Injection Test in a Large Diameter Well in South Portugal and Contribution to the Understanding of the Local Hydrogeology. In: 10º Seminário de Águas Subterrâneas - Associação Portuguesa de Recursos Hídricos (APRH). Universidade de Évora, 9 e 10 de Abril de 2015, Évora. pp 61–64

Costa L, Neves MC, Monteiro JP (2015d) Efeito Conjugado da Geologia e do Clima na Piezometria do Aquífero Querença-Silves – Combined Geological and Climatic Forcings on the Querença-Silves Piezometry. In: 9º Simpósio de Meteorologia e Geofísica da Asosciação Portuguesa de Meteorologia e Climatologia – APMG2015

Costa LRD, Hugman RT, Stigter TY, Monteiro JP (2021) Predicting the impact of management and climate scenarios on groundwater nitrate concentration trends in southern Portugal. Hydrogeol J 29:2501–2516. https://doi.org/10.1007/s10040-021-02374-4

Cunha MC, Nunes L (2011) Groundwater Characterization, Management and Monitoring. WIT Press, Southampton, UK

Daubechies I (1990) The wavelet transform time-frequency localization and signal analysis. IEEE Trans. Inform. IEEE Trans Inf 36:961–1004

de Lima MIP, Santo FE, Ramos AM, Trigo RM (2014) Trends and correlations in annual extreme precipitation indices for mainland Portugal, 1941-2007. Theor Appl Climatol 1–21. https://doi.org/10.1007/s00704-013-1079-6

Dettinger MD, Ghil M, Strong CM, et al (1995) Software expedites singular-spectrum analysis of noisy time series. Eos (Washington DC) 76:12, 14, 21

Diamantino C (2009) Recarga artificial de aquíferos:aplicação ao sistema aquífero da Campina de Faro. Dissertation, Faculdade de Ciências, Universidade de Lisboa

Dias R (2001) Neotectónica da Região do Algarve (Neotectonics of the Algarve Region). PhD Thesis. Universidade de Lisboa, Portugal.

Dickinson JE, Hanson RT, Ferré TPA, Leake SA (2004) Inferring time-varying recharge from inverse analysis of long-term water levels. Water Resour Res 40:W07403. https://doi.org/10.1029/2003WR002650

Diersch H-JG, Kolditz O (1998) Coupled groundwater flow and transport: 2. Thermohaline and 3D convection systems. Adv Water Resour 21:401–425. https://doi.org/10.1016/S0309-1708(97)00003-1

Diersch HJG (2014) FEFLOW: Finite Element Modeling of Flow, Mass and Heat Transport in Porous and Fractured Media. Springer-Verlag Berlin Heidelberg, Berlin

Dillon P (2005) Future management of aquifer recharge. Hydrogeol J 13:313–316. https://doi.org/10.1007/s10040-004-0413-6

Dillon P, Pavelic P, Page D, et al (2009) Managed aquifer recharge : An Introduction. Waterlines Report Series No. 13, National Water Commission. Canberra

Dillon P, Stuyfzand P, Grischek T, et al (2019) Sixty years of global progress in managed aquifer recharge. Hydrogeol J 27:1–30. https://doi.org/10.1007/s10040-018-1841-z

Doherty J (2002) Model-Independent Parameter Estimation, 4th edn. Watermark Numerical Computing

Domènech L, Saurí D (2011) A comparative appraisal of the use of rainwater harvesting in single and multi-family buildings of the Metropolitan Area of Barcelona (Spain): social experience, drinking water savings and economic costs. J Clean Prod 19:598–608. https://doi.org/10.1016/j.jclepro.2010.11.010

Dong L, Shimada J, Kagabu M, Fu C (2015) Teleconnection and climatic oscillation in aquifer water level in Kumamoto plain, Japan. Hydrol Process. https://doi.org/10.1002/hyp.10291

Dwivedi SN, Shukla RR, Singh R, et al (2015) Determining the recharging capacity of an injection

well in a semi-confined alluvial aquifer. Curr Sci 109:1177–1181. https://doi.org/10.18520/v109/i6/1177-1181

El Janyani S, Massei N, Dupont J-P, et al (2012) Hydrological responses of the chalk aquifer to the regional climatic signal. J Hydrol 464–465:485–493. https://doi.org/10.1016/j.jhydrol.2012.07.040

Espírito Santo F, Ramos AM, de Lima MIP, Trigo RM (2014) Seasonal changes in daily precipitation extremes in mainland Portugal from 1941 to 2007. Reg Environ Chang 14:1765–1788. https://doi.org/10.1007/s10113-013-0515-6

Ferguson G, Gleeson T (2012a) Vulnerability of coastal aquifers to groundwater use and climate change. Nat Clim Chang 2:342–345. https://doi.org/10.1038/nclimate1413

Ferguson G, Gleeson T (2012b) Vulnerability of coastal aquifers to groundwater use and climate change. Nat Clim Chang 2:342–345. https://doi.org/10.1038/nclimate1413

Fragoso M, Tildes Gomes P (2008) Classification of daily abundant rainfall patterns and associated large-scale atmospheric circulation types in Southern Portugal. Int J Climatol 28:537–544. https://doi.org/10.1002/joc.1564

Freeze RA, Cherry JA (1979) Groundwater. Prentice-Hall. Inc., Englewood Cliffs, NJ

Fretwell BEN, Burgess W, Barker J (2000) Contaminant retardation within the seasonally unsaturated zone of the Chalk aquifer : the SUZ process. In: Dassargues A (ed) Tracers and Modelling in Hydrogeology. IAHS Press, Wallingford, UK, pp 385–390

Fu C, James AL, Wachowiak MP (2012) Analyzing the combined influence of solar activity and El Niño on streamflow across southern Canada. Water Resour Res 48:. https://doi.org/10.1029/2011WR011507

Gale I (2005) Strategies for Managed Aquifer Recharge (MAR) in semi-arid areas. United Nations Educational, Scientifi c and Cultural Organization (UNESCO), Paris

Gale IN, Neumann I, Calow RC, Moenich M (2002) The effectiveness of Artificial Recharge of groundwater : a review. Keyworth, Nottingham.

Gámiz-Fortis S, Pozo-Vázquez D, Trigo RM, Castro-Díez Y (2008) Quantifying the predictability of winter river flow in Iberia. Part I: Interannual predictability. J Clim 21:2484–2502. https://doi.org/10.1175/2007JCLI1774.1

Gámiz-Fortis SR, Pozo-Vázquez D, Esteban-Parra MJ, Castro-Díez Y (2002) Spectral characteristics and predictability of the NAO assessed through Singular Spectral Analysis. J Geophys Res Atmos 107:ACL 11-1-ACL 11-15. https://doi.org/10.1029/2001JD001436

García-Herrera R, Hernández E, Barriopedro D, et al (2007) The Outstanding 2004/05 Drought in the Iberian Peninsula: Associated Atmospheric Circulation. J. Hydrometeorol. 8:483–498

Gelhar LW, Welty C, Rehfeldt KR (1992) A critical review of data on field-scale dispersion in aquifers. Water Resour Res 28:1955–1974. https://doi.org/10.1029/92WR00607

Ghil M, Allen MR, Dettinger MD, et al (2002) Advanced spectral methods for climatic time series. Rev Geophys 40:1–41. https://doi.org/10.1029/2001RG000092

Ghyben W (1888) 1888–1889. Nota in verband met de voorgenomen putboring nabij Amsterdam. Koninklyk Instituut Ingenieurs Tijdschrift (The Hague). pp. 8– 22. Koninklyk Inst Ingenieurs Tijdschr (The Hague) 8–22

Giorgi F (2006) Climate change hot-spots. Geophys Res Lett 33:1–4. https://doi.org/10.1029/2006GL025734

Goodess CM, Jones PD (2002) Links between circulation and changes in the characteristics of Iberian rainfall. Int J Climatol 22:1593–1615. https://doi.org/10.1002/joc.810

Grinsted A, Moore JC, Jevrejeva S (2004) Application of the cross wavelet transform and wavelet coherence to geophysical time series. Nonlinear Process Geophys 11:561–566. https://doi.org/10.5194/npg-11-561-2004

Gurdak J, Hanson R, Green T (2009) Effects of climate variability and change on groundwater resources. U.S. Geol. Surv. Fact Sheet FS09-3074. U.S. Geol. Surv. Denver, Color.

Gurdak JJ (2017) Groundwater: Climate-induced pumping. Nat. Geosci. 10:71–72

Gurdak JJ, Hanson RT, McMahon PB, et al (2007) Climate Variability Controls on Unsaturated Water and Chemical Movement, High Plains Aquifer, USA. Vadose Zo J 6:533–547. https://doi.org/10.2136/vzj2006.0087

Hanson RT, Newhouse MW, Dettinger MD (2004) A methodology to asess relations between climatic variability and variations in hydrologic time series in the southwestern United States. J Hydrol 287:252–269. https://doi.org/10.1016/j.jhydrol.2003.10.006

Hashemi H, Berndtsson R, Persson M (2014) Artificial recharge by floodwater spreading estimated by water balances and groundwater modelling in arid Iran. Hydrol Sci J 60:336–350. https://doi.org/10.1080/02626667.2014.881485

Hemker C, Post V (2014) MLU for Windows. Well flow modeling in multilayer aquifer systems. MLU Users Guide.

Her Y, Yoo SH, Cho J, et al (2019) Uncertainty in hydrological analysis of climate change: multi-parameter vs. multi-GCM ensemble predictions. Sci Rep 9:1–22. https://doi.org/10.1038/s41598-019-41334-7

Herzberg A (1901) Die wasserversorgung einiger Nordseebades. J Gasbeleucht Wasserver 44:815–819, 842–844

Holman IP, Rivas-Casado M, Bloomfield JP, Gurdak JJ (2011) Identifying non-stationary groundwater level response to North Atlantic ocean-atmosphere teleconnection patterns using wavelet coherence. Hydrogeol J 19:1269–1278. https://doi.org/10.1007/s10040-011-0755-9

Horne R (1990) Modern Well Test Analysis: A Computer-Aided Approach. Petroway Inc., Palo

Alto, USA

Hugman R (2017) Numerical Approaches to Simulate Groundwater Flow and Transport in Coastal Aquifers – From Regional Scale Management to Submarine Groundwater Discharge. PhD Thesis, University of the Algarve

Hugman R, Stigter T, Costa L, Monteiro JP (2017a) Numerical modelling assessment of climate-change impacts and mitigation measures on the Querença-Silves coastal aquifer (Algarve, Portugal). Hydrogeol J 25:2105–2121. https://doi.org/10.1007/s10040-017-1594-0

Hugman R, Stigter T, Costa L, Monteiro JP (2017b) Modeling Nitrate-contaminated Groundwater Discharge to the Ria Formosa Coastal Lagoon (Algarve, Portugal). Procedia Earth Planet Sci 17:650–653. https://doi.org/10.1016/j.proeps.2016.12.174

Hugman R, Stigter TY, Monteiro JP (2013) The importance of temporal scale when optimising abstraction volumes for sustainable aquifer exploitation: A case study in semi-arid South Portugal. J Hydrol 490:1–10. https://doi.org/10.1016/j.jhydrol.2013.02.053

Hugman R, Stigter TY, Monteiro JP, Nunes L (2012) Influence of aquifer properties and the spatial and temporal distribution of recharge and abstraction on sustainable yields in semi-arid regions. Hydrol Process 26:2791–2801. https://doi.org/10.1002/hyp.8353

Hugman R, Viegas J, Góis A, et al (2016) Re-Assessing Coastal Groundwater Management Policy in the Algarve : Estimating the Potential for Seawater Intrusion. In: Aqua 2015 - 42nd IAH Congress. p 620

Huno SKM, Rene ER, Van Hullebusch ED, Annachhatre AP (2018) Nitrate removal from groundwater: A review of natural and engineered processes. J Water Supply Res Technol - AQUA 67:885–902. https://doi.org/10.2166/aqua.2018.194

Hurrell JW, Kushnir Y, Ottersen G (2003) An overview of the North Atlantic Oscillation,. Clim Significance Environ Impact 1–35. https://doi.org/10.1029/GM134

Hurrell JW, Van Loon H (1997) Decadal variatons in climate associated with the North Atlantic Oscillation. Clim Chang 36:301–326

Ibánhez JSP, Leote C, Rocha C (2011) Porewater nitrate profiles in sandy sediments hosting submarine groundwater discharge described by an advection-dispersion-reaction model. Biogeochemistry 103:159–180. https://doi.org/10.1007/s10533-010-9454-1

IPMA (2019) Instituto Português do Mar a e da Atmosfera. In: Port. Inst. Sea Atmos.

Jackson BM, Browne CA, Butler AP, et al (2008) Nitrate transport in Chalk catchments: monitoring, modelling and policy implications. Environ Sci Policy 11:125–135. https://doi.org/10.1016/j.envsci.2007.10.006

Jerez S, Trigo RM (2013) Time-scale and extent at which large-scale circulation modes determine the wind and solar potential in the Iberian Peninsula. Environ Res Lett 8:. https://doi.org/10.1088/1748-9326/8/4/044035

Jones MP, Hunt WF (2010) Performance of rainwater harvesting systems in the southeastern United States. Resour Conserv Recycl 54:623–629. https://doi.org/10.1016/j.resconrec.2009.11.002

Kalimeris A, Ranieri E, Founda D, Norrant C (2017) Variability modes of precipitation along a Central Mediterranean area and their relations with ENSO, NAO, and other climatic patterns. Atmos Res 198:56–80. https://doi.org/10.1016/j.atmosres.2017.07.031

Keller J, Bliesner RD (1990) Sprinkle and Trickle Irrigation. The Blackburn Press

Kim Y, Lee B (2013) MAR for Sustainable Water Curtain Cultivation Method in Rural Area. In: 8th International Symposium on Managed Aquifer Recharge (ISMAR8). Beijing, China

Kim Y, Lee B, Ha K, et al (2013) Groundwater level deterioration issues and suggested solution for the water curtain cultivation area in South Korea. In: EGU General Assembly 2013. Vienna

King A, Jensen V, Fogg GE, Harter T (2012) Groundwater Remediation and Management for Nitrate. Technical Report 5. In: Addressing Nitrate in California's Drinking Water with a Focus on Tulare Lake Basin and Salinas Valley Groundwater. Report for the State Water Resources Control Board Report to the Legislature. p 51

Kolditz O, Ratke R, Dierschb HG, Zielke W (1998) Coupled groundwater flow and transport : 1 . Verification of variable density flow and transport models. 21:

Kruseman GP, de Ridder NA (1990) Analysis and evaluation of pumping test data, 2nd editio. International Institute for Land Reclamation and Improvement, Wageningen

Kuss AJM, Gurdak JJ (2014) Groundwater level response in U.S. principal aquifers to ENSO, NAO, PDO, and AMO. J Hydrol 519:1939–1952. https://doi.org/10.1016/j.jhydrol.2014.09.069

Leitão T, Lobo-Ferreira JP, Carvalho T, et al (2015) MARSOL : Demonstrating Managed Aquifer Recharge as a Solution to Water Scarcity and Drought. In: 10.o Semin. sobre Águas Subterrâneas, APRH. Évora, Portugal, p 4

Leitão T, Lobo Ferreira J, Oliveira M, et al (2016) Deliverable 4.3 Monitoring Results from the South Portugal MARSOL Demonstration Sites. UE MARSOL project - Demonstrating Managed Aquifer Recharge as a Solution to Water Scarcity and Drought. FP7 MARSOL-619120 Project

Leitão TE, Mota R, Novo ME, Lobo-Ferreira JP (2014) Combined Use of Electrical Resistivity Tomography and Hydrochemical Data to Assess Anthropogenic Impacts on Water Quality of a Karstic Region: A Case Study from Querença-Silves, South Portugal. Environ Process 1:43–57. https://doi.org/10.1007/s40710-014-0002-1

Leote C, Ibánhez JS, Rocha C (2008) Submarine groundwater discharge as a nitrogen source to the Ria Formosa studied with seepage meters. Biogeochemistry 88:185–194. https://doi.org/10.1007/s10533-008-9204-9

Liang X, Zhang Y (2013) Temporal and spatial variation and scaling of groundwater levels in a

bounded unconfined aquifer. J Hydrol 479:139–145. https://doi.org/10.1016/j.jhydrol.2012.11.044

Lorenzo-Lacruz J, Vicente-Serrano SM, López-Moreno JI, et al (2011) The response of Iberian rivers to the North Atlantic Oscillation. Hydrol Earth Syst Sci 15:2581–2597. https://doi.org/10.5194/hess-15-2581-2011

Loureiro NS, Coutinho MA (1995) Rainfall changes and rainfall erosivity increase in the Algarve (Portugal). Catena 24:55–67. https://doi.org/10.1016/0341-8162(94)00026-B

Lovejoy S, Schertzer D (2013) The climate is not what you expect. Bull Am Meteorol Soc 130715075145003

Luque-Espinar J a., Chica-Olmo M, Pardo-Igúzquiza E, García-Soldado MJ (2008) Influence of climatological cycles on hydraulic heads across a Spanish aquifer. J Hydrol 354:33–52. https://doi.org/10.1016/j.jhydrol.2008.02.014

Malta E jan, Stigter TY, Pacheco A, et al (2017) Effects of External Nutrient Sources and Extreme Weather Events on the Nutrient Budget of a Southern European Coastal Lagoon. Estuaries and Coasts 40:419–436. https://doi.org/10.1007/s12237-016-0150-9

Mandelbrot B (1982) The fractal geometry of nature. Freeman, San Francisco

Mangin A (1984) Pour une meilleure connaissance des systèmes hydrologiques à partir des analyses corrélatoire et spectrale [For a better knowledge of the hydrological systems starting from the cross-correlation and spectral analysis]. J Hydrol 67:25–43

Manuppella G, Ramalho M, Rocha R, et al (1993) Carta geológica da região do Algarve, folha Ocidental, na escala 1:100 000 [Geological map of the Algarve Region, scale 1:100 000]. Serviços Geolóicos de Portugal

Martin R (2014) Clogging issues associated with managed aquifer recharge methods, IAH Commis. IAH Commission on Managing Aquifer Recharge, Australia

Massei N, Durand a., Deloffre J, et al (2007) Investigating possible links between the North Atlantic Oscillation and rainfall variability in Northwestern France over the past 35 years. J Geophys Res Atmos 112:1–10. https://doi.org/10.1029/2005JD007000

Mendonça JL, Almeida C (2003) A Exploração de Recursos Hídricos Subterrâneos: O Exemplo do Sistema Aquífero Querença-Silves [Exploitation of groundwater resources: the example of aquifer system Querença-Silves]. J dos Recur Hídricos 24(3):53–61

Miranda, P., Coelho, F.E.S., Tomé, A.R., Valente MA (2002) 20th century Portuguese climate and climate scenarios. Clim Chang Port Scenar Impacts Adapt Meas SIAMproject, pp. 23–83

Missimer TM, Maliva RG, Ghaffour N, et al (2014) Managed aquifer recharge (MAR) economics for wastewater reuse in low population wadi communities, Kingdom of Saudi Arabia. Water (Switzerland) 6:2322–2338. https://doi.org/10.3390/w6082322

Monteiro JP (2006) Mudanças no uso, gestão e conhecimento da água na segunda metade do

século xx – o caso do algarve. In: 5º congresso Ibérico sobre Gestão e Planeamento da Água. Fundação Nova Cultura da Água. Faro, Dezembro de 2006. p 10pp

Monteiro JP, Costa M, Martins R, Oliveira A (2006a) Estudo das Potencialidades de Reutilização de Águas residuais na Região do Algarve – Caracterização da Procura. Relatório Técnico Hidroprojecto & Universidade do Algarve

Monteiro JP, Costa MS (2004) Dams, Groundwater Modelling and Water Management at the Regional Scale in a Coastal Mediterranean Area (The Southern Portugal Region–Algarve). Larhyss J 3:157–169

Monteiro JP, Nunes L, Vieira J, et al (2003) Síntese Bidimensional dos Modelos Conceptuais de Funcionamento Hidráulico de Seis Sistemas Aquíferos do Algarve, Baseada em Modelos Numéricos de Escoamento Regional. In: Ribeiro L, Peixinho de Cristo F (eds) As Águas Subterrâneas no Sul da Península Ibérica. International Association of Hydrologists, Lisboa, pp 159–169

Monteiro JP, Oliveira MM, Costa JP (2002) Impact of the Replacement of Groundwater by Dam Waters in the Albufeira-Ribeira de Quarteira and Quarteira Coastal Aquifers. 1–10

Monteiro JP, Ribeiro L, Martins J (2007a) Modelação Matemática do Sistema Aquífero Querença-Silves. Validação e Análise de Cenários. Relatório Técnico. Instituto da Água (INAG). Inédito.

Monteiro JP, Ribeiro L, Reis E, et al (2007b) Modelling stream-groundwater interactions in the Querença-Silves aquifer system. In: XXXV AIH Congress, Groundwater and Ecosystems. Lisbon, p 10

Monteiro JP, Vieira J, Nunes L, Younes F (2006b) Inverse Calibration of a Regional Flow Model for the Querenca-Silves Aquifer System. In: Proceedings of the International Congress on Integrated Water Resources Management and Challenges of the Sustainable Development. Marrakech

Moore C, Doherty J (2005) Role of the calibration process in reducing model predictive error. Water Resour Res 41:1–14. https://doi.org/10.1029/2004WR003501

Moore GWK, Renfrew IA, Pickart RS (2013) Multidecadal mobility of the north atlantic oscillation. J Clim 26:2453–2466. https://doi.org/10.1175/JCLI-D-12-00023.1

Musacchio A, Re V, Mas-Pla J, Sacchi E (2020) EU Nitrates Directive, from theory to practice: Environmental effectiveness and influence of regional governance on its performance. Ambio 49:504–516. https://doi.org/10.1007/s13280-019-01197-8

Neves MC, Costa L, Hugman R, Monteiro JP (2019a) The impact of atmospheric teleconnections on the coastal aquifers of Ria Formosa (Algarve, Portugal). Hydrogeol J 27:2775–2787. https://doi.org/10.1007/s10040-019-02052-6

Neves MC, Costa L, Monteiro JP (2016) Climatic and geologic controls on the piezometry of the Querença-Silves karst aquifer, Algarve (Portugal). Hydrogeol J 24:.

https://doi.org/10.1007/s10040-015-1359-6

Neves MC, Jerez S, Trigo RM (2019b) The response of piezometric levels in Portugal to NAO, EA, and SCAND climate patterns. J Hydrol 568:1105–1117. https://doi.org/10.1016/j.jhydrol.2018.11.054

Newton A, Icely JD, Falcao M, et al (2003) Evaluation of eutrophication in the Ria Formosa coastal lagoon, Portugal. Cont Shelf Res 23:1945–1961. https://doi.org/10.1016/j.csr.2003.06.008

Nicolau R (2002) Modelação e mapeamento da distribuição espacial da precipitação – Uma aplicação a Portugal Continental (Modeling and mapping of the spatial distribution of rainfall). Ph.D. thesis, Universidade Nova de Lisboa, Lisbon

NOAA (2019) National Oceanic and Atmospheric Administration, Climate Preciction Center

Nunes G, Monteiro JP, Martins J (2006) Quantificação do consumo de água subterrânea na agricultura por métodos indirectos (Quantifying groundwater use in agriculture by inderect methods). In: IX Encontro de Utilizadores de Informação Geográfica. Oeiras, pp 15–17

Oliveira L, Leitao T, Lobo-Ferreira JP, et al (2011) Água, Ecossistemas Aquáticos e Actividade Humana – Projecto PROWATERMAN. Terceiro Relatório Temático – Resultados Quantitativos e Qualitativos das Campanhas de 2011 e Balanços Hídricos. Referência do Projecto n.º PTDC/AACAMB/105061/2008, 2011

Oliveira MM, Oliveira L, Lobo-Ferreira JP (2008) Estimativa da recarga natural no sistema aquífero de Querença-Silves (Algarve) pela aplicação do modelo BALSEQ_MOD. In: 9.º Congresso da Água - Água: desafios de hoje, exigências de amanhã, Cascais (Portugal), 2 - 4 Abril

Pyne RDG (1995) Groundwater Recharge and Wells: A Guide to Aquifer Storage Recovery, CRC Press. Boca Raton : Lewis Publishers, Florida

Quelhas dos Santos J (1991) Fertilização - Fundamentos da utilização dos adubos e correctivos [Fertilisation: Fundamentals of the utilisation of fertilisers and correctors] m Martins, Portugal, 1991; 441 pp, In Portuguese. Francisco Lyon de Castro, Publ. Europa- América, Mem Martins, Portugal

Raymond F, Ullmann A, Tramblay Y, et al (2019) Evolution of Mediterranean extreme dry spells during the wet season under climate change. Reg Environ Chang 19:2339–2351. https://doi.org/10.1007/s10113-019-01526-3

RBMP (2012) Plano de Gestão das Bacias Hidrograficas que Integram a Região Hidrográfica das Ribeiras do Algarve (RH8) 2012-2015 (River Basin Management Plan for the Hidrografic Regin of the Algarve Streams(RH8) 2012-2015). Faro, Portugal

Rivett MO, Buss SR, Morgan P, et al (2008) Nitrate attenuation in groundwater: A review of biogeochemical controlling processes. Water Res 42:4215–4232. https://doi.org/10.1016/j.watres.2008.07.020

Rocha C, Veiga-Pires C, Scholten J, et al (2015) Assessing land–ocean connectivity via Submarine Groundwater Discharge (SGD) in the Ria Formosa Lagoon (Portugal): combining radon measurements and stable isotope hydrology. Hydrol Earth Syst Sci Discuss 12:12433–12482. https://doi.org/10.5194/hessd-12-12433-2015

Roseiro CM dos SD (2009) Recarga artificial de aquíferos:aplicação ao sistema aquífero da Campina de Faro. Universidade de Lisboa

Russo TA, Lall U (2017) Depletion and response of deep groundwater to climate-induced pumping variability. Nat Geosci 10:105–108. https://doi.org/10.1038/ngeo2883

Salvador N, Monteiro JP, Hugman R, et al (2012) Quantifying and modelling the contribution of streams that recharge the Querença-Silves aquifer in the south of Portugal. Nat Hazards Earth Syst Sci 12:3217–3227. https://doi.org/10.5194/nhess-12-3217-2012

Sang YF (2013) A review on the applications of wavelet transform in hydrology time series analysis. Atmos Res 122:8–15. https://doi.org/10.1016/j.atmosres.2012.11.003

Santos D, Miranda P (2006) Alterações climáticas Portugal. Cenários, impactos e medidas de adaptação (Climatic change in Portugal: Scenarios, Impacts and adaptation measures). Projecto SIAM II - 1ª edição. Gradiva.

Scanlon BR, Mace RE, Barrett ME, Smith B (2003) Can we simulate regional groundwater flow in a karst system using equivalent porous media models? Case study, Barton Springs Edwards aquifer, USA. J Hydrol 276:137–158. https://doi.org/10.1016/S0022-1694(03)00064-7

Silva AV, Portugal A, Feitas L (1986) Modelo de Fluxo Subterrâneo e Salinização dos Aquíferos Costeiros entre Faro e Fuseta [Groundwater and salinization model of the coastal aquifers between Faro and Fuseta]. Comun dos Serviços Geológicos Port 72:71–87

Silva M (1988) Hidrogeologia do Miocénico do Algarve [Hydrogeology of the Miocene of the Algarve]. PhD Thesis, Universidade de Lisboa, Lisboa, Portugal

Slimani S, Massei N, Mesquita J, et al (2009) Combined climatic and geological forcings on the spatio-temporal variability of piezometric levels in the chalk aquifer of Upper Normandy (France) at pluridecennal scale. Hydrogeol J 17:1823–1832. https://doi.org/10.1007/s10040-009-0488-1

Smith AJ, Turner J V. (2001) Density-dependent surface water-groundwater interaction and nutrient discharge in the Swan-Canning Estuary. Hydrol Process 15:2595–2616. https://doi.org/10.1002/hyp.303

SNIRH (2021) Sistema Nacional de Informação de Recursos Hídricos. In: Natl. Inf. Syst. Water Resour.

Soares PMM, Cardoso RM, Lima DCA, Miranda PMA (2017) Future precipitation in Portugal: high-resolution projections using WRF model and EURO-CORDEX multi-model ensembles. Clim Dyn 49:2503–2530. https://doi.org/10.1007/s00382-016-3455-2

Stefan C, Ansems N (2018) Web-based global inventory of managed aquifer recharge

applications. Springer International Publishing

Steirou E, Gerlitz L, Apel H, Merz B (2017) Links between large-scale circulation patterns and streamflow in Central Europe: A review. J Hydrol 549:484–500. https://doi.org/10.1016/j.jhydrol.2017.04.003

Stigter T (2005) Integrated Analysis of Hydrogeochemistry and Assessment of Groundwater Contamination Induced by Agricultural Practices. PhD thesis, Instituto Superior Técnico, Lisbon, Portugal

Stigter T, Carvalho Dill AMM, Ribeiro L, Reis E (2007) Groundwater status in the two nitrate vulnerable zones of the Algarve – concerns for the adjacent wetland and agro-ecosystems. In: Ribeiro L, Chambel A, Condesso de Melo MT (eds) XXXV IAH Congress, Groundwater and Ecosystems, Lisbon, Portugal, 17-21 September 2007. Lisbon, Portugal, pp 142–143

Stigter T, Mazimpaka C, Zhou Y (2015) Modelling nitrate transport towards a coastal lagoon under the influence of aquifer properties, contaminating activities , restoration poilices and climate change. In: Aqua 2015 - 42nd IAH Congress. International Association of Hydrogeologists (IAH), Rome, Italy, p 1

Stigter TY, Carvalho Dill a. MM, Ribeiro L, Reis E (2006a) Impact of the shift from groundwater to surface water irrigation on aquifer dynamics and hydrochemistry in a semi-arid region in the south of Portugal. Agric Water Manag 85:121–132. https://doi.org/10.1016/j.agwat.2006.04.004

Stigter TY, Carvalho Dill AMM, Malta E, Santos R (2013) Nutrient sources for green macroalgae in the Ria Formosa lagoon - assessing the role of groundwater. In: Ribeiro L, Chambel A, Condesso de Melo MT (eds) Groundwater and Ecosystems. CRC Press, Lisbon, Portugal, pp 153–167

Stigter TY, Carvalho Dill AMM, Ribeiro L (2011) Major issues regarding the efficiency of monitoring programs for nitrate contaminated groundwater. Environ Sci Technol 45:8674–8682. https://doi.org/10.1021/es201798g

Stigter TY, Monteiro JP, Nunes LM, et al (2009) Screening of sustainable groundwater sources for integration into a regional drought-prone water supply system. Hydrol Earth Syst Sci Discuss 6:85–120. https://doi.org/10.5194/hessd-6-85-2009

Stigter TY, Nunes JP, Pisani B, et al (2014) Comparative assessment of climate change and its impacts on three coastal aquifers in the Mediterranean. Reg Environ Chang 14:41–56. https://doi.org/10.1007/s10113-012-0377-3

Stigter TY, Ribeiro L, Carvalho Dill a. MM (2006b) Application of a groundwater quality index as an assessment and communication tool in agro-environmental policies - Two Portuguese case studies. J Hydrol 327:578–591. https://doi.org/10.1016/j.jhydrol.2005.12.001

Stigter TY, Ribeiro L, Dill a. MMC (2006c) Evaluation of an intrinsic and a specific vulnerability assessment method in comparison with groundwater salinisation and nitrate contamination levels in two agricultural regions in the south of Portugal. Hydrogeol J

14:79–99. https://doi.org/10.1007/s10040-004-0396-3

Stigter TY, Van Ooijen SPJ, Post VEA, et al (1998) A hydrogeological and hydrochemical explanation of the groundwater composition under irrigated land in a Mediterranean environment, Algarve, Portugal. J Hydrol 208:262–279. https://doi.org/10.1016/S0022-1694(98)00168-1

Taylor RG, Scanlon B, Döll P, et al (2013a) Ground water and climate change. Nat Clim Chang 3:322–329. https://doi.org/10.1038/nclimate1744

Taylor RG, Todd MC, Kongola L, et al (2013b) Evidence of the dependence of groundwater resources on extreme rainfall in East Africa. Nat Clim Chang 3:374–378. https://doi.org/10.1038/nclimate1731

Terrinha P (1998) Structural geology and tectonic evolution of the Algarve Basin, South Portugal. Dissertation, Imperial College, Univ. London

Torrence C, Compo GP (1998) A Practical Guide to Wavelet Analysis. Bull Am Meteorol Soc 79:61–78. https://doi.org/10.1175/1520-0477(1998)079<0061:APGTWA>2.0.CO;2

Torrence C, Webster PJ (1998) The annual cycle of persistence in the El Nino/Southern Oscillation. Q J R Meteorol Soc 124:1985–2004. https://doi.org/10.1002/qj.49712455010

Tremblay L, Larocque M, Anctil F, Rivard C (2011) Teleconnections and interannual variability in Canadian groundwater levels. J Hydrol 410:178–188. https://doi.org/10.1016/j.jhydrol.2011.09.013

Trigo RM, Pozo-Vázquez D, Osborn TJ, et al (2004) North Atlantic oscillation influence on precipitation, river flow and water resources in the Iberian Peninsula. Int J Climatol 24:925–944. https://doi.org/10.1002/joc.1048

Trigo RM, Valente MA, Trigo IF, et al (2008) The impact of North Atlantic wind and cyclone trends on European precipitation and significant wave height in the Atlantic. Ann N Y Acad Sci 1146:212–234. https://doi.org/10.1196/annals.1446.014

Vallejos A, Sola F, Pulido-Bosch A (2014) Processes Influencing Groundwater Level and the Freshwater-Saltwater Interface in a Coastal Aquifer. Water Resour Manag 29:679–697. https://doi.org/10.1007/s11269-014-0621-3

van der Linden P, Mitchell JFB (2009) ENSEMBLES: Climate Change and its Impacts: Summary of research and results from the ENSEMBLES project. Met Office Hadley Centre, FitzRoy Road, Exeter EX1 3PB, UK

Vautard R, Yiou P, Ghil M (1992) Singular-spectrum analysis: A toolkit for short, noisy chaotic signals. Phys. D Nonlinear Phenom. 58:95–126

Velasco EM, Gurdak JJ, Dickinson JE, et al (2017) Interannual to multidecadal climate forcings on groundwater resources of the U.S. West Coast. J Hydrol Reg Stud 11:250–265. https://doi.org/10.1016/j.ejrh.2015.11.018

Verruijt A (1968) A NOTE ON THE GHYBEN-HERZBERG FORMULA. Int Assoc Sci Hydrol Bull 13:43–46. https://doi.org/10.1080/02626666809493624

Vicente-Serrano SM, López-Moreno JI (2008) Nonstationary influence of the North Atlantic Oscillation on European precipitation. J Geophys Res Atmos 113:D20120. https://doi.org/10.1029/2008JD010382

Vieira J, Monteiro JP (2003) Atribuição de Propriedades a Redes Não Estruturadas de Elementos Finitos Triangulares (Aplicação ao Cálculo da Recarga de Sistemas Aquíferos do Algarve). In: Ribeiro L, Peixinho de Cristo F (eds) As Águas Subterrâneas no Sul da Península Ibérica

Wang L, Stuart ME, Lewis MA, et al (2016) The changing trend in nitrate concentrations in major aquifers due to historical nitrate loading from agricultural land across England and Wales from 1925 to 2150. Sci Total Environ 542:694–705. https://doi.org/10.1016/j.scitotenv.2015.10.127

Werner AD, Simmons CT (2009) Impact of sea-level rise on sea water intrusion in coastal aquifers. Ground Water 47:197–204. https://doi.org/10.1111/j.1745-6584.2008.00535.x

Wick K, Heumesser C, Schmid E (2012) Groundwater nitrate contamination: factors and indicators. J Environ Manage 111:178–186. https://doi.org/10.1016/j.jenvman.2012.06.030

Zhang J, Hao Y, Hu BX, et al (2017) The effects of monsoons and climate teleconnections on the Niangziguan Karst Spring discharge in North China. Clim Dyn 48:53–70. https://doi.org/10.1007/s00382-016-3062-2

Zhou Z, Ansems N, Torfs P (2015) A Global Assessment of Nitrate Contamination in Groundwater. Int Groundw Resour Assess Cent 1–27